Title

A cortisol-driven gene expression signature from circulating monocytes and neutrophils during severe inflammation.

Authors

Arthur Molendijk, PhD

Affiliation :

Center for Translational Immunology,

University Medical Center Utrecht,

Netherlands

Email : molendijkarthur@gmail.com

Leo Koenderman, PhD

Department of Respiratory Medicine,

Center for Translational Immunology,

University Medical Center, Utrecht,

Netherlands

Email : l.koenderman@umcutrecht.nl

Abstract

Background. Glucocorticoids are used as anti-inflammatory and immunosuppressive drugs in the treatment of many inflammatory diseases, such as rheumatoid arthritis and systemic lupus erythematosus (SLE), but their use in treatment of severe inflammation in sepsis and shock is controversial. This is at least in part caused by the lack of information regarding responding cell types and the genes which are the targets of glucocorticoids *in vivo*. Here, we aim to get an overview of glucocorticoid regulated genes in blood cells and to describe their expression in health, mild and severe inflammation depending on cell type.

Methods and Findings. We used 2 different sets of cortisol induced query genes in a gene expression correlation search of 375+ blood based gene transcription datasets to obtain 2 gene signatures of GC induction, either in the relative absence or in the presence of severe inflammation. Additional searches provided gene expression correlation profiles for separate immune cells and control tissues. Many well known GC target genes were recovered, as well as candidate GC regulated genes, which were further tested for upregulation by GC *in vitro* in different immune cells. Genes from GC signature 1, present in the relative absence of severe inflammation, and gene markers for cell type and inflammation were evaluated for expression correlation characteristics in a meta analysis of 62 datasets exluding severe inflammation, allowing delineation of a core group of GC induced genes including TSC22D3 and DDIT4. Several genes from this core group were highly upregulated in whole blood by circadian GC, and by GC treatment of healthy people, and suitable for combined use as biomarker of GC action, in the absence of severe inflammation. GC signature 2, present in severe inflammation, originated from gene expression in neutrophils and monocytes, as determined by correlation analysis using 38 datasets on severe inflammation, such as sepsis and trauma, and from gene expression profiles of isolated blood cells from sepsis patients. Genes expressed specifically in monocytes included VSIG4 and ADAMTS2, while genes such as OLAH and ARG1 were preferentially expressed in neutrophils, or expressed in both cell types such as CD163. GC driven signature 2 genes expressed in monocytes, included several markers for alternatively activated macrophages, that were strongly upregulated in severe inflammation. GC signature 2 was present in sepsis, trauma, and ARDS, and found in many other inflammatory diseases such as Kawasaki disease. The gene signature for cortisol induction in severe systemic inflammation might depend on elevated blood cortisol levels

and/or the appearance of the distinct neutrophils and monocytes populations as seen in severe inflammation. This points to endogenous cortisol as an important factor for immunosuppression *in vivo*.

Conclusion. We present a large number of cortisol regulated genes in different blood cells, obtained by transcriptomic meta-analysis, including gene markers that will be potentially useful for monitoring cortisol action in severe inflammation at the cellular level. We further demonstrate that gene induction by GCs in monocytes and neutrophils, associated with severe inflammation, is frequently present in many different inflammatory illnesses.

Introduction

Use of glucocorticoids in therapy, and objective

Endogenous cortisol links the endocrine and immune system, and has an important role in regulating inflammatory events. Synthetic glucocorticoids (GCs) are widely used in medicine because of their strong anti-inflammatory, and immunosuppressive mode of action. Systemic corticosteroid therapy is routinely used in autoimmune diseases such as rheumatoid arthritis (RA) and systemic lupus erythematosus (SLE), during severe exacerbation in pulmonary diseases such as COPD and asthma, in (kidney) transplantion, in severe COVID-19, in acute lymphoblastic leukemia (ALL), and as cortisol replacement in Addison's disease (Chan et al., 2020; De Lucena & Rangel, 2018; Johannsson et al., 2015; Recovery, 2021; Strehl et al., 2019). GCs with reduced systemic bioavailability are also used in active inflammatory bowel disease (IBD) (Dubois-Camacho et al., 2017). A controversy is present concerning the use of GCs in the treatment of acute inflammation such as found during septic/burn shock as well as in ARDS, and COVID-19 (Annane et al., 2017; Briegel et al., 2018; Carlet et al., 2020; Chan et al., 2020; Vandewalle & Libert, 2020; Venet et al., 2015). Considering the physiological importance of endogenous GCs and the wide use of systemic GC therapy, biomarkers for monitoring GC activity at the cellular level are very useful (Alder et al., 2018; Chan et al., 2020; Russell, 2018). Blood transcriptomics is an important technology for obtaining such biomarkers, and has been used to develop an 8 gene expression signature, to monitor cellular GC activity especially in RA and SLE (Hu et al.,

2018). Blood transcriptomics has also been used to classify heterogeneity in sepsis (Leligdowicz & Matthay, 2019; Tsakiroglou et al., 2023), but without using GC induced genes, as biomarkers, to assist in classification. Furthermore, the use of GC induced genes for monitoring the cellular effects of GC therapy in septic and burn shock has not been adequately applied. Our objective here was to use large collections of blood transcriptomics datasets to obtain GC driven gene signatures in the absence or presence of severe systemic inflammation, such as found in sepsis, ARDS, and trauma. Secondly, profiling signature gene expression based on cell type and inflammatory state was performed to help select suitable biomarkers for monitoring cortisol activity in different illnesses.

Cortisol, GR, and cellular effects

Cortisol is a steroid hormone and the major end product of the HPA (Hypothalamic Pituitary Adrenal) axis, which plays an important role in the body's stress response. Different stresses, both physical or psychosocial, stimulate the HPA axis and thereby transiently increase systemic cortisol concentrations (Oster et al., 2017). Moreover, circadian stimulation of the HPA axis results in increasing cortisol concentration during late sleep, before sunrise, peaking around the sleep wake transition at 6h-10h, and bottoming in the evening, early night between 22h-2h (Oster et al., 2017). Changes in cortisol concentration affect blood cell trafficking and mobilization, resulting in stress and circadian rhythm related shifts in different immune cell percentages (Ince et al., 2019; Olnes et al., 2016; Sautron et al., 2015; Shimba & Ikuta, 2020). In sepsis, the central HPA axis is first transiently activated, and then becomes dysfunctional, while different peripheral adaptations still maintain increased cortisol availibility (Van den Berghe et al., 2022; Vandewalle & Libert, 2020). Natural (cortisol in humans) and synthetic (eg dexamethasone) GCs are lipohilic molecules, that can traverse cell membranes. Cellular effects of GCs can be genomic (transcriptional) mediated by the glucocorticoid receptor (GR), or non-genomic (transcription independent), involving GR or other putative GC receptors (Escoter-Torres et al., 2019; Timmermans et al., 2019). In the absence of GC ligand, the glucocorticoid receptor (GR) is a part of a matured protein heterocomplex in the cytoplasm (Escoter-Torres et al., 2019; Timmermans et al., 2019). Upon ligand binding, GR translocates to the nucleus, and binds as a dimer or tetramer to pseudo-palindromic GREs (glucocorticoid response elements) in DNA, which are situated in promoters and enhancers, to activate or repress its target genes. Important GR gene targets

for activation produce anti-inflammatory factors (Escoter-Torres et al., 2019; Gerber et al., 2021; Johnson et al., 2021; Petta et al., 2016; Strickland et al., 2022; Timmermans et al., 2019; Vettorazzi et al., 2021). Many effects of GCs on neutrophils, monocytes, and monocyte derived macrophages, are thought to relate to the cell biology of different phases of the local inflammatory response to injury and infection, where a pro-inflammatory phase triggered by DAMPS and PAMPS, is followed by a resolution phase, and a tissue repair phase (Desgeorges et al., 2019; Ehrchen et al., 2019; Ronchetti et al., 2018). GCs affect monocytes, and monocyte derived macrophages depending on their differentiation and activation status, suppressing the pro-inflammatory phenotype, and stimulating the anti-inflammatory phenotype by increasing their phagocytosis of apoptotic cells (Desgeorges et al., 2019; Ehrchen et al., 2019). Effects of GCs on immune cells can be observed, to some degree, from their transcriptomes and epigenomes. Transcriptomes of different isolated blood cells and primary cell types, treated *in vitro* with GC, are highly cell type dependent, and predict testable phenotypic effects such as impaired BCR en TLR7 signaling in B cells (Franco et al., 2019). Such transcriptomes are potentially valuable data for development of selective therapies (Buttgereit, 2021; Franco et al., 2019), which would also be true for cell specific transcriptomes induced by endogenous cortisol *in vivo*, as accessible by a gene expression correlation approach.

Trauma and sepsis

Impaired immunity to infections can occur after trauma, and agents that block inflammation in sepsis are not very successful and can even be harmful (Ward et al., 2008). This led to the idea of pro-inflammatory mediators being balanced by anti-inflammatory mediators in return to homeostasis, but not in inflammation named SIRS (systemic inflammatory response syndrome), nor during immunosuppression named CARS (compensatory anti-inflammatory response syndrome) (Bone, 1996; Ward et al., 2008). Pro and anti-inflammatory and immunosuppressive processes were later found to occur together after trauma, and SIRS and CARS concepts have changed as a result (Binkowska et al., 2015; Gentile et al., 2012; Xiao et al., 2011). After severe injury DAMP exposure leads to activation of complement and coagulation pathways, and to activation of innate immune cells. Trauma can lead to remote organ injury and sepsis (Huber-Lang et al., 2018; Pottecher et al., 2019). Sepsis is defined as a life-threatening organ dysfunction caused by a dysregulated host

response to infection (Singer et al., 2016). The degree of organ dysfunction is represented by a SOFA (sequential organ failure assessment) score (Singer et al., 2016). For therapy of sepsis, the immunology of the host response is very important besides the nature of the infection (Jarczak et al., 2021). Sepsis is heterogenous, for example in the relative presence of hyperinflammation and immune suppression which may also change over time, and a major effort is ongoing in patient stratification, including the use of blood leucocyte transcriptomics, to possibly improve effects of standard and future therapies (van der Poll et al., 2021; Van Der Poll et al., 2017). Sepsis starts with detection of PAMPs from pathogens, and DAMPs from tissue damage, causing a systemic inflammatory response. Several pro-inflammatory mechanisms become deregulated including activation of complement and coagulation, immune cells, endothelial cells, and platelets. On the other hand, immunosuppressive responses are induced in parallel including lymphocyte apoptosis, reduced antigen presentation by APCs, and macrophages shifting to an alternative (M2) activation state (Hotchkiss et al., 2016; Jarczak et al., 2021; van der Poll et al., 2021; Van Der Poll et al., 2017).

Monocytes and neutrophils in severe inflammation

Low surface expression of HLA-DR on blood monocytes is an important marker for immunosuppression in sepsis, in surgery, and in cancer (Hibbert et al., 2018; Venet & Monneret, 2018), and correlates negatively with serum cortisol concentrations (Kim et al., 2010; Mengos et al., 2019; Tulzo et al., 2004). Monocytes found in sepsis are more phagocytic, and less responsive to endotoxin stimulation (endotoxin tolerant), but express higher levels of cytokines and interleukins compared to monocytes from healthy controls (Shalova et al., 2015). They display an activation pattern that is also found in macrophages as judged by gene expression analysis (Liepelt et al., 2020; Washburn et al., 2019). Recently, single cell sequencing has allowed a better description of monocyte heterogeneity in sepsis, ARDS, and COVID-19, and different monocyte cellular states have been identified, some of which are strongly expanded (Jiang et al., 2020; N. Liu et al., 2021; Reyes et al., 2020; Reyes et al., 2021; Schulte-Schrepping et al., 2020; Wang et al., 2021; Wen et al., 2020). No cortisol gene expression signature has been identified from these transcriptomics studies, neither on bulk nor single cell 'sepsis monocytes'. Neutrophils in severe systemic inflammation, such as found after trauma and in sepsis, are dysfunctional which is associated with the

susceptibility to infections and cause of tissue damage. The functions of neutrophils in acute inflammation act as a double edged sword. At the one hand, neutrophils are essential in pathogen defense and tissue repair, but on the other hand deregulated neutrophils are involved in collateral damage to host healthy tissue (Hesselink et al., 2019; Kovtun et al., 2018; Leliefeld et al., 2016; Mortaz et al., 2018). Neutrophils isolated from the blood of sepsis or ARDS patients are functionally altered including reduced chemotaxis, and delayed apoptosis. Interestingly enough no change in phagocytic capacity was found for these cells (Demaret et al., 2015; Juss et al., 2016). Different neutrophil populations occur in severe systemic inflammation, based on cell surface markers, nuclear shape, cellular density, and functional characteristics (Hellebrekers et al., 2018; Hesselink et al., 2019; Leliefeld et al., 2016; Mortaz et al., 2018; Pillay et al., 2012; Shen et al., 2017). Severe systemic inflammation results in the appearance of low density neutrophils (LDNs), with different origins, including degranulated neutrophils, immature neutrophils, granulocytic MDSCs, and pro-inflammatory/primed LDNs (Hesselink et al., 2019). Granulocytic MDSCs obtained from LDNs express degranulation markers on mature and immature subsets and produce arginase activity as a main characteristic, which causes arginine depletion and inhibition of T cell proliferation in *in vitro* assays (Darcy et al., 2014; Uhel et al., 2017; Van Der Poll et al., 2017). Transcriptomic studies, on bulk neutrophils or single cells in systemic severe inflammation including severe COVID-19 (Aschenbrenner et al., 2021; de Kleijn et al., 2012; Demaret et al., 2015; Juss et al., 2016; Kwok et al., 2020; Reusch et al., 2021; Schulte-Schrepping et al., 2020; Sinha et al., 2022; Vieira Da Silva Pellegrina et al., 2015) have not evaluated the identification of co-expressed cortisol induced genes.

Result, importance

Here we used a meta-analysis to overcome some of the limitations of identifying cortisol induced genes in single blood transcriptomics datasets. Different cortisol inducible query genes were used on 375 + blood datasets applying an expression correlation search to obtain two large, robust cortisol driven gene signatures. Signature genes were profiled for cell type dependent expression, induction by GC *in vitro*, as well as for circadian expression, and upregulation during mild and severe inflammation. We delineate a 119 gene signature of cortisol driven gene expression in the relative absence of severe inflammation, largely derived from responses to circadian and stress cortisol in neutrophils, also with some

contribution of NK and T cells. A set of genes (GC-1) selected from this signature was suitable for use as a blood transcriptional biomarker in the absence of severe inflammation. Gene expression correlation profiles of GC induction obtained for different immune cells indicated both common and cell type specific regulation, accompanying more general transcriptional reprogramming. A second 136 gene signature of cortisol driven gene expression in severe inflammation, was derived from "severe inflammatory" neutrophils, among others characterized by upregulation of ARG1 encoding arginase 1, and from monocytes including M2 alternatively activated macrophage-like monocytes. Many signature 2 genes were specifically upregulated upon GC treatment in septic and burn shock. A selection of genes (GC-2) was used to demonstrate the presence of signature 2 in a wide range of inflammatory illnesses, originating both from exogenous and endogenous GC, which indicated a general importance of GCs in immunosuppression. This analysis extends the description of cortisol action on different immune cells *in vivo*, and genes or gene modules derived from signature 2 will potentially be useful biomarkers for stratification of sepsis and other inflammatory diseases, and for monitoring of cellular responses to GC in severe inflammation.

Methods

Datasets

This study made use of data in the public domain. Microarray gene expression data were downloaded from the NCBI GEO database (Barrett et al., 2013) and loaded into R, using Biobase and GEOquery packages from the Bioconductor software repository (Huber et al., 2015; Sean & Meltzer, 2007). Expression matrices from GSE expression sets were put into GEO DataSet (GDS) format-like expression tables (i.e. dataframes with ID_REF and IDENTIFIER columns for platform probe ID and gene symbol, respectively, and followed by sample value columns). If gene symbols were not directly provided with the platform, other platform probe identifiers were used to obtain matching gene symbols, via HGCN custom downloads, using the approved gene symbols from HGNC (Braschi et al., 2019). RNA-sequencing phenotypic data were downloaded from NCBI GEO using GEOquery. The corresponding expression data were downloaded from the GEO website, and put into a GDS expression table-like format. Processed microarray and RNA-seq expression data were also downloaded from the ArrayExpress website (Athar et al., 2019), and read into R, along with the corresponding sample and data relationship (sdr) files, and array design files. Microarray

and RNA sequencing data from ArrayExpress were also put into a GDS expression table-like format, using HGCN custom downloads in case of missing gene symbol columns in expression tables or platform. In case of RNA sequencing data, a first column named ID-REF contained alternative identifiers, if provided such as Ensemble ID, or else a duplicate of gene symbols, with the second IDENTIFIER column always preserved for gene symbols. Phenotypic metadata were edited as required for later analysis. Expression dataframe files were indexed depending on tissue source (mostly PBMCs and whole blood), separated cell types, number of samples in a dataset, platform (specific expression arrays or RNA-seq), and different illnesses.

Selecting genes and datasets for GC signatures

Gene expression tables were left unchanged, without new transformation of the original values, which mostly come in either base 2 logarithmic or linear scales. Single microarray platform IDs correspond with probe in Illumina or probeset in Affymetrix datasets, and are hereafter named probe for simplicity. The number of probes present in the ID-REF column corresponding to a single gene varies depending on microarray platform, whereas in case of the RNA seq expression tables, each gene was uniquely represented by a single observation (row). Pearson correlation coefficients between the different probe expression variables corresponding with a single query gene and all other gene probes in a expression table were calculated. A given query gene was used to obtain ranked expression correlation profiles for different datasets using the corresponding gene query probes present in each gene expression table from a collection of 375 + blood transcriptomic datasets (whole blood and PBMCs, excluding datasets on separated blood cells and tissues). The number of profiles acquired per query gene depended on the presence of genes and corresponding probe numbers on dataset platforms. Gene modules (test genes), containing the query gene, were used to select profiles depending on the calculated number of test genes present in the top G (top genes nr., start at 25) ranking genes in each profile (intersect size).The top P (selected profiles nr., start at 20) ranking gene expression correlation profiles, according to intersect size, were used to obtain an initial combined correlation profile with average gene rankings as follows: Multiple probes present for single genes in each profile where aggregated per gene taking the maximal correlation value with the query gene. Average gene expression

correlation values were calculated as mean, without applying Fisher's Z transform, or taking into account unequal sample sizes of the datasets (see below), and then used to obtain corresponding average rankings for a combined profile. Genes present in fewer than X (use, start at 10) supporting profiles were discarded from the combined profile. Depending on output, including evaluation of distribution of intersect sizes and presence of top ranking genes, variables test genes, top genes nr. (G), selected profiles nr. (P), and use (X), were iteratively adjusted in R script to obtain a final combined profile for one query gene. Next, profiles obtained for different query genes in a module were combined, and genes in the combined profile were ordered according to the mean ranking of genes in the different profiles. In case of drafting the GC signatures, a cut off was decided as mentioned in results. The results from this method (S1 Table), showing the presence of GC signatures 1 and 2 in blood, can be replicated using an annotated R script with preset variables (genesignaturesindatasets.R, in folder "code"), and a smaller number (n = 30) of whole blood datasets, containing 15 sets without severe inflammation, and 15 sets with severe inflammation in a GitHub repository (https://github.com/ArthurJohannes/GCblood_repo , Zenodo).

Gene expression correlation profiles, using separate dataset collections

Pooling correlation coefficients in meta analysis, as used here of Pearson correlation coefficients of expression values for a pair of genes in different transcriptomic datasets, can be performed either after Z transform, weighing, taking mean, and transformation of weighted mean value back to average correlation coefficient according to Fisher, or by taking mean of weighted correlations coefficients directly (Alexander, 1990; Field, 2005). Weighting of different studies is applied according to within and between study variances, or according to study sample size, depending on method. Both methods are sufficiently accurate in obtaining an estimate, when population correlations vary (Field, 2005). Here, average correlation coefficients were directly taken as mean, without weighing for sample size, not to give too much weight to a few large datasets, and to have equal contributions of all datasets, which are potentially unique with respect to biased sampling of illnesses and other conditions. Average correlations obtained from meta analysis were primarily used for ranking, and less as estimates of "true" correlations. Collections of datasets were based on

experimental description as provided in metadata. Gene expression tables, or subsets thereof, were left unchanged, without transformation of the original values except in a few cases where mentioned in results and supporting information for different collections. Dataset collections varied in size, from blood in the absence of severe inflammation (62), blood in the presence of severe inflammation (38), to smaller sizes in case of separated blood cells (4-8), and control tissues (5-11). A query gene was used to obtain ranked gene expression correlation profiles using the corresponding gene query probes present in each gene expression table from a dataset collection, as described before. An average gene expression correlation profile per query gene was derived by first selecting different profiles for consistent results between probes, and between datasets, instead of using testgenes, and also using maximally one probe per dataset. Profiles were selected by setting low thresholds for overlap of the 200 highest ranking genes between profiles. Not all datasets gave correlation hits, and this may depend on the quality of specific probes on different platforms, number of samples in a dataset, or type of experiment. Since probes for a single gene on a microarray platform can perform differently, also with some probes being inadequate, it was important to select for each microarray dataset the query probe giving the largest average overlap with the correlation results of all other datasets. Average correlation profiles were obtained, as before, by aggregation of probes per gene in each profile using the maximal correlation value, and then taking the mean correlation value of the contributing profiles for ranking, without applying Fisher Z transform, or weighing by dataset sample sizes. Genes present in fewer than X (variable named use) supporting datasets were discarded from the combined profile. Since inadequate gene probes, if present, will have higher correlation values with the query (closer to 0), than corresponding adequate gene probes, in case of actual negative correlation, this averaging method is best suited for the positive correlation part of the profiles. To reliably determine the negative correlation end of ranked average gene expression correlation profiles, probes were also aggregated per gene taking the minimal correlation value in one case (S4 Table, sheet 4). A multiple gene query can also be used with the corresponding R script (multigenequerycorrelationmeta.R in folder “code” in GitHub repository https://github.com/ArthurJohannes/GCblood_repo) on each of 2 separate dataset collections, as provided, one without (n = 15), and one with severe inflammation (n =15), respectively. Results for different genes can also be combined to give robust average

correlation results in case of using a selected gene set or gene module as a multigene query. For example, GC signatures 1 and 2 in blood can be replicated using precalculated results as obtained with R script (multigenequerycorrelationmeta.R in folder "code") on the 2 separate dataset collections, by combining results for GC signature 1 and 2 query genes (script multigenematrix.R part 1, in folder "code" in the GitHub repository).

Characterization of average correlation profiles

Average gene expression correlation profiles were compared for reciprocal ranking of genes in related profiles to determine the existence of clusters of correlated gene expression by meta analysis. Using the method described above, reciprocal average correlation values between gene pairs (a,b and b,a) were identical in case of identical corresponding gene probes used, which mostly applies to RNA sequencing data, and when using the same (all) datasets in the dataset collection for both genes. In this way, the dataset collection on muscle tissue (consisting of 10 RNAseq datasets, and one microarray dataset with mostly unique gene probes; gse 111551, gpl17586) often yielded symmetrical gene expression correlation matrices in meta analysis. Ranking gene expression correlation values in profiles obtained either on a single dataset or from meta analysis, results in different reciprocal rankings for gene pairs (rankings for a,b and b,a different), and asymmetric matrices of gene rankings. An "inside" gene in a large tight co-expression cluster may have higher ranking (closer to 1) in a profile of an "outside" gene than the other way around. This allows easier grouping of the "outside" gene with the large cluster which can be useful, and indicate (marginal) gene induction in case of such clusters resulting from specific gene induction. The order of gene rows and columns was arbitrarily set to indicate relevant gene groups, not using clustering algorithms. Reciprocal expression correlation ranking of set GC-1 and set GC-2 genes, as shown in meta analysis (Fig. 4 and 8), can be replicated using R script multigenematrix.R part 2, in GitHub subfolder "code" on precalculated expression profiles obtained with R script (multigenequerycorrelationmeta.R) on each of the 2 separate dataset collections, one without, and one with severe inflammation.

Transcriptional gene modules

Gene expression correlation, and deriving gene modules based on co-expression in samples, is strongly dependent on the origin and cellular complexity of source material, separated cell type, and other conditions (van Dam et al., 2018). Modules were determined by using only blood (whole and PBMC), and for some modules differentiating between the presence and absence of severe inflammation. No distinction was made for whole blood or PBMC datasets, since apart from eosinophils, mature neutrophils, neutrophil bands, and basophils, were generally present in sufficient amounts for detection of the corresponding co-expression clusters. Many different transcriptional gene module detection methods exist including more commonly used network-based approaches (Saelens et al., 2018), to identify modules in co- expression networks, using single (Langfelder & Horvath, 2008), or multiple datasets (Altman et al., 2021; Chaussabel & Baldwin, 2014; Chaussabel et al., 2008). Here we used multiple blood transcriptomic datasets, from different platforms, in meta-analysis of gene expression correlation, and bypassed construction of a complete co-clustering network in module identification. High ranking genes by average correlation value, present in profiles obtained with a suitable starting query gene were tested in turn, using the same dataset collection, to get an overview of the correlation structure. Genes with high reciprocal ranking to the query gene were considered module worthy, while genes with higher correlations to other / outside co-expression clusters were removed from the list. The correlation structure of high ranking genes was also visualized in individual datasets as a clustered heatmap of the pairwise correlation matrix of up to about 200 genes, with added marker genes, using the R package pheatmap (Kolde, 2019).The bigger picture emerging from the figures was used to delineate clusters of co-expression. As a rule both procedures were used in combination to arbitrarily define transcriptional modules. A single use repertoire of gene modules corresponding with different clusters for cell types, cellular processes, and gene inductions was acquired. Not all genes were assigned to modules.

Using gene sets and modules

Different methods exist to summarize gene set expression values using a single score, such as mean and median expression value of genes in the set, mean of Z scores for each gene, eigengene values (Langfelder & Horvath, 2008), and GSEA (Hu et al., 2018). Ranking of gene transcriptional modules and gene sets in gene expression correlation profiles was done by

taking the mean ranking in the profile of all genes in the module or set. For plotting module expression in all samples (Fig. 6), a dataset was first converted to linear scale. Gene expression values were aggregated per gene taking mean probe expression. The data was then scaled (value - mean, and divide by sd), and the mean of Z scores of genes in the module were taken as module Z value after rescaling. For plotting the distribution of sample gene expression values for genes and modules in different experimental groups, datasets were first converted to linear scale, if necessary. In case of using gene modules with microarray data, only adequate and identical gene probes were used per platform in case of GPL570 and GPL10558. In case of other microarray platforms, probes with highest expression levels in the experiment were used. To obtain module expression values, expression values for individual genes were combined, adjusting for expression range, and background / basal expression seen in the whole dataset, for each gene in the module. In case of RNA sequencing data, such adjustment was only made for the expression ranges of different genes in the module, but not for basal expression. Values were plotted on the log2 scale using similar Y axis interval sizes to allow for a better comparison between datasets. Distributions of module expression were examined within datasets, and also between datasets, using identical probes in case of microarray platforms. The differences between ill and healthy control groups were compared between datasets, to score a relative strength of induction occurring for different illnesses, for use in an overview (Fig. 16). Annotated R scripts and datasets to reproduce figure 9E, and 9F (single genes, gse154918, RNAseq (Herwanto et al., 2021), replicate results of gene module expression in severe inflammation, (gene modules, gse154918, RNAseq), and to reproduce figure S4A (gene modules, gse66099, microarray gpl570 (Sweeney et al., 2015), and figure S5F (gene modules, gse34404, microarray gpl10558 (Idaghdour et al., 2012) are provided in github repository folder (https://github.com/ArthurJohannes/GCblood_repo/tree/main/plotting , Zenodo).

Using R and figures preparation

Data were analyzed using R programming language for statistical computing and graphics, in RStudio IDE desktop. The ggplot2 R package (Wickham, 2016) was used for plotting. For aligning plots, use was made of the R packages grid (Murrell, 2002), gridExtra (Auguie et al., 2017), and package gtable contained in ggplot2. Package pheatmap (Kolde, 2019) was used

for hierarchical clustering of correlation matrices, using Euclidean distance (not directly using correlation dissimilarity as a distance), and clustering method complete, and for custom annotation. R packages xlsx (Dragulescu, 2012), and readxl (Wickham et al., 2019) were used for writing and reading Excel files, or WPS spreadsheet files. Tables were edited in WPS spreadsheets. Figure PDFs were arranged and edited in Inkscape (Inkscape project, 2020), or created with BioRender.com.

Results

PART1 (obtaining GC 1 and GC 2 gene signatures)

Clusters of co-expression for GC induced genes in homeostasis and in severe inflammation

In the course of drafting gene modules of co-expressed genes using a meta analysis of blood transcriptomic datasets, 2 different clusters of cortisol induced gene expression were observed, one in healthy people and another in severe inflammation. A cluster of genes co-expressed with cortisol induced genes TSC22D3 and DDIT4, could be seen in several datasets with circadian sampling, *in vivo* GC treatment, and in large datasets on whole blood of healthy people. For example, in healthy PBMCs and whole blood for datasets gse11761, gse14642, and gse57065 (Cazalis et al., 2014; Radom-Aizik et al., 2009a, 2009b)(Fig 1A, 1C). Another cluster of genes co-expressed with ADAMTS2 and VSIG4 was visible in most datasets on severe inflammation, including sepsis and trauma, for example in inflammatory PBMCs and whole blood in case of datasets gse9960 (Tang et al., 2009), and gse57065 (Fig 1B, 1D). Several strong DEGs in severe inflammation from cluster 2 were absent in cluster 1 including monocyte expressed ADAMTS2, and VSIG4, and predominantly neutrophil expressed OLAH, and DAAM2 (Fig 1A, 1C).

Obtaining 2 signatures of GC induction in homeostasis and in severe inflammation

To obtain robust gene expression correlation signatures, the best datasets for observing clusters 1 or 2 were selected from a collection of 375+ blood transcriptomic datasets for each of a number of “best“ cluster 1 and exclusive cluster 2 genes (Fig 2A). Average gene expression correlation rankings based on selected datasets for each query gene were then averaged for either cluster 1 or cluster 2 query genes to obtain 2 final gene rankings (S1 Table). Cortisol driven gene expression signature 1 (more generally, also in the absence of

severe inflammation), was derived from the final gene ranking obtained with cluster 1 query genes PER1, ZBTB16, DDIT4, TSC22D3, KLF9 and IRS2 (S1 Table, sheet 1). The first 100 genes were taken along with 19 genes with high rankings for only some of the 6 query genes, especially for TSC22D3 and DDIT4. Cortisol driven gene expression signature 2 (in the presence of severe inflammation) was obtained similarly to signature 1, but using 3 query genes exclusive to cluster 2 (ADAMTS2, VSIG4, OLAH), and 4 additional genes with strong correlated expression to the first 3 query genes, and with high fold induction in monocytes or neutrophils in severe inflammation (DAAM2, CD163, ADORA3, and FLT3 (S1 Table , sheet 2). ADAMTS2, encoding a metalloproteinase in procollagen processing, is glucocorticoid (GC) inducible in monocytes and macrophages *in vitro* (Hofer et al., 2008), and VSIG4, encoding a complement receptor immunoglobulin (CRIg), is GC inducible in macrophages *in vitro* (Gorgani et al., 2011). CD163 and ADORA3 are GC induced genes in monocytes, and CD163 is an important marker for alternative anti-inflammatory macrophage (M2) activation (Ehrchen et al., 2019). OLAH and DAAM2 are genes, which like ADAMTS2 and VSIG4 are highly expressed in severe inflammation but more so in neutrophils than in monocytes. OLAH, encoding thioesterase 2 in premature fatty acid chain release from fatty acid synthase (Ritchie et al., 2016), and DAAM2, encoding a formin family protein, are not known as cortisol induced genes but were implicated based on high average correlation with ADAMTS2 and VSIG4 expression in severe inflammation. FLT3, encoding a receptor tyrosine kinase important in regulating haematopoietic cell proliferation, is not known as a GC induced gene, but was also strongly implicated based on average gene expression correlation results (S1 Table, sheet 2). The final average ranked list of genes correlating with the 7 query genes in datasets on severe inflammation was cut off taking the first 100 genes (except PER1 and IFNGR1, including 28 genes also present in signature 1), and taking additional high ranking genes that were absent from signature 1, or had high rankings for only 2-3 query genes (eg C1QA/B/C, RNASE1/4, ANG, with monocyte biased queries ADAMTS2 , VSIG4, and FLT3), and were not previously assigned to a very large group of genes (such as SERPINB1, NLRC4, RAB27A, GYG1 in neutrophils) upregulated in severe inflammation, more generally (S1 Table, sheet 2). Gene sets for signature 1 (n = 119) and 2 (n = 136) overlapped for 28 genes (S2 Table, sheet 1).

Testing *in vitro* induction of GC sigature genes obtained *in vivo*

The signature genes found by correlation search may come from variable differential gene expression due to upregulation by GCs, or more indirectly due to cell type shifts caused by cortisol in healthy people (signature 1), or the appearance of specific cell types in severe inflammation (signature 2). Therefore, it was important to determine which signature genes could be observed as DEGs *in vitro*, and at the same time determine the cell types involved at basal and induced gene expression levels. Total genes (n = 227) from both signature sets were compared with 8 sets of *in vitro* GC induced DEGs, taken at a cut off of 2 fold induction and with unadjusted p value < 0.05, in different immune cells and PBMC preparations (Fig 2B, 2C, S2 Table). Overlap with different DEG sets was in in the range of 10-54% of signature genes, and higher with myeloid cells than with lymhoid cells in experiment gse112101 (Franco et al., 2019), suggesting a relatively high contribution of monocyte and neutrophil gene expression to the gene correlation signatures (Fig 2B). Counting the occurrence of individual genes in different DEG sets showed best representation for several well known cortisol induced genes (DUSP1, FKBP5, SESN1,TSC22D3, TXNIP, etc) (S2 Table, sheet 10), and these were also present in the signatures obtained by correlation search (Fig 2C). Several frequent DEGs, which were absent from the correlation signatures (eg SLCO4A1, TBC1D16, TBC1D8, KLF4, SPON2, FPR1) (S2 Table, sheet 10), were not further pursued in analysis. The DEG sets excluded 64 potentially cortisol induced genes present in the signatures while 49 genes were detected only once in these experiments. The high proportion of genes upregulated by GC *in vitro* strongly indicated that the signatures mainly originated from GC gene induction rather than from shifts in cellular blood count.

Basal gene expression and induction by GC in different cell types *in vitro*

In a next step, all GC signature genes were directly compared for basal expression levels in separated blood cells and for their induction by GC *in vitro*. Gene expression was profiled using experiment gse60424 on separated immune cells from different illnesses, excluding sepsis (Linsley et al., 2014), experiment gse112101 which studies GC gene induction *in vitro* in different cell types including separated immune cells (Franco et al., 2019), and experiment gse109439 on GC gene induction *in vitro* in monocytes and macrophages (Wang et al., 2019). Since these 3 experiments are RNA sequencing data, they lack the probeset specific background signals present in similar experiments on microarray platforms, and allow more accurate comparisons. Additionally, gene expression profiles were examined using

experiment gse100521 on GC gene induction in M1 macrophages analysed on a microarray platform (Gharib et al., 2019). Basal level expression data from experiment gse60424 and gse112101 were largely similar as expected, although with some differences, eg in case of CXCR4, and FLT3 (S3 Table). Most signature 1 genes were generally expressed, while several genes were expressed more specifically in lymphocytes, monocytes or neutrophils (Fig 3, S3 Table). Signature 2, obtained from datasets on severe inflammation, and using GC induced query genes expressed preferentially in myeloid cells, contained more genes expressed specifically in monocytes or neutrophils as might have been expected (S3 Table). Differential expression of many signature genes, in one or more cell types, was well visible in a range of up to +100 fold induction in case of FKBP5 and ZBTB16 (Fig 3, S3 Table). Of 64 genes without differential expression in the earlier comparison, additional genes were now found as DEGs, while 8 genes remained negative (S3 Table). These additional DEGs resulted from using a paired t test in case of dataset gse112101, inclusion of dataset gse100521, and not using a cut off at 2 fold expression difference. Signature 1 query genes were ubiquitously expressed and induced, except for relatively high IRS2 and low KLF9 basal expression in neutrophils in both experiments gse60424 and gse112101, and ZBTB16 being preferentially expressed in B and NK cells (Fig 3, S3 Table). CXCR4 was another good example of a signature 1 gene, and used in a GC-1 gene set (n= 7), drawn up for biomarker purpose (see below). Signature 2 query genes ADAMTS2, CD163 and VSIG4 were specifically expressed in monocytes, FLT3 preferentially in monocytes, ADORA3 in both monocytes and neutrophils, while OLAH and DAAM2 were preferentially expressed in neutrophils (Fig 3, S3 Table). Important examples of signature 2 genes were FKBP5, also expressed in lymphocytes, HPGD, also expressed in T cells and NK cells, ALOX5AP, and ARG1 expressed in neutrophils, and ALOX15B, and MAOA expressed in monocytes (Fig 3, S3 Table). Additional examples of genes found in GC signature 2 were AMPH and MACIR, which were later selected in a GC-2 biomarker gene set (n = 9) (see below). Basal expression of ADAMTS2 and FLT3 was higher in monocytes than in monocyte derived macrophages, while expression of CD163, VSIG4, ALOX15B, MAOA, and ADORA3 genes was higher in macrophages instead. *In vitro* upregulation by GC was visible for all signature 2 query and example genes, sometimes even in cell separations with very low/absent basal expression as in case of CD163 and VSIG4 (Fig 3). Genes ARG1 and MAOA were upregulated by GC treatment in neutrophils, and ALOX15B in monocytes (Fig 3).

PART 2 (gene induction by GC in homeostasis)

Selection of gene set GC-1 from GC signature 1

Not all genes present in GC signature 1 would be suitable for use as biomarkers of GC action, since gene expression might be too dependent on cell type or alternative regulation, or fold induction might be too low. GC target genes include several negative regulators in activation and inflammation (Gerber et al., 2021; Xavier et al., 2016), which are otherwise also required for negative feedback regulation in these same processes, with accompanying gene induction, for example, genes DUSP1, NFKBIA, and TNFAIP3 (Altonsy et al., 2014; Chen et al., 2002). Such induction during inflammation would severely limit the use of GC target genes as specific biomarkers. Therefore, GC signature genes, and a selection of relevant marker genes were examined each for gene expression correlation characteristics, and for upregulation during mild inflammation. Average gene expression correlation profiles were obtained using a collection of 62 blood transcriptomic datasets which excluded datasets on severe inflammation based on experimental description. The absence of severe systemic inflammation in the datasets was indicated by a relatively low correlation signal for several important GC signature 2 genes and other gene markers for severe inflammation (S4 Table, sheet 2), and no correlation signal for ADAMTS2. Different clusters of marker gene expression related to mild inflammation were visible for monocytes and neutrophils, most obviously in case of induction involving interferon (S4 Table, sheet2). Signature 1 genes with higher ranking correlation to induction by GC (n= 31) (S4 Table, sheet1), were tested each for reciprocal correlation ranking. A “core group” for induction by GC, of approximately 20 genes was visible with this selection of 31 GC signature 1 genes (Fig. 4). This core group included all query genes used to obtain GC signature 1, and variably originated from homeostasis in lymhocytes and myeloid cells, for example, DDIT4 being expressed more in NK cells, and TSC22D3 more in neutrophils. Expression of several genes in GC signature 1 also correlated with marker gene expression in inflammation, indicating alternative gene regulation, eg in case of TNFAIP3, NFIL3, and SOCS1 (Fig. 4, S4 Table, sheet 1). Potential upregulation of GC signature gene expression during mild inflammation was further examined using datasets gse73072 (Liu et al., 2016) on experimental respiratory viral infection of volunteers, and gse68310 (Zhai et al., 2015), from a prospective experiment for respiratory viral infection on a non-hospital population. Under these conditions, blood cells

would likely show gene induction by interleukins and interferon, but less so by DAMPs, and MAMPs which are more associated with severe inflammation (see below). A number of GC signature 1 genes, including TNFAIP3, NFIL3, and SOCS1, was upregulated during mild inflammation, more than, or comparible to positive marker gene IL1B (S4 Table, sheet 1). The next step in selecting a biomarker gene set for GC action in blood, was determining fold induction in the presence of GC *in vivo*. Differential expression of GC signature 1 and 2 genes in healthy people was analysed using 4 experiments on the effect of different GC treatments (gds3864, PBMC, (Carlet et al., 2010); gse67255, PBMC, (Olnes et al., 2016); gse110160, whole blood, (Hu et al., 2018); gse46743, whole blood, (Arloth et al., 2015), and using 2 experiments on the effects of fatty acid or alcohol intake, which both provided adequate circadian sampling (gds3704, PBMC, (Bouwens et al., 2010); gds2767, whole blood, (Baty et al., 2006). Many glucocorticoid induced genes in the core group, as well as additional GC signature 1 en 2 genes, were present in these experiments as high ranking DEGs, relative to gene markers used to observe changes in NK and neutrophil percentages, as caused by GC (Olnes et al., 2016) (S1 Fig A, S5 Table). Not all GC signature 1 genes were seen as DEGs *in vivo,* possibly because of low fold changes of induction compared to shifts in cellular percentages. Conversely, relative upregulation of several genes exclusively present in GC signature 2, indicated their induction, also by GC in homeostasis. Experiment gds3704 with circadian sampling of PBMCs (Bouwens et al., 2010) showed relatively few circadian changes in cellular composition (S1 Fig A). Cluster analysis combining cell type marker genes and GC signature 1 and 2 genes that were expressed as DEGs in this experiment, showed differential clustering of these GC signature genes with either lymphoid or myeloid cells (S1 Fig B), in good agreement with the results from correlation meta analysis. High ranking DEGs, especially from this experiment, were selected from the “core group” of 20 GC induced genes, also leaving out genes that were highly upregulated in severe inflammation (FKBP5, ECHDC3, TPST1, FLT3), or sensitive to early induction *in vitro* (AREG, NR4A2, DUSP1, DUSP2, FOS). Selection GC-1 (PER1, TSC22D3, ZBTB16, KLF9, DDIT4, IRS2, CXCR4) corresponded with the 6 query genes used to obtain GC signature 1, but with added CXCR4.

Signature 1 is GC driven, not molecular clock driven

Peripheral clocks regulate cellular circadian rhythms, and clock genes are also functional in immune cells (Labrecque & Cermakian, 2015) . Circadian expression of core clock genes in

immune cells has been documented in case of lymphocytes, macrophages and monocytes (Labrecque & Cermakian, 2015; Wittenbrink et al., 2018) . Molecular clock function involves transcription of clock genes such as PERs and CRYs driven by the CLOCK/BMAL1 heterocomplex bound to their E-box enhancers (Cox & Takahashi, 2019) . GCs also regulate circadian rhythms and entrain the cellular circadian clock, and clock genes PER1, PER2, and NFIL3 are primary targets of the GC-receptor (Oster et al., 2017; Shimba & Ikuta, 2020; So et al., 2009). Circadian, CLOCK driven gene expression in human tissues is strong in fat (Loboda et al., 2009), muscle (Lundell et al., 2020; Perrin et al., 2018), and skin, but not in blood (Wu et al., 2018). To answer whether molecular clock driven gene expression might have contributed to GC signature 1 obtained on blood, averaged gene expression correlation profiles for both GC and CLOCK driven gene expression were obtained for these tissues, combining results for different relevant query genes (S6 Table, sheet 7-12), and using smaller collections of datasets (S6 Table, sheet 16). A tight correlated expression of clock genes was well visible in dataset collections on muscle, skin, and fat tissues, by the presence of PER1-3, NR1D2, TEF, DBP, and HLF genes (S6 Table, sheet 10-12), in agreement with the transcriptional architecture of the cellular circadian clock (Cox & Takahashi, 2019). Furthermore, a strong negative correlation existed between the expression of CLOCK/BMAL1 regulated genes, and both ARNTL (encoding BMAL1) and NFIL3 clock genes (S6 Table, sheet 13-15), which are both usually expressed in circadian anti-phase to PER1 (Yan et al., 2008). Gene expression correlation profiles obtained with either GC inducible genes or CLOCK regulated genes for specific tissues were relatively similar, with clock genes present in GC profiles, and GC inducible genes in clock profiles (S6 Table, sheet 7-12). In contrast to results for tissues, GC driven gene expression profiles, but not CLOCK driven profiles, could readily be obtained for separated immune cells, using relevant GC inducible query genes, and small corresponding dataset collections (S6 sheet 1-6,16). Similarly, no CLOCK driven gene expression profiles could be obtained using large blood transcriptomic dataset collections. Next, GC-1 set genes and several CLOCK regulated genes were compared for reciprocal expression correlation ranking using dataset collections for blood, monocytes, and muscle (Fig 5A, 5B, 5C). Much tighter clustering of GC-1 set genes in monocytes compared to blood was observed, which may relate to lower complexity of the monocyte source material. GC-1 set genes in muscle showed strong subclustering of KLF9 and ZBTB16, and additionally of TSC22D3 and DDIT4, while gene CXCR4 ranked very low. CLOCK regulated genes including

PER1, DBP, and TEF strongly grouped together in muscle, less so in monocytes, and not in blood (Fig 5A, 5B, 5C). Expression of CLOCK regulated genes in blood also did not strongly correlate with GC-1 set genes, indicating that GC signature 1 obtained on blood was primarily GC driven with little contribution from CLOCK regulated circadian gene expression. GC driven gene expression correlation profiles derived from immune cells and tissues showed strong evidence for transcriptional reprogramming (histone modification and RNA splicing), and ubiquitin dependent protein degradation, in GO term enrichment analysis of top 1000 ranking genes (S7 Table). The profiles were also directly compared with each other, taking the top ranking 200 genes of each profile, and all genes were examined for transcriptional induction *in vitro* using data by Franco et al. (2019) on GC treatment of immune cells and different cell cultures (S8 Table). This analysis indicated likely gene targets of GC, more generally, as well as in specific cell types, and also additional genes absent in GC signatures 1 and 2. For example, FOXO3, a known target of the GC receptor (Lützner et al., 2012), with a critical role in muscle atrophy and autophagy (Zhao et al., 2007), recurred in different profiles, including tissues (Fig 5D, S8 Table). Genes PTGER4, present in lymphocyte profiles, and VSIR in neutrophil, represented interesting examples of candidate GC induced genes *in vivo* (Fig 5D, S8 Table).

Using GC-1 gene set as biomarker for GC action in blood cells in the absence of severe inflammation

Major sources of intra-individual variability in cellular blood count, in health, are circadian rhythm (Ackermann et al., 2012), and exercise (Gustafson et al., 2017). As a result, many genes are expressed in circadian fashion, sometimes roughly in phase with induction by GCs, in case of genes expressed in NK cells and neutrophils. While these changes may represent confounders for the use of gene set GC-1 as a biomarker in blood, at another level they also correspond to effects of GC on cell trafficking (Shimba & Ikuta, 2020). Set GC-1 contained high ranking genes in differential expression, to minimize the confounding effect of circadian change in cell percentages. A good example for visualizing both circadian gene expression, and gene upregulation during inflammation was provided by longitudinal respiratory viral challenge experiment gse73072 (Liu et al., 2016). This experiment sampled whole blood, during several days, mostly at 3 time points per twenty-four hours, for a larger number of individuals, using a microarray platform. Expression of all 7 genes in set GC-1 was visibly

circadian with highest expression at early day (S4 Table, sheet 1), as shown for DDIT4, which was the strongest example for circadian expression seen in plotting many genes from this dataset (Fig 6A, 6B). Inflammation in this experiment was indicated by upregulation of IL1B, and interferon inducible OASL (Fig 6A, 6B). Several signature 1 genes were visibly upregulated during inflammation in mild respiratory viral infection (S4 Table, sheet 1), as shown for known GC regulated genes NFIL3 and TNFAIP3 (Fig 6C), but not genes selected in set GC-1 (S4 Table, sheet 1), as shown for DDIT4 (Fig 6A, 6B). Genes in set GC-1 were used together as a robust module to visualize induction by circadian cortisol without inflammatory induction (Fig 6C, 6D, 6E). Circadian expression of set GC-1 continued during mild inflammation, but from a lower basal level, possibly related to shifts in cell percentages occurring during inflammation (Fig 6D, 6E). Fold downregulation of gene expression in set GC-1 during inflammation was highest for DDIT4, ZBTB16, and IRS2 (S4 Table, sheet 2). Some variability in mean and range of expression of DDIT4, and set GC-1 between healthy individuals was apparent, which may relate to longer lasting differences in cellular percentages, as a confounder, or to actual differences in GC induction. Intra-individual DDIT4 and set GC-1 expression levels sampled 24h apart were more similar (Fig 6D). In conclusion, gene set GC-1 was suitable for longitudinal monitoring of GC activity in whole blood, and was not induced by systemic mild inflammation caused by uncomplicated respiratory viral infection.

PART 3 (gene induction by GC in severe inflammation)

Comparing mild inflammation and severe inflammation

GC inducible gene expression was upregulated during severe inflammation, but not during mild inflammation, as shown in case of set GC-1 in experimental respiratory viral infection (Fig 6, S4 Table, sheet 1,2). For a better view of GC signature gene expression in severe inflammation, it was important to first differentiate gene expression in mild and severe inflammation more generally. Mild inflammation occurring in numerous samples, in datasets from the collection excluding severe inflammation (n= 62), allowed a basic description of relevant marker gene expression in inflammation, using correlation analysis (S4 Table, sheet 2). Correlation results agreed well with differential gene expression during mild

inflammation in experimental, and prospective respiratory viral infection, used for comparison (Liu et al., 2016; Zhai et al., 2015). (S4 Table, sheet 2). Most obvious was transcriptional induction involving interferon (eg GBP5 by IFN gamma, and MX1 by IFN alpha). Upregulation during inflammation, not involving interferon, included marker gene IL1B, and, for example, GK in neutrophils (S4 Table, sheet 2). Large differences existed in gene expression correlation for myeloid cells between the collection excluding severe inflammation, and a second dataset collection on severe inflammation, assembled according to experimental description (n = 38) (S4 Table, sheet 4, Fig 7A, 7B). Ordering genes according to hierarchical clustering of gene expression in single datasets on mild respiratory viral infection (Zhai et al., 2015), and sepsis (Burnham et al., 2017) (Fig 7C, 7D) showed the presence of matching gene groups in meta analysis (Fig 7A, 7B). Genes expressed in neutrophil bands clustered together in the absence of severe inflammation, whereas separate clusters for myelocytes (pro-neutrophils), and metamyelocytes (pre-neutrophils) existed in severe inflammation, as also reported in case of severe Covid-19 (Reusch et al., 2021; Schulte-Schrepping et al., 2020) (Fig 7C, 7D). The appearance of immature neutrophils in severe, but not in mild inflammation, was also indicated by corresponding differential gene expression analysis (Fig 7E, 7F). Other genes that were highly upregulated in severe inflammation, but not in mild inflammation, included GC signature 2 genes OLAH (upregulated mainly in neutrophils), and VSIG4 (upregulated mainly in monocytes), as well as genes not regulated by GCs such as FAM20A (Fig 7E, 7F, S4 Table, sheet 4). Inductions involving interferon were also visible in severe inflammation, in sepsis, but from a relatively lower basal expression level, possibly due to large shifts in global gene expression (Fig 7E, 7F).

Selection of gene set GC-2 from GC signature 2

To select suitable genes from GC signature 2, for use as biomarkers of GC action in blood in severe inflammation, a similar approach was taken, as in case of selecting set GC-1 from GC signature 1. Average gene expression correlation profiles for all GC signature 2, and relevant marker genes were obtained using the blood dataset collection on severe inflammation (n = 38) (S4 Table, sheet 3,4). Signature 2 genes with higher ranking correlation to induction by GC (n = 41), were tested each for reciprocal correlation ranking, with relevant marker genes, such as those indicating severe inflammation, included (Fig 8). Selected GC signature 2

genes could largely be grouped according to their relative expression in neutrophils and monocytes. Several GC signature 2 genes that were predominantly expressed in neutrophils (eg IL1R2) also grouped with marker genes for severe inflammation, more generally (eg GYG1), and were therefore not used in the biomarker gene set (Fig 8). Required high fold upregulation of gene expression in blood, separated monoctes, and separated neutrophils, between sepsis and healthy control samples, was examined for candidate biomarker genes (S4 Table, sheet 3), also using RNA seq experiment gse60424 on separated blood cells from different diseases (Linsley et al., 2014). Differential expression of GC signature 2 genes between monocytes and neutrophils in sepsis, agreed well with corresponding groups of gene expression correlation seen in severe inflammation (S4 Table, sheet3, Fig 8). Selected gene set GC-2 (MACIR/C5orf30, ADORA3, DAAM2, OLAH, ADAMTS2, FLT3, VSIG4, AMPH, MAOA) contained genes expressed in both monocytes and neutrophils to minimize the potential effect of cell type when using the set as a biomarker in blood. The set contained 6 genes that were also used from the start, as query genes to obtain GC signature 2 (Fig 3). Genes in set GC-2 were all reported as DEGs in blood in GC treatment of pediatric septic shock by Wong (2014), and were among the highest ranking DEGs in blood in GC treatment of severe inflammation as seen in datasets gse106878 (Kolte, 2020) and gse77791 (Plassais et al., 2017) (see below).

Monocytes and neutrophils in severe inflammation in blood transcriptomic data

Analysis of gene expression correlation using the collection of blood datasets on severe inflammation, in combination with corresponding gene differential expression data, established a robust framework for a description of severe inflammation (S4 Table, sheet 4). Different cell types, gene inductions, and cellular processes were recognizable using marker genes with a focus on myeloid cells. A cluster of genes, including marker gene HLA-DRA, expressed in antigen presentation by monocytes, dendritic cells, and B cells, was downregulated in blood in severe inflammation, but not during mild inflammation in respiratory viral infection (S4 Table, sheet 4). A large cluster of co-expressed genes, including GYG1, was highly upregulated in neutrophils during severe inflammation, and also upregulated in monocytes to a lower extent, and was named severe inflammatory myeloid (SIM) for simplicity. Expression of SIM genes was in strong negative correlation to genes expressed in T cells, consistent with opposite shifts in neutrophil and T cell percentages

occurring during severe inflammation (S4 Table, sheet 4). Many SIM genes were not, or less upregulated during mild inflammation caused by respiratory viral infection (S4 Table, sheet 4). A discernible, small (n = 4) subcluster of co-expressed, highly upregulated genes, in severe inflammation included FAM20A (S4 Table, sheet 4). A gene BLOC1S1, "close" to this correlation cluster, and genes ITGA7 and METTL7B in the small cluster are 3 neighbouring genes on chromosome 12, which might suggest coordinated regulation of gene expression. An informative selection of genes, predominantly expressed in either monocytes, or neutrophils during severe inflammation was examined separately in meta correlation analysis, and in corresponding correlation clustering and differential expression analysis using a single RNAseq dataset on whole blood from sepsis and bacterial infection (Herwanto et al., 2021) (Fig 9). Genes used in meta analysis were ordered according to hierarchical clustering of the same genes in the single RNAseq dataset. Two clusters corresponding to intermediate / non-classical / MS3 (including C1QA), and classical / MS1 monocytes (including VCAN and CCR2) were visible in whole blood, with monocyte states MS1 and MS3 as defined by Reyes et al. (2020) (Fig 9A, 9C). C1Q genes expression in severe inflammation was strongly associated with VSIG4, and not strongly associated with induction by interferon (Fig 9A), in stark contrast to expression of C1Q genes in the absence of severe inflammation (Fig 7A). C1Q expression in blood in severe inflammation also correlated with MERTK and PPARG expression. Gene PPARG, which is associated with monocyte/macrophage alternative activation (Bouhlel et al., 2007), ranked relatively high in expression correlation profiles of MARCO (encoding a macrophage scavenger receptor), HMOX1, MAFB, and GC inducible genes VSIG4 and ADAMTS2 (Fig 9A). Expression of C1QA was upregulated in severe inflammation, while expression of CDKN1C, a marker gene for non-classical monocytes, was downregulated instead (Fig 9E). Two clusters corresponding to immature neutrophils were again visible, with myelocytes expressing AZU1 and MPO, encoding azurophil granule proteins, key transcription factors CEBPE, MYB and ERG, and genes in proliferation, and secondly, inflammatory metamyelocytes expressing MMP8, HP, and RETN . GC signature 2 genes IL1R2, IL18R1, and ARG1, could be grouped together with OLAH, DAAM2 and TPST1 (Fig 9B), while hierarchical clustering using a single dataset broke this connection (Fig 9D). In contrast to many genes shown to be upregulated in severe inflammation, expressed mainly in neutrophils (eg GYG1 in SIM cluster), gene MME encoding CD10 was downregulated in whole blood (Fig 9F).

Gene expression in separated monocytes and neutrophils in severe inflammation

Next, gene expresssion was examined in separated monocytes and neutrophils using 2 smaller dataset collections of monocytes / PBMCs (n = 7), and of neutrophils / granulocytes (n = 6) in severe inflammation (S9 Table, sheet 10). Genes tested included many genes relevant to inflammation, selected genes from GC signatures 1 and 2, as well as novel candidate genes of GC induction, which were found in additional gene expression correlation profiles obtained using either dataset collection (see below). Tested genes were grouped based on expression correlation characteristics, using a panel of different marker genes and gene sets. Results were compared to differential gene expression in severe inflammation, either in separated monocytes (Washburn et al., 2019), or in granulocytes (Coulibaly et al., 2019), and to *in vitro* induction by GC treatment in the corresponding cell type (Franco et al., 2019). Observed gene groups in monocytes and neutrophils also included immediate early gene expression (eg with marker gene FOSB), likely due to *in vitro* activation, and contaminating neutrophils in monocytes / PBMC separations (eg using marker gene CD177) (S9 Table, sheet 2,4). A group of genes including HLA-DRA was downregulated in separated "sepsis" monocytes. A group of genes including C1Qs, was highly upregulated in separated "sepsis" monocytes, while gene CDKN1C was in a different group, with genes expressed in non-classical monocytes, and was downregulated. A group of genes including FAM20A was visible, and was highly upregulated compared to control monocytes. Gene sets GC-1 and GC-2 were used to mark expression correlation with GC induction in monocytes, and showed 2 overlapping groups of genes, which were generally upregulated in sepsis, in monocytes, and inducible *in vitro* by GC in monocytes (S9 Table, sheet 2). Using the collection of datasets on separated neutrophils, 2 groups of gene expression corresponding with myelocytes, and inflammatory meta-myelocytes were visible (S9 Table, sheet 4), similar to the presence of immature neutrophils detected in blood in severe inflammation (S4 Table, sheet 4). A large cluster of co-expressed genes, including GYG1, was highly upregulated in separated neutrophils during severe inflammation, and was similar to the SIM (severe inflammatory myeloid) gene group seen in blood. A group of genes including FAM20A was highly upregulated in severe inflammation, and overlapped with the corresponding FAM20A gene group in monocytes. Many genes were downregulated together with MME, encoding CD10, which is a marker for old/mature neutrophils, either due to shifts in neutrophil cell type

composition, or to shifts in overall gene expression in the same cells that upregulated GYG1. Using marker gene TSC22D3, and 2 different marker gene sets to indicate GC induction, many tested gene expression correlation profiles were positive, and present in gene groups loosely corresponding with different levels of upregulation in neutrophils in severe inflammation (S9 Table, sheet 4). Hierarchical cluster analysis of gene expresssion using representative datasets on monocytes in sepsis (gse133822, (Washburn et al., 2019)), and granulocytes in sepsis and SIRS (gse123729, (Coulibaly et al., 2019)) showed the presence of genes upregulated more exclusively in severe inflammation, and, on the other hand, genes frequently induced in severe inflammation, and generally during mild inflammation (S2 Figure). Clustering in these datasets was also directly compared to similar results from correlation meta analysis focusing on genes co-expressed with FAM20A, and genes induced by GC more specific to each cell type (Fig 10). Monocyte states MS1 (classical-monocyte -like) and MS3, as defined by Reyes et al. (2020), using single cell sequencing, and myelocyte (pro-neutrophil) and inflammatory metamyelocyte (pre-neutrophil) clusters were present in case of monocytes and granulocytes, respectively (Fig 10C, 10D). Gene groups and clusters of GC regulated expression were well visible in separated monocytes and neutrophils (Fig 10A, 10B, 10C, 10D). Genes in the FAM20A group, as visible in blood in severe inflammation (S4 Table, sheet 4), were found in similar groups, but with different additional genes in either monocytes or neutrophils (Fig 10A, 10B). HP (encoding haptoglobin, an acute phase protein), and RETN grouped with FAM20A in monocytes, but in neutrophils, with genes expressed in metamyelocytes (pre-neutrophils) instead (Fig 10C, 10D). Single cell expression data of monocytes in sepsis (Reyes et al., 2020), and of neutrophils in severe Covid-19 (Schulte-Schrepping et al., 2020) could not be used systematically to associate all GC induced expression with different cellular subtypes, due to low signals for many important genes. Exceptions were IL1R2 and CD163, as markers for monocyte state MS1, and C1Q genes for MS3 (IL1R2, (Reyes et al., 2020); other genes, https://singlecell.broadinstitute.org/single_cell/study/SCP548)).

To extend the number of candidate GC regulated genes found in GC signature 2, we also obtained GC driven correlation profiles using the dataset collections of separated monocytes and neutrophils in severe inflammation (S10 Table, sheet 8,9). These profiles were in good agreement with GC signature 2, and contained additional high ranking genes, some of which

were inducible *in vitro* by GC in immune cells, eg FMN1 in monocytes (S10 Table, sheet 11). A comparison of induction profiles by GC in health, and during severe inflammation, in monocytes and neutrophils, predicted wide ranging effects of GCs on cell biology, based on gene functional categories, such as modulation of secretory pathway activity, increased sphingolipid synhesis during severe inflammation, and uptake of apoptotic cells (efferocytosis) by monocytes during severe inflammation (Fig 11).

For completion, gene expression in the absence of severe inflammation was also examined, using suitable dataset collections on separated monocytes (gse56045 + 4 subsets thereof, (Reynolds et al., 2014)), and neutrophils (n = 5) (S9 Table, sheet 10). Immediate early gene expression, likely due to *in vitro* activation, was again clearly visible for both monocytes and neutrophils (S9 Table, sheet 1,3). To some extent, this interfered with a description of *in vivo* gene expression during inflammation, especially for genes that were not (also) induced by interferon. In case of neutrophils, a gene group including GK and ACSL1 was associated with inflammation (S9 Table, sheet 3), and this was supported by gene expression correlation analysis of datasets on blood in the absence of severe inflammation, where a similar gene group mainly originated from inflammatory neutrophils (S4 Table, sheet 2). Inductions involving interferon were well visible in monocytes (eg C1Q genes) and neutrophils, as well as inductions by GC in homeostasis (S9 Table, sheet 1,3). Overall results based on combined gene expression analysis are summarized, showing the presence of different cell types and inductions in homeostasis, inflammation, and in severe inflammation (Fig 12).

Upregulation of GC signature genes by GC treatment in septic shock and burn shock

Direct transcriptomic comparisons between healthy and severe inflammation show abundant DEGs in blood, only a few of which will be due to direct induction by glucocorticoids. Datasets on the effects of exogenous GCs on blood cell gene transcription in severe inflammation are available for septic shock, and burn shock (Kolte, 2020; Plassais et al., 2017; Wong et al., 2014). While modulation of gene expression by GC treatment in septic shock and burn shock was reported (Plassais et al., 2017; Wong et al., 2014), GC activated genes were not identified beyond those present in known gene networks and signaling pathways (Plassais et al., 2017). GC signature 2 genes, as reported here, were among the highest DEGs present in hydrocortisone treated burn shock patients and septic shock patients (gse77791 (Plassais et al., 2017); gse106878 (Kolte, 2020)), and also in the 319

DEGs in GC treatment of pediatric septic shock reported by Wong et al. (2014) (S11 Table, sheet 2,3,4). Upregulated DEGs in these 3 datasets largely overlapped, were frequently upregulated in immune cells by GC treatment *in vitro* (gse112101, (Franco et al., 2019)), and also ranked highly in GC driven gene expression correlation profiles obtained for blood, monocyte, and neutrophils in severe inflammation (S11 Table, sheet 5). Several DEGs, absent from GC signatures 1 and 2, were supported by GC driven correlation profiles such as MFGE8 (efferocytosis marker), induced by GCs in monocytes (Lauber et al., 2013) (S11 Table, sheet 5). A selection of GC signatures genes, including GC-1 and GC-2 sets, and relevant marker genes was used in differential expression analysis for datasets on GC treatment of septic shock and burn shock, and for datasets on sepsis/SIRS (gse66099 (Sweeney et al., 2015)), and sepsis (gse65682 (Scicluna et al., 2015)), comparing healthy controls and patients (Fig 13). Large shifts in cell percentages, with lymphoid cells decreased, and an altered metabolic state, indicated by increased expression of GK, GYG1, HK3 and LDHA, were visible when comparing severely ill and healthy individuals in case of burn shock, sepsis/SIRS or sepsis (Fig. 13D, 13E, 13F). In contrast, GC treatment of septic shock patients resulted in induction of set GC-1 and GC-2 genes, more exclusively, over 24h compared to placebo (MACIR / c5orf30 in set GC-2 absent, and OLAH in set GC-2 present as alias THEDC1, in dataset gse106878 (Kolte, 2020)), (S11 Table, sheet 2), while gene markers for severe inflammation, more generally, were down regulated in both GC and placebo treated patients after 24h (LDHA, HK3, GPR84, MMP8). An increase related to 24h time difference was visible both in GC and placebo treated patients for genes AZU1 (neutrophil bands/myelocytes), and MME (mature/old neutrophils CD10), (Fig. 13A, 13B). In severe burn shock, hydrocortisone treatment of severely ill patients resulted in a relatively small shift in cell percentages and metabolic state of myeloid cells, as indicated by the absence of GK, GYG1, HK3 and LDHA upregulation (Fig. 13C), likely because GC did not strongly influence the percentages of severe inflammatory myeloid cells which are present in the patients receiving the treatment. Consequently, a specific transcriptomic effect of hydrocortisone on severe inflammatory neutrophils and monocytes can be clearly seen by upregulation of genes in sets GC-2 and GC-1, except for CXCR4, but not simply in the DEGs comparing ill and healthy patients from the same experiment, which showed upregulation of gene markers in severe inflammation, more generally (Fig. 13C).

Using set GC-2 as biomarker for GC action in blood cells during severe inflammation

To get a better overview of GC regulated gene expression in systemic inflammation, the presence of GC signature 2, and associated differential gene expression was determined for many different illnesses, starting with longitudinal data on severe injury. Set GC-2 was used as a transcriptomic biomarker in whole blood using a measure of combined gene expression in the set. For a more complete description of systemic inflammation, several additional gene modules, and gene sets were also included. Module T cell (n = 13, with bias for naive T cell), was used to follow decreased percentages of T cells during severe inflammation. A SIM gene set (n = 16) was selected from the large corresponding expression cluster, as highly upregulated genes especially in neutrophils in severe inflammation. Module FAM20A consisted of genes co-induced specifically in severe inflammation, unrelated to GC induction (n = 4). Inducible gene modules interferon gamma (n = 23), and interferon alpha (n = 8), which were frequently upregulated in mild and in severe inflammation, were also used. Whole blood transcriptomic datasets from Affymetrix, Illumina, or RNA seq platforms, were compared per platform for gene module expression, using adequate identical gene probes in case of Affymetrix and Illumina platforms (S12 Table), as confirmed by expression correlation clustering in representative datasets (S3 Figure). Gene module / set expression values were calculated adjusting for the expression range of single genes, and also for background / basal expression levels for single genes in case of microarray platforms (see methods).

In case of severe injury, but not in case of sepsis, longitudinal data provide a precise time point for the start of severe inflammation. Several public datasets are available on gene expression in whole blood after severe injury, which differ in number of samples and range of sampling time points. The dataset on a genomic storm occurring after critical injury (Xiao et al., 2011) was good to visualize gene (module) expression in comparison to marker gene expression in immature neutrophils (Fig 14). Neutrophil bands appeared in circulation immediately after injury, while later immature neutrophils likely corresponded with myelocytes and metamyelocytes originating from emergency granulopoiesis. Induction by GC of genes in set GC-2 was frequently visible before, and after appearance of cells from emergency granulopoiesis, both in monocytes (eg VSIG4, ADAMTS2), and in neutrophils (eg OLAH, DAAM2). VSIG4 expression peaked earlier than ADAMTS2, suggesting a different course for monocyte subtypes after injury. Upregulation of SIM set genes occurred

immediately after injury, closely followed by upregulation of the FAM20A set, while relative expression of module T cells in blood was decreased instead. Relative expression of T cell module and SIM set was still different from healthy controls at week 4, indicating continued systemic severe inflammation. Combined expression of genes in set GC-2 was increased in most patient blood samples, expression of gene module interferon gamma was relatively unchanged, while expression of module interferon alpha was decreased (Fig 14). Next, whole blood transcriptomic data covering many different diseases, and preferably including healthy controls, were examined by plotting gene set expression value distributions for patient groups. Gene module / set expression value distributions were skewed and often with many outliers in case of the inducible modules (Fig. 15). Increased expression of GC-1 and GC-2 sets was visible upon systemic GC treatment in healthy people, in burn shock, and septic shock, in GC treated SLE (Fig. 15), and in additional examples, upon systemic GC treatment in SLE and rheumatoid arthritis, and also upon GC treatment in asthma exacerbation (S7 Figure). Set GC-1 had relatively strong expression in GC treated healthy people (Fig. 15A), while GC-2 was relatively strong in GC treated patients with burn shock or septic shock (Fig. 15B, 15C). These results demonstrated that set GC-1, but not set GC-2 could be used as a biomarker in the absence of severe inflammation, and secondly, that in case of severe inflammation, set GC-2 was a stronger biomarker of GC action in whole blood than set GC-1. Increases in GC-1 and GC-2 expression in RA and SLE patients upon treatment with GCs, and a strong increase in set GC-1 expression upon treatment of healthy people agreed with results by Hu et al. (2018), who used an 8 gene molecular signature to monitor GC responses. SIM gene set and module FAM20A expression was highly upregulated in burn shock and septic shock, but relatively unchanged by GC treatment (Fig. 15B, 15C). Interferon alpha and gamma modules were upregulated in SLE as expected, while a marked decrease was visible in case of burn shock, possibly related to more general shifts in gene expression in myeloid cells (Fig. 15D, 15B). Both the SIM and FAM20A signature and associated differential expression was present in datasets on sepsis, septic shock, trauma, burn shock, and SIRS, and the signatures were also found in additional illnesses by correlation detection (including Kawasaki disease, IBD, childrens malaria, severe COVID-19, SJIA, lung cancer), with strength of differential expression and frequency of cases depending on illness (Fig 16 , S4 Figure, S5 Figure, S6 Figure, S7 Figure). The expression of FAM20A module in PBMCs from COVID-19 patients remained relatively high compared to the SIM set, consistent with a

strong bias in the SIM set for genes more upregulated in neutrophils than in monocytes in severe inflammation (Fig 16, S7 Figure F). GC signature 2 and corresponding differential expression was also detected in a large number of additional inflammatory diseases, also including Kawasaki disease, IBD, severe COVID-19, childrens malaria, SJIA, and lung cancer (S4 Figure, S5 Figure, S6 Figure, S7 Figure), as summarized (Fig 16). At least, in case of data on Kawasaki disease (Wright et al., 2018), septic shock (Kolte, 2020), and burn shock ((Plassais et al., 2017), the absence of GC use in several shown patient groups is explicitly mentioned, indicating an origin of GC signature 2 in induction also by endogenous cortisol (Fig 16). Upregulation of set GC-2 genes in SLE, RA, sarcoidosis, asthma, and possibly also in IBD, SJIA and TB, might primarily be due to the frequent use of systemic GCs in treatment of inflammation, while upregulation in other illnesses might be due to high levels of endogenous cortisol present in severe inflammation, also in COVID-19 (Tan et al., 2020), in the acute phase of Kawasaki disease (Sano et al., 2010), and in children's malaria (Enwonwu et al., 1999). In conclusion, additional illnesses besides sepsis and severe injury showed both cases of severe inflammation, and frequent upregulation of the GC-2 set genes, due to GC treatment or endogenous cortisol depending on illness.

Discussion

Aim of study and short summary of results

In this study, we aimed to develop gene expression biomarkers for GC action on blood cells. We obtained gene signatures of GC induction by using correlated expression with several well known GC target genes, used as queries, in meta analysis of a large collection of public blood transcriptomic datasets. Different signatures were found depending on the absence or presence of severe inflammation, as in case of sepsis and critical injury. These 2 signatures, which both showed good overlap with GC upregulated genes in immune cells *in vitro*, originated from *in vivo* expression, thereby providing an alternative starting point for selecting biomarker genes. GC signature 1 mainly originated from circadian gene induction by GC in different blood cells. From this signature, we selected a set of genes (GC-1) as best biomarkers for GC action, for use on whole blood in the absence of severe inflammation. Set GC-1 could be used efficiently, to detect induction by endogenous cortisol, and by GC

treatment, and was not upregulated during mild inflammation. Using meta analysis, we also provide an overview of gene expression, in homeostasis, inflammation, and severe inflammation in circulating monocytes and neutrophils, more generally. GC signature 2 originated from alternatively activated monocytes and neutrophils in severe inflammation, and upregulation of key signature genes was visible in whole blood, upon GC treatment in burn shock, and septic shock. We demonstrate that expression of a selected set of GC signature 2 genes (GC-2) was well suited to detect gene induction in blood upon systemic GC treatment in SLE, RA, asthma, in septic shock, and in burn shock. GC signature 2 was found in many more different inflammatory illnesses, including Kawasaki disease, severe malaria, severe COVID-19, and lung cancer, resulting from both exogenous and endogenous GC. Use of set GC-2 indicated different frequencies and strength of induction in patients depending on illness.

Meta analysis of gene expression correlation is a useful method

Differential gene expression in blood cells upon *in vivo* GC or ACTH treatment has been widely studied in humans and animals. The change in blood cell percentages caused by these treatments enormously complicates the interpretation of the transcriptomic data. Potential GC regulated DEGs in these experiments were mostly identified from existing literature, and by comparing with *in vitro* induction results, for example in PBMCs or isolated immune cells (Franco et al., 2019; Hu et al., 2018). More exceptionally, a set of co-expressed, GC induced genes in blood of ACTH injected pigs was directly identified by cluster analysis using a single experiment (Sautron et al., 2015). We noticed induction signals originating from circadian and stress related changes in endogenous cortisol, and sometimes also from GC usage, in gene expression correlation profiles in many blood transcriptomic datasets, which provided a useful starting point for finding candidate GC regulated genes. It indicated that a search would not necessarily be limited to GC administration experiments or studies with documented GC usage, and that Pearson's correlation might be used in meta analysis to obtain robust gene expression correlation profiles. In case of the initial GC signatures, datasets were selected from a total number of 375+ blood transcriptomic datasets, based on the quality of correlation hits. Subsequent gene expression correlation profiles were obtained in meta-analysis using several datasets collections based on experimental description. Gene expression correlation profiles for different GC regulated query genes

were combined to best show induction by GC. The recovery of known GR target genes in GC signatures, and in additional gene expresion correlation profiles, many recurrent candidate genes, and the large overlap with GC upregulated DEGs in blood cells in different *in vitro* and *in vivo* experiments showed that the approach was generally very effective. A general advantage of using correlation is its independence from gene expression range and basal expression levels, or background signals often present in microarray data, allowing easier detection of GC regulated genes at low fold induction. A difficulty with correlation analysis was that GC regulated DEGs may drop down in gene expression correlation profiles due to overriding alternative correlations, and thus escape detection. Meta-analysis, in case of separated immune cells, was limited here to some extent, by the smaller number of available data (sub) sets, and by *in vitro* activation, and the presence of confounding contaminating cells.

GC signatures and molecular clock

GC signature 1 originated mainly from circadian GC in different blood cells, while GC signature 2 originated from alternatively activated monocytes and neutrophils in severe inflammation. However, GC signature 1 and 2 genes were not simply expressed in either homeostasis or severe inflammation, as evident from gene expression correlation profiles obtained for separated immune cells, and from *in vivo* differential expression upon GC treatment. Instead, the difference between signatures was related to both quantitative and qualitative changes in gene induction by GC in homeostasis compared to severe inflammation, and to the specific cell types appearing in severe inflammation. Genes induced by GC in monocytes and neutrophils in homeostasis, with the exception of CXCR4, were mostly induced as well in severe inflammation, while additional genes were induced in severe inflammation (eg ADAMTS2 and VSIG4 in monocytes). A question was whether gene regulation by the local molecular clock in blood cells might have contributed to GC signature 1, since both circadian GC production and the molecular clock can drive circadian gene expression in similar phase. Molecular clock and clock associated genes in skin transcriptomics data are present in 2 strongly negatively correlated and tight co-expression clusters, that include the E box and RORE target genes, respectively (Wu et al., 2018). These tight clusters are absent in data from whole blood, T cells, and monocytes, showing that the clock oscillator is much weaker in blood cells (Wu et al., 2018). In agreement, we found

similar strong co-expression clusters in skin, and also in fat and muscle tissue, but not in blood or separated blood cells, using correlation profiling in meta analysis of corresponding transcriptomic datasets. This indicated that signature 1 was primarily GC driven and that expression of strong GC target genes in blood cells, will show direct induction by GCs. Several methods exist to predict the circadian phase from transcriptomic measurements of whole blood (Braun et al., 2018; Hughey, 2017; Laing et al., 2017), and monocytes (Wittenbrink et al., 2018). A glucocorticoid driven network links many of the top ranked biomarker genes for circadian phase in whole blood, indicating gene induction by circadian GC either via local circadian clocks or directly (Laing et al., 2017). In agreement, among the circadian expressed, best time telling genes in these studies were many genes present here in GC signatures 1 and 2 (9/15 (Hughey, 2017); eg 13/76 (Laing et al., 2017); 3/40 (Braun et al., 2018); eg 10/34 (Wittenbrink et al., 2018)).

Tissue and cell type specific induction by GC

Recently, it has been argued that a better understanding of cell type and tissue specific effects of GCs, would be important for adjusting or developing new therapies (Quatrini & Ugolini, 2021) . Highly cell type specific gene induction upon *in vitro* GC treatment was reported in isolated immune cells and in proliferating non immune cell cultures, and the global effects of GC in different cells were compared at the molecular pathway level (Franco et al., 2019). Here, we traced *in vivo* effects of endogenous GC on the transcriptome of different lymphocytes, monocytes, neutrophils, muscle, skin, and fat, by using expression correlation with GC induced query genes in meta-analysis. The combination of GO terms (S7 Table), and upregulated genes suggested that a general state of cellular stress (Pakos-Zebrucka et al., 2016; Vihervaara et al., 2018), including unfolded protein response (UPR), might be associated with GC effects, which would be interesting to explore further. The varied effects of GC on the transcriptomes, often left open interpretation for effects of GCs on cell biology. The presence in 4 lymphocyte profiles of PTGER4, encoding the EP4 receptor for immunosuppressive prostaglandin E2 (PGE2), and a target in cancer immunotherapy (Kalinski, 2012; Take et al., 2020), suggested a role for GC in increasing PGE2 sensitivity in immunosuppression. Finding VSIR, encoding VISTA, as a novel GC regulated gene in neutrophils added to the importance given recently to VISTA as a possible therapeutic target in managing cytokine storms (ElTanbouly et al., 2021).

Modules, homeostasis, and mild inflammation

Variable gene expression in blood represents a rich source for drafting gene modules based on gene expression correlation characteristics (Altman et al., 2021; Chaussabel & Baldwin, 2014; Chaussabel et al., 2008). For developing more precise gene modules, it is important to also take into account differential co-expression between health or disease conditions (van Dam et al., 2018). A commonly used module repertoire for blood has recently been updated, but does not use differential co-expression to also incorporate conditional modules (Altman et al., 2021). Although generally useful, it contains no modules functionally annotated for induction by glucocorticoid, and no module corresponding to the 20 "core" GC signature 1 genes. A 29 gene module M16.70 contained 14 genes present in GC signatures, especially in GC signature 2, but without ADAMTS2 or VSIG4, for example. We used marker genes and "single use" gene transcriptional modules from meta-analysis, to study gene expression correlation in blood, monocytes, and neutrophils, in the absence of severe inflammation, to describe homeostasis and mild inflammation. Mild inflammation as seen in uncomplicated respiratory viral infection was especially marked by induction by interferon and upregulation of IL1B as expected. The upregulation of GK, encoding glycerol kinase, expressed in correlation with ACSL1 and AQP9, mainly in neutrophils in mild inflammation, might indicate increased triacylglycerol synthesis in support of lipid body biogenesis, which is important in the production of inflammatory mediators from arachidonic acid (Melo & Weller, 2016; Weller, 2016). Upregulated expression of CDKN1C and C1QA/B/C genes (Table S4) was consistent with increased frequencies of intermediate monocytes present in blood in mild respiratory viral infection (Vangeti et al., 2023). Our analysis showed several GC signature 1 genes that were upregulated during mild inflammation, even among "core" GC induced genes. This agreed with the notion that negative regulators of inflammation are frequently upregulated by GCs, sometimes through cooperation of GR and NF-kB (Gerber et al., 2021), and indicated that some of these same factors are also negative feedback regulators in inflammation, irrespective of GC induction. A selection of "core" GC induced genes, which were also high ranking DEGs in experiments of *in vivo* GC treatment, and in circadian sampling, and not induced during mild inflammation, was used as biomarker set GC-1 . Genes in this set GC-1 (PER1, TSC22D3, ZBTB16, KLF9, DDIT4, IRS2, CXCR4) have all been described as direct GR target genes, in different cell types (Guo et al., 2017; Hoffman et al.,

2021; Mostafa et al., 2021; Prekovic et al., 2021; Wang et al., 2019), as might be expected for GC inducible "core group" genes. Decreased expression in whole blood of several GC-1 genes during inflammation might either be due to confounding shifts in blood cell percentages, or to gene repression, for example by interferon as has been reported in case of TSC22D3 (Dankers et al., 2022). This could not be determined for lack of public data on separated cells in mild respiratory viral infection. Only in case of actual gene repression, would set GC-1 be useful to show decreased cortisol action on blood cells during inflammation.

Severe inflammation occurring in different illnesses

A very large quantitative and qualitative difference existed between blood gene expression during inflammation in mild respiratory viral infection, and in severe inflammation. Blood gene expression, specific to severe inflammation, is likely ultimately due to gene induction by systemic DAMPs and MAMPs, as in trauma and sepsis (Raymond et al., 2017; Relja & Land, 2020). Blood transcriptomics, including gene expression in monocytes and neutrophils, has been used to correlate gene expression with degrees of severity in COVID-19 (Wang et al., 2022). Immature neutrophils originating from emergency myelopoiesis are a heightened characteristic in severe COVID-19 (Aschenbrenner et al., 2021; Schulte-Schrepping et al., 2020). Based on their complete absence, we suggest that data on experimental, and prospective, seasonal respiratory viral infection, may represent a clean example of systemic mild inflammation, without a transition to severe inflammation as frequently occurring in COVID-19 patients.

A gene set (SIM, n= 16), selected from a much larger group of upregulated genes in severe inflammation in myeloid cells, contained LDHA, was less based on co-expression, and probably remained more heterogeneous with respect to gene regulation. Expression of LDHA, encoding lactate dehydrogenase, and lactic acid levels are increased in blood neutrophils in severe inflammation, more so in appendicitis than in sepsis, and are indicative for aerobic glycolysis (Pan et al., 2022). Within the very large SIM group, a small subcluster of genes co-expressed with FAM20A could be made out. FAM20A is one of only relatively few genes reported to be induced *in vitro* by single stimuli of IL10 and IL6 in macrophages (Gupta et al., 2018; Lurier et al., 2017). IL6 and IL10 lead to distinct cellular responses both acting through STAT3, which is an important transcription factor in inflammatory pathways in sepsis (Braun et al., 2013; Lei et al., 2021). Gene induction by IL6 of HP, encoding acute

phase protein haptoglobin, is also dependent on STAT3 (Kim & Baumann, 1997). Therefore, a strong correlated expression of FAM20A and HP, as seen in separated monocytes, suggested that induction of FAM20A would also be dependent on STAT3 *in vivo*, but the specific inducer(s) remained unknown.

Another group of upregulated genes in severe inflammation in myeloid cells were GC inducible genes, from which gene set GC-2 (MACIR/C5orf30, ADORA3, DAAM2, OLAH, ADAMTS2, FLT3, VSIG4, AMPH, MAOA) was selected. GC treatment in septic shock and burn shock induced many genes in GC signatures 1, and 2 above the expression level reached by endogenous GC. Previously, upregulated DEGs in GC treatment in septic shock were not discussed as potential GC target genes, possibly since IPA (Ingenuity Pathway Analysis) at the time showed down-regulation of glucocorticoid signaling pathways instead (Wong et al., 2014). A small number of well known GC target genes were reported as upregulated DEGs in GC treatment in burn shock (Plassais et al., 2017), but not identified within a larger cluster of co-expressed GC regulated genes. Differential expression related to GC treatment could be demonstrated in septic shock, burn shock, asthma, SLE and RA, using set GC-2 as a transcriptional biomarker, in agreement with expression of a GC gene signature developed to monitor cellular responses to GC treatment in case of SLE and RA (Hu et al., 2018). Upregulation of VSIG4 in correlation with GC usage in SLE (Northcott et al., 2021), and of ADAMTS2 in separated monocytes from giant cell arteritis patients treated with GC (Estupiñán-Moreno et al., 2022), also support the possible use of set GC-2 in these autoimmune diseases. Furthermore, upregulation of set GC-2 was frequent in GC untreated Kawasaki disease, severe malaria, severe COVID-19, and other illnesses, indicating induction by endogenous GC, and not just by exogenous GC in treatment. Serum cortisol and cortisol availability are increased in critical illness (Annane et al., 2017; Van den Berghe et al., 2022), and endogenous GC has been discussed as a possible factor in immunosuppression in sepsis (He et al., 2020; Vandewalle & Libert, 2020), although not commonly so (Hibbert et al., 2018; Liu et al., 2022; Ono et al., 2018; Torres et al., 2022; Venet & Monneret, 2018). On the other hand, myeloid cells have been widely implicated in immunosuppression in severe inflammation, in case of monocytes (Avendaño-Ortiz et al., 2018; Mengos et al., 2019; Shalova et al., 2015), neutrophils (Darcy et al., 2014; Demaret et al., 2015; Hesselink et al., 2019; Mortaz et al., 2018; Reusch et al., 2021; Silvestre-Roig et al., 2019; Sinha et al., 2022),

or both cell types (Reyes et al., 2021; Schrijver et al., 2019; Schulte-Schrepping et al., 2020; Uhel et al., 2017; Venet et al., 2021). In fact, low expression of HLA-DR is typical for monocytes in sepsis, and is an important biomarker for immunosuppression (Hibbert et al., 2018; Monneret & Venet, 2014; Torres et al., 2022). Low monocyte HLA-DR expression in septic shock, and after surgery was found to correlate with high serum cortisol in earlier reports, while treatment by GC *in vitro* downregulated HLA-DR (Kim et al., 2010; Tulzo et al., 2004). Here, we find a wide functional range of genes induced by GCs in circulating monocytes and neutrophils in severe inflammation. This likely pointed to an important role for endogenous GCs in immunosuppression in sepsis, via myeloid cells, which would be worthwhile to explore.

GC and cell biology of monocytes and neutrophils in severe inflammation

In vitro treatment of monocyte derived macrophages with interleukins IL4, IL10, and GC separately induce alternatively activated (M2) subtypes with roles in wound repair, tissue remodeling, and efferocytosis. M2 macrophage subtypes induced by IL10 (M2c-IL10) and GC (M2c-GC) are more similar to each other than the one induced by IL4 (M2a-IL4), while the *in vivo* existence of these exact subtypes in tissues remains difficult to determine (Abdelaziz et al., 2020; Roszer, 2015). GC action on monocytes and macrophages is immunosuppressive and also anti-inflammatory, promoting a cellular phenotype involved in resolving inflammation and in tissue repair (Desgeorges et al., 2019; Ehrchen et al., 2019). *In vitro* GC treatment of isolated monocytes triggers an extensive transcriptional program, directing monocyte to macrophage differentiation to a specific alternatively activated state with anti-inflammatory phenotype (Ehrchen et al., 2007; Ehrchen et al., 2019; Heideveld et al., 2018; Wang et al., 2019). Well known examples of genes upregulated by GC in monocytes *in vitro*, were present in GC signature 2 obtained from blood transcriptomic datasets on severe inflammation such as ADAMTS2, CD163, and C1QA/B/C, as well as key marker genes of alternative activation like PPARG (Bouhlel et al., 2007), and MERTK, which were co-expressed and upregulated along with additional marker gene IL10 for M2c activation (Abdelaziz et al., 2020; Roszer, 2015). Functionally, many GC signature 2 genes expressed in monocytes, also indicated an efferocytosis and tissue repair phenotype. Notable with respect to wound healing was induction by GC of genes ANG, RNASE1, and RNASE4, encoding angiogenic factors. In this way, the response of blood monocytes to GC in severe

inflammation resembled alternative activation by GCs *in vitro*. Different monocyte subpopulations (classical, intermediate, and non-classical) exist in health. Mammalian C1Q genes and CDKN1C are preferentially expressed by intermediate and non-classical monocytes compared to classical monocytes, and more so in non-classical monocytes (Talker et al., 2022; Wong et al., 2011). As determined by expression of surface markers CD14 and CD16, percentages of classical monocytes are unchanged, intermediate monocytes are increased, while non-classical monocytes are decreased in severe inflammation (Liepelt et al., 2020). Using single-cell RNA sequencing, 4 different monocyte states have been defined in sepsis including a population similar to non-classical monocytes named MS3, expressing high FCGR3A (CD16), and a CD14 +, HLA-DR low subpopulation named MS1. MS1 expresses IL1R2, is expanded in sepsis and COVID-19, and originates from altered myelopoiesis in bone marrow (Reyes et al., 2020; Reyes et al., 2021). Additional marker genes can be found for MS1 (eg CD163, RETN), and for MS3 (eg CDKN1C, C1Q genes) in the study by Reyes et al. (2020), https://singlecell.broadinstitute.org/single_cell/study/SCP548. Here, the existence of different gene expression clusters in monocytes in severe inflammation, with either C1Q genes (intermediate-like) or CDKN1C (non-classical-like), suggested some heterogeneity in MS3 cells. C1q is part of the C1 complex in classical complement activation, which results in cellular uptake of targeted immune complexes and pathogens. C1q also functions in efferocytosis and uptake of necrotic debris as described for macrophages (Galvan et al., 2014; Thielens et al., 2017; Westman et al., 2020). Induction of C1Q genes during mild inflammation involved interferon, but GC in severe inflammation instead. The C1q expressing intermediate-like monocyte in severe inflammation might be specialized more in uptake of apoptotic and/or necrotic cells than in uptake of immune complexes or antibody/complement opsonized pathogens.

Low density neutrophils (LDNs) containing immature (myelocytic) and mature granulocytes expand in sepsis (Mortaz et al., 2018; Uhel et al., 2017). In agreement, proliferating immature granulocytes in whole blood and in isolated neutrophils were indicated in transcriptomic datasets on sepsis by strong correlated upregulation of proliferation and azurophilic granule marker genes. Immature low density granulocytic cells more or less equate with immunosuppressive PMN-MDSCs (PMN myeloid derived suppressor cells) or neutrophil precursors, which appear in blood during sepsis and other inflammatory illnesses

including cancer and COVID19, often in high percentages, and which represent promising biomarkers (Reusch et al., 2021; Schrijver et al., 2019; Schulte-Schrepping et al., 2020). Responses of neutrophils to GCs are complex and not simply anti-inflammatory (Ronchetti et al., 2018). Several GC upregulated genes in neutrophils are known such as LTB4R encoding the leukotriene B4 receptor, and IL1R1 encoding the interleukin 1 receptor (Ronchetti et al., 2018), and were also found as neutrophil expressed genes in GC signature 2. The signature genes indicated important effects of GCs on inflammatory neutrophils during severe inflammation, for example modulation of IL1 and IL18 signaling (eg by upregulation of IL1 decoy receptor IL1R2 and IRAK3). Secretion of arginase 1, encoded by ARG1, has been implicated in immunosuppression by low density neutrophils in severe inflammation, and arginase derived from tumor infiltrating myeloid cells is an important factor in suppression of the cancer immune response (Grzywa et al., 2020; Mortaz et al., 2018). ARG1 was present as a neutrophil expressed gene in GC signature 2, clustered with GC induced genes in sepsis neutrophils, was highly upregulated in sepsis neutrophils, and was also upregulated by GC *in vitro* in neutrophils. Furthermore, ARG1 was upregulated in blood after GC treatment in septic shock and burn shock (S11 Table, sheets 2,3,4). As ARG1 is also upregulated in neutrophils by *in vivo* dexamethasone treatment of severe COVID-19 (Sinha et al., 2022), and ARG1 is a GC receptor targeted gene in liver (Okun et al., 2015), our results strongly suggest it might be a GC target gene in neutrophils as well. Neutrophils and monocytes in severe inflammation shared upregulation of many genes, including genes co-expressed with FAM20A, and many GC-regulated genes. Upregulation of CD163 and MERTK seen in gene expression datasets in severe inflammation agreed with flow cytometric data of both monocytes and neutrophils in sepsis (Groselj-Grenc et al., 2008; Guignant et al., 2013), and also indicated similar functional changes occurring in neutrophils and monocytes.

Transcriptional biomarkers

Blood gene transcriptional modules of co-expression can be used as a basis for biomarker discovery (Chaussabel & Baldwin, 2014; Chaussabel et al., 2008). Here, we selected 2 gene sets GC-1, and GC-2 for use as blood transcriptomic biomarkers for GC action on cells, based on expression correlation and differential expression analysis of many public datasets. Different sets of GC induced genes have recently been selected for monitoring the response of blood cells to GC treatment in SLE, RA and Addison's disease (Hu et al., 2018; Northcott et

al., 2021; Sævik et al., 2021). Set GC-1 might represent a set suitable for use on whole blood in the absence of severe inflammation, similar to a set of 3 genes (TSC22D3, DDIT4, and FKBP5) proposed for guiding GC replacement therapy in Addison's disease (Sævik et al., 2021). Set GC-1 genes are among the high ranking DEGs in PBMCs in GC therapy of Addison's disease reported in a separate study (Chantzichristos et al., 2021), supporting their potential use as biomarkers. In case of inflammatory illnesses, GC-1 set genes would become less suitable for straightforward use on whole blood or PBMCs due to changes in cell percentages, and large shifts in differential gene expression in specific cell types, especially neutrophils, which tend to obscure the existing induction signal. Hu and coworkers developed a set of 8 biomarker genes for GC activity (FKBP5, ECHDC3, IL1R2, ZBTB16, IRS2, IRAK3, ACSL1, DUSP1), based on differential expression seen upon GC treatment both in health and in SLE, which can be applied to whole blood using qPCR (Hu et al., 2018). An alternative set of 5 genes (VSIG4, ALOX15B, CD163, AMPH, IL1R2), based on expression correlation with GC usage in both PBMC and whole blood datasets on SLE, was also tested for biomarker potential (Northcott et al., 2021). These selections apparently originated from induction by GC, in neutrophils and monocytes, respectively. Here, set GC-2 combined several genes highly induced by GC in monocytes and neutrophils in severe inflammation, and was adequate for monitoring effects of GC usage in both autoimmune diseases, and in sepsis and burn shock. If required, the present data analysis would also allow a precise selection of GC biomarker genes expressed in either monocytes or predominantly in neutrophils. Upregulation of TSC22D3 (encoding GILZ) in blood, seen upon GC treatment in septic shock and burn shock (S11 Table, sheets 2,3,4), supports the idea of using GILZ as a possible monitoring molecule, for example, in the RECORDS trial on responsiveness to GC treatment in sepsis (Fleuriet et al., 2023; He et al., 2020). In case of using whole blood transcriptomic data, set GC-2 would provide a more robust alternative. Blood transcriptional markers, and recently serum IFN gamma and Il 10 ratio, have been developed to stratify sepsis patients for receiving GC treatment (König et al., 2021; Sweeney & Wong, 2021). Activity by endogenous GC before treatment, as detectable by set GC-2 expression, would likely also influence the outcomes of GC treatment. In general, it would be worthwhile to relate set GC-2 expression to other measurements and clinical data, such as possibly immunosuppression by endogenous GC in sepsis, as well as by exogenous GC in treatment. Relevant gene module / biomarker combinations have been used for patient stratification in

subclasses, for example in bacterial infection, severe RSV infection, and sepsis (Altman et al., 2021; Banchereau et al., 2012; Rinchai et al., 2020). In contrast, gene modules have not been applied in most other studies on stratification of sepsis in endotypes as reviewed (Komorowski et al., 2022; Tsakiroglou et al., 2023). A smart combination of biomarker features, closely corresponding to gene transcriptional modules, would allow a basic description of patient immunological status in different inflammatory illnesses. Gene induction by GC will likely be a relevant feature, as well as, for example, inductions by interferon alpha and gamma in a larger biomarker panel. In future, such panels might then be used for initial classification, and for immune status monitoring, building on more easily understandable features, than in case of existing sepsis endotypes.

conclusion

In conclusion, we present an overview of GC regulated gene expression in blood cells in relation to inflammation, using meta analysis of transcriptomic datasets. Besides known GC target genes in immune cells, we found several candidate genes, induced differently in lymphocytes, monocytes, and neutrophils. Adding to known GC targets, and comparing expression in different cells is important, since GC regulated genes and proteins are also potential therapeutic targets in GC treated diseases. Extensive transcriptomic analysis allowed an informed selection of biomarker genes for cellular action of GCs. Depending on the presence of severe inflammation, different gene expression signatures of induction by GC, were obtained. A core set of GC induced genes (GC-1) was suitable for use as a biomarker in whole blood, in the absence of severe inflammation, and showed circadian gene induction by GC. A second gene expression signature of induction by GC originated from alternatively activated monocytes and neutrophils seen in severe inflammation, and was present in many different diseases, strongly suggesting an important general role for GCs in immunosuppression occurring in these diseases. A set of genes selected from this signature (GC-2) was used to compare frequency and strength of induction in whole blood, which was highest in sepsis and trauma. We think that gene induction by GCs in circulating monocytes and neutrophils in severe inflammation, as described here, will be an important feature in multi-gene biomarker panels for inflammatory disease.

FIGURE LEGENDS

Figure 1

Different expression correlation clusters of cortisol induced genes in health and severe inflammation.

A, hierarchical clustering of a 20 gene expression correlation matrix from combined, related datasets gse11761 and gse14642 on PBMCs and exercise in healthy people (Radom-Aizik et al., 2009a, 2009b). Signal quality as indicated, with several probesets not (3) or barely (4) above background level. B, hierarchical clustering of a 20 gene expression correlation matrix from dataset gse9960 on PBMCs of critically ill and sepsis patients (Tang et al., 2009). Adjusted differential gene expression comparing to gse11761 and gse14642 as indicated. C, same from dataset gse57065 on whole blood of septic shock patients, subsetted for healthy controls (Cazalis et al., 2014). Signal quality as indicated with 6 probesets barely above background level. D, same from dataset gse57065 subsetted for septic shock patients. Differential gene expression in blood from septic shock patients and healthy controls as indicated. Cluster 1, genes clearly present in an expression correlation cluster in health. Cluster 2, genes not (clearly) present in cluster 1 in health, and present in an expression correlation cluster in severe inflammation. Cell type of main gene expression as indicated. All datasets are obtained from the same platform (GPL570, Affymetrix Human Genome U133 Plus 2.0 Array), with good and identical probesets used for the correlation matrices.

Figure 2

Obtaining cortisol driven gene signatures and comparison with *in vitro* DEGs

A, work diagram for obtaining cortisol gene signatures by blood transcriptomic analysis, illustrated for signature 2 (severe inflammation). A dataset collection “severe inflammation” included 38 datasets as selected by experimental description. Scrolls symbolize gene lists ordered by Pearson correlation values with query genes. Datasets (375 +) were ranked and selected for use, based on the number of cluster 2 gene hits present in the highest correlating 50-200 genes, for a given query gene. Results for individual cluster 2 query genes, most tight to cluster 2, were combined to obtain a final ordered gene list which was cut off

to obtain signature 2 genes for further analysis; B, Venn diagrams of combined cortisol signature 1 and 2 gene set with 8 DEG sets from GC induction of immune cells *in vitro*. PBMC (gse110156, 6h, 1 mM prednisolone (Hu et al., 2018)), macrophage (gse61880, time series 1-24h, 100 nM dexamethasone (Jubb et al., 2016)), macrophage b, monocyte (gse109439, 4h, 1 mM, triamcinolone acetonide (Wang et al., 2019)), monocyte b, neutrophil, CD4 T cell, and B cell (gse112101, 2h and 6h, 22.7 mM methylprednisolone (Franco et al., 2019)); C, frequency distribution of all GC induced DEG genes and cortisol signature 1 and 2 genes, as present in total of 8 DEG sets, overlap of DEGs and signature genes as indicated.

Figure 3

Cell type specific expression and *in vitro* induction of GC signature genes.

Summary of cell type specific expression and upregulation of signature query and example genes using RNAseq datasets on *in vitro* GC treatment. Query genes used to obtain gene expression correlation signatures 1 and 2, and genes present in signature 1, 2, or both as indicated. Genes that were selected in this study as biomarker sets GC-1 and GC-2, as indicated. Basal, relative gene expression in different immune cell controls as a ratio of total expression in the 4 cell types shown (B, B cell; T, CD4 T cell; M, monocyte; N, neutrophil) for experiment gse112101 (Franco et al., 2019), and as a ratio of total expression in monocytes (M) and macrophages (Mf) in experiment gse109439 (Wang et al., 2019), with table cells color coded blue. Induced, differential expression upon GC treatment for different cell types in experiments gse112101 (4 cell types, 22.7 mM methylprednisolone, 2h and 6h), and gse109439 (monocytes, macrophages,1 mM triamcinolone acetonide, 4h). DEG values are log2 fold change of induced and control expression levels, with table cells shaded red (up regulation) and green (down regulation), accordingly. NS, not significant ($p > 0.05$); NA, absent p value. Log2 fold change, and unadjusted p values used for experiment gse109439 according to Wang et al., (2019).Protein/function, protein names, function, and enzyme pathway products as indicated (SPM, Specialized Pro-resolving Mediators; LTB4, Leukotriene B4).

Figure 4

A core group of gene induction by GC, in blood, in the absence of severe inflammation.

Reciprocal ranking in gene expression correlation profiles (rows) obtained using a collection of 62 blood transcriptomic datasets excluding severe inflammation. Gene rankings as derived from minimally 25 contributing datasets, except for gene AREG (11 datasets), approximately 50-55 contributing datasets on average. Profile rankings color coded in green from 1 (high) to 400 (low). A selection of 31 genes from GC signature 1, and 25 relevant marker genes for cell type and inflammation as indicated. Genes selected as biomarker GC-1 set as indicated. Gene IL1B with NF-kB dependent induction (NF-kB), genes IL1RN and TNFAIP6, both with NF-kB dependent induction and induction by interferon (NF-kB + IFN), 2 interferon alpha (IFN alpha), and 2 interferon gamma (IFN gamma) inducible genes were used together as different markers for inflammation. Gene CIRBP (cold inducible RNA-binding protein) was added as a marker for circadian expression. A "core group" of GC inducible genes, with some subclustering related to differential expression in lymphoid cells or myeloid cells was visible. Several GC signature 1 genes showed correlated expression with inflammation markers. Collection of 62 blood datasets excluding severe inflammation as given (S4 Table, sheet5).

Figure 5

Molecular clock does not interfere with GC driven gene expression correlation profiles in blood and separated immune cells.

A, B, C) reciprocal ranking in gene expression correlation profiles (rows) for 12 relevant genes regulated by GCs or molecular clock, shown in same order in A (blood), B (control monocytes) and C (muscle). A) correlation profiles obtained using a collection of 62 blood datasets excluding severe inflammation. Gene rankings derived from minimally 25 contributing datasets, approximately 50-55 contributing datasets on average. B) correlation profiles obtained using a collection of 4 datasets on monocytes excluding severe inflammation, with rankings derived from minimally 3 contributing datasets, with 9 profile query genes being present in 4 datasets, and 3 genes (ZBTB16, KLF9, TEF) in 3 datasets. C) correlation profiles obtained using a collection of 11 datasets on muscle, with rankings derived from minimally 6 contributing datasets, with 11 profile query genes being present 11 times and query gene PER1 7 times. Shown are groups of genes corresponding with regulation by GC (GC), or regulation by CLOCK/BMAL1 heterocomplex (clock). D) selected genes in ranked gene expression correlation profiles (columns) obtained for different immune cells, combining different single gene expression correlation profiles (n = 3-10) in

each case as given (S6 Table). Genes present in GC signatures 1 and 2 as indicated. Profile rankings color coded in green from 1 (high) to 200 (low) in each panel. Dataset collections used in A (S4 Table, sheet 5), and B, C, and D (S6 Table, sheet 16) as given.

Figure 6

Expression of cortisol induced genes in time series of experimental respiratory viral infection

A, circadian expression for DDIT4 (gene inducible by cortisol), and upregulated expression during inflammation for IL1B (marker gene for NF-kB dependent induction), and OASL (marker gene inducible by interferon alpha) in 7 not responding, and 7 responding individuals infected with RSV in experiment gse73072 (Liu et al., 2016); B, same as A, in 7 not responding and 7 responding individuals infected with H1N1; C, circadian expression for biomarker gene set GC-1, and upregulated expression during inflammation for dually cortisol and interleukin inducible genes NFIL3, and TNFAIP3 in same H1N1 infected individuals shown in B; D, circadian expression for biomarker gene set GC-1, and DDIT4, and no upregulation of gene module interferon alpha in not responding individual to H1N1 infection; E, same as D with upregulation of gene module interferon alpha in responding individual during inflammation (time point 69h missing from data). For A, B, and C, scale in STDV units for each gene or module based on whole of gse73072, for D and E scale in log2 values (for use of gene set composite expression values see methods).

Figure 7

Large difference in gene expression in myeloid cells depending on severity of systemic inflammation

Comparing mild and severe inflammation using gene expression correlation (meta) analysis and DEGs in blood. A) reciprocal ranking in gene expression correlation profiles for 23 relevant genes in homeostasis and inflammation, obtained on a collection of 62 datasets excluding severe inflammation (S4 Table, sheet 5). Gene rankings derived from minimally 25 contributing datasets except for VSIG4 profile (minimally 20), approximately 50-55 contributing datasets on average. Rankings from 1 (high) to 1000 (low) color coded in green. Gene order presented in A corresponds to C. Different groups of genes as indicated, such as corresponding with neutrophil bands, and induction involving interferon. B) reciprocal ranking in gene expression correlation profiles for 23 relevant genes in severe inflammation

obtained on a collection of 38 datasets on severe inflammation (S4 Table, sheet 5). Gene rankings derived from minimally 20 contributing datasets, approximately 30-35 datasets on average. Rankings are color coded in green. Gene order in B corresponds to D. Different gene groups as indicated, such as induction involving interferon, induction by GC, myelocytes, and metamyelocytes. C) hierarchical clustering of gene expression correlation matrix for mild respiratory viral infection (gse68310, gpl10558 (Zhai et al., 2015)), using all samples. Module marker genes as derived from meta analysis. Clusters named according to the presence of marker genes. Highest level clusters named according to origin in homeostasis or inflammation (inflammatory type). D) hierarchical clustering of gene expression correlation matrix from sepsis (e-mtab-5273, gpl10558 (Burnham et al., 2017)), using all samples. Module marker genes as derived from meta analysis as shown, with clusters named according to the presence of marker genes. Highest level clusters named according to a more general occurrence in inflammation (mainly induction involving interferon), or to a more specific presence in severe inflammation (inflammatory type). E) distribution of DEGs in experiment gse68310 on prospective, seasonal respiratory viral infection, using samples ill (0 and 2 days) versus healthy (baseline and spring). F) distribution of DEGs in dataset e-mtab-5273 on sepsis using samples ill versus healthy. X-axis values on log-2 scale, with interval of 9 log 2 units for each panel, except for MMP8 with interval of 12 log 2 units. Shown are box plots with added binned dot plots.Identical gene probes from platform gpl10558 used in E and F.

Figure 8

Groups of gene induction by GC, in blood, in the presence of severe inflammation.

Reciprocal ranking in gene expression correlation profiles (rows) obtained using a collection of 38 blood transcriptomic datasets on severe inflammation. Gene rankings as derived from minimally 20 contributing datasets, except for genes CPM, SRGAP1, INSR, DNASE4, SIGLEC16, and MARVELD1 (15 datasets), approximately 30-35 contributing datasets on average. Profile rankings color coded in green from 1 (high) to 400 (low). A selection of 41 genes from GC signature 2, genes in set GC-1 , and 18 relevant marker genes for cell type and inflammation as indicated. Genes that were selected as biomarker GC-2 set as indicated. Gene IL1B (NF-kB), genes GK and NAMPT which are upregulated mainly in

neutrophils during inflammation, genes IL1RN and CASP1 (NF-kB + IFN), 2 interferon alpha (IFN alpha), and 2 interferon gamma (IFN gamma) inducible genes were used together as different markers for inflammation. Also included are marker genes mainly expressed in neutrophils during severe inflammation. Gene groups related to differential expression in monocytes or neutrophils were visible. Several GC signature 2 genes , mainly expressed in neutrophils, showed strong correlated expression with marker genes for severe inflammation. Collection of 38 blood datasets on severe inflammation as given (S4 Table, sheet 5).

Figure 9

Monocyte and neutrophil derived gene expression in severe inflammation in blood.

A and B) reciprocal ranking in gene expression correlation profiles for 23 genes, mostly expressed in either monocytes (A), or neutrophils (B), obtained on a collection of 38 datasets on severe inflammation (S4 Table, sheet 5). Gene rankings derived from minimally 20 contributing datasets, approximately 30-35 datasets on average. Rankings from 1 (high) to 500 (low) color coded in green. Gene order in figure A and B corresponds to figure C and D, respectively. Gene groups shown for monocytes, are induction involving interferon, induction by GC, and genes with relatively high ranking of C1QA, or PPARG in the expression correlation profiles (A). Shown groups for neutrophils are induction by GC, induction by interferon, and genes expressed in myelocytes and metamyelocytes (B). C and D) hierarchical clustering of gene expression correlation matrices for 23 genes mostly expressed in either monocytes (C) or neutrophils (D), using sepsis and bacterial infection samples from dataset gse154918 (whole blood, RNAseq, (Herwanto et al., 2021)). C) module marker genes as derived from meta analysis as shown, with clusters named according to relative gene expression between monocyte states MS1 and MS3 as defined in sepsis (Reyes et al., 2020), and clusters for induction involving interferon, and induction by GC in severe inflammation. D) module marker genes as derived from meta analysis as shown, with clusters named according to expression in myelocytes and metamyelocytes, and a cluster for induction by GC in severe inflammation. Cluster combinations also named according to a more general occurrence in inflammation (mainly induction involving interferon), or to a more specific presence in severe inflammation (inflammatory type). E and F) differential gene expression between sepsis and bacterial infection samples (ill), and healthy controls in dataset

gse154918 for genes predominantly expressed in either monocytes (E) or neutrophils (F). Normalized X-axis values on log-2 scale, with interval of 9 log 2 units for each panel, except for OLAH with interval of 12 log 2 units. Shown are box plots with added binned dot plots.

Figure 10

Gene expression in separated monocytes and neutrophils in severe inflammation

A) reciprocal ranking in gene expression correlation profiles for 23 genes, obtained on a collection of 7 datasets on monocytes and PBMCs in severe inflammation. Gene rankings derived from minimally 5 contributing datasets, except for profile FCGR3A (minimally 4). Profile query genes were present in all 7 datasets, except for VCAN (6 times), and FCGR3A (5 times). B) reciprocal ranking in gene expression correlation profiles obtained on a collection of 7 datasets on neutrophils and granulocytes in severe inflammation, including PMNCs from gse180387. Gene rankings derived from minimally 4 contributing datasets for each profile. Profile query genes were present 5-7 times in 7 neutrophil datasets. Rankings from 1 (high) to 100 (low) color coded in green in panels A and B. Gene order in figure A and B corresponds to figure C and D, respectively. Gene groups shown for monocytes and neutrophils, are induction by GC in severe inflammation, and a group of genes induced in severe inflammation, co-expressed with FAM20A. C) hierarchical clustering of gene expression correlation matrices for 23 genes expressed in separated CD14 positive monocytes in severe inflammation, using CD14 samples sepsis and critically ill from RNAseq dataset gse133822 (Washburn et al., 2019). Genes in GC signatures, and genes co-expressed with FAM20A in blood as shown. Clusters of gene expression correlation corresponding with MS1 / classical monocytes and MS3 / non-classical monocytes in severe inflammation as shown. Relative gene expression between monocyte states MS1 and MS3 taken from monocyte single cell expression data for sepsis (Reyes et al., 2020). Of note, a MS3 related cluster was visible in CD14 cells. D) hierarchical clustering of gene expression correlation matrices for 23 genes expressed in granulocytes in severe inflammation, using samples sepsis and SIRS from dataset gse123729 (Coulibaly et al., 2019). Genes in GC signatures, and genes co-expressed with FAM20A in blood as shown. Clusters of gene expression correlation corresponding to myelocytes and metamyelocytes as shown. Relative gene expression in pro-neutrophils (myelocytes), pre-neutrophils (metamyelocytes), and mature neutrophils, taken from neutrophil single cell expression data for severe Covid-19 (Schulte-Schrepping et

al., 2020). E and F) differential gene expression of GC inducible genes, and genes in FAM20A set in separated monocytes and granulocytes in severe inflammation. E) differential expression between CD14 sepsis samples and CD14 healthy controls from dataset gse133822 (Washburn et al., 2019). F) differential expression in sepsis and SIRS samples, versus presurgical controls from dataset gse123729 (Coulibaly et al., 2019). X-axis values on log-2 scale (cpm in E), with interval of 12 log 2 units for each panel, except for ADAMTS2 with interval of 13 log 2 units. Shown are box plots with added binned dot plots.

Figure 11

Wide ranging effects of GCs on monocytes and neutrophils predicted *in vivo*.

Gene induction by GCs in monocytes (M) and neutrophils (N) as detected in homeostasis and during severe inflammation. Functional categories of genes induced by GCs in monocytes and neutrophils include regulation of gene expression, secretory pathway, and phagocytosis among others. Phagocytosis of apoptotic cells (efferocytosis) was associated with monocytes in severe inflammation. A summary is presented based on gene expression correlation analysis using dataset collections for separated monocytes and neutrophils (S10 Table, S9 Table, sheets 1-9), and as supported by differential gene expression in PBMCs, and whole blood upon GC treatment in health (S1 Figure, S5 Table, S11 Table , sheet1), and during severe inflammation (S11 Table, sheet 2,3,4).

Figure 12

Different signatures of gene induction by GCs in homeostasis and during severe inflammation.

Overview of gene expression as detected in circulating monocytes and neutrophils, in homeostasis, inflammation, and during severe inflammation. Many genes are upregulated by GCs in health, and by interleukins/interferon during systemic inflammation as represented by mild respiratory viral infection. GC exposed monocytes and neutrophils upregulated a class of genes encoding negative regulators of inflammation, that are otherwise upregulated in inflammation, providing negative feedback (examples NFIL3, NFKBIA). Other genes were more specifically upregulated either by GCs (examples IRS2, TSC22D3, KLF9, IL1R2), or in inflammation (eg IL1B, OASL, GBP2), depending on cell type. Genes MCL1 and CLEC4E represented additional examples of dual upregulation. C1Q genes

were upregulated in intermediate and non-classical monocytes during inflammation (I/NC). Systemic severe inflammation involves exposure of monocytes and neutrophils to DAMPS and MAMPS, resulting in large changes in gene expression profiles. Monocytes in severe inflammation expressed PPARG indicative for alternative activation, and neutrophils expressed LDHA, indicative for ongoing aerobic glycolysis. Genes MMP8, HP, and RETN in neutrophils were preferentially upregulated in immature cells (IM). Endogenous or exogenous GCs induced genes in monocytes, in neutrophils or in both. Other stimuli (X) induced similar gene expression in monocytes and neutrophils, including gene FAM20A. Differential gene expression in MS1 and MS3 monocytes, according to data by Reyes et al., (2020) as indicated. Overview is mainly based on comparative *in vivo* gene expression analysis of GC inducible genes, and marker genes in separated cells (S10 Table, S9 Table), and in blood (S10 Table, S4 Table), either in the absence or presence of severe inflammation. Genes NFIL3, NFKBIA, MCL1, and IL1B, were likely upregulated due to *in vitro* activation in separated cells , which hampered assigning *in vivo* expression for these genes in case of monocytes, as indicated (*).

Figure 13

Gene induction by GC treatment in severe inflammation

A; Differential expression of a selection of candidate cortisol induced genes and relevant marker genes (dataset lacks genes OLAH and GYG1) in whole blood comparing 24h hydrocortisone treatment with baseline in septic shock (gse106878, whole blood, sequential hydrocortisone injections, 24 GC treated patients, 23 placebo treated patients, gse106878 (Kolte, 2020). Values for gene expression as log2 ratios, and genes ordered according to expression ratio. B; genes in same order comparing 24h placebo treatment with baseline. C; differential expression of a selection of candidate cortisol induced genes and relevant marker genes in whole blood of burn shock patients, comparing effects of hydrocortisone at one day and 120h time points with placebo treatment at one day and at 120h timepoints (gse77791, whole blood, priming dose and continuous infusion of hydrocortisone, time series, 15 GC treated individuals, 15 placebo treated individuals (Plassais et al., 2017)). Values for gene expression as log2 ratios, and genes ordered according to expression ratio (C); D, genes in same order compared for expression in whole blood between all 30 ill and all 13 healthy individuals in gse77791; E, whole blood gene expression compared between ill

and healthy individuals in sepsis/SIRS in dataset gse66099 (Sweeney et al., 2015); F, similar comparison of whole blood gene expression between ill and healthy individuals in sepsis dataset gse65682 (Scicluna et al., 2015). 95% confidence intervals according to Fieller as indicated. Marker genes include LEF1 (naive T cells), BANK1 (B cells), SPON2 (NK cells), PRF1 (cytotoxic cells more generally), FCGR3B (neutrophils), MME (old/mature neutrophil CD10), AZU1 (band/pro-neutrophil), MMP8 (band/pre-neutrophil), VCAN and CCR2 (MS1/classical monocyte,) GK, GYG1, HK3, and LDHA (enhanced lipid synthesis and glucose metabolism in myeloid cells), OASL (interferon alpha), GBPs (interferon gamma), IL1B and TNF (NF-kB signalling), and HLA-DRA (interferon gamma and antigen presentation).

Figure 14

Longitudinal gene expression during severe inflammation after trauma.

Expression of marker genes, marker gene modules, GC inducible genes, and set GC-2 in whole blood, after trauma, and compared to healthy controls (gse36809 (Xiao et al., 2011)). Expression values and time after injury shown at log 2 scales (h, hours; d, days; w, weeks). Mean value for healthy controls (H) was set at zero . In case of genes OLAH, DAAM2, VSIG4, and ADAMTS2, maximal expression values in healthy controls, which possibly still correspond to gene probe background levels, are indicated by horizontal lines. Expression values for modules and gene sets were calculated using adequate gene probes, with subtraction of background / basal expression, and adjusting for different gene expression ranges as detailed in methods. Neutrophil bands appeared immediately after trauma, while later immature neutrophils likely originated from emergency granulopoiesis. Relative expression of T cell and SIM modules / sets was still different from healthy control at week 4. Induction by GC of genes in set GC-2 was frequently visible before and after appearance of cells from emergency granulopoiesis. In monocytes, VSIG4 expression peaked earlier than ADAMTS2.

Figure 15

Distribution of gene module expression in health and during inflammatory illnesses

Increase of GC-1 and GC-2 gene module expression upon GC treatment in healthy people, and in patients with burn shock, septic shock, and systemic lupus erythematosus (SLE). Included for comparison are expression values for gene modules T cell, severe inflammatory

myeloid (SIM), FAM20A, (4 genes including FAM20A), interferon gamma (inf gamma), and interferon alpha (inf alpha). Datasets used different assay platforms and log fold change between module expression values in one set are not directly comparable to log fold changes in other datasets. A; gse110160 (Hu et al., 2018), healthy, and healthy 2-8 h after prednisolone intake (GC 2-8h). B; gse77791 (Plassais et al., 2017), healthy, severe burn shock (1-5 days, excluding 7 days samples; b.shock), severe burn shock with hydrocortisone treatment (1-5 days, excluding 7 days samples; b.shock GC). C; gse106878 (Kolte, 2020), septic shock placebo 0 h (Ssh P0), septic shock hydrocortisone 0 h (Ssh GC0), septic shock placebo 24 h (Ssh P24), septic shock hydrocortisone 24 h (Ssh GC 24). D; gse110174 (Hu et al., 2018), healthy, SLE low and medium prednisone usage (SL l/m GC), SLE high prednisone usage (SL hGC), SLE unknown prednisone usage (SL uGC). X-axis values on log-2 scale, with interval of 9 log 2 units for each panel. Shown are box plots with added dot histograms.

Figure 16

GC-2 gene expression is upregulated by endogenous and exogeneous GC depending on disease

Overview of gene expression in blood during different diseases and upon treatment with GCs using 5 relevant features; a gene set for severe inflammatory myeloid (SIM), a gene module of 4 induced genes including FAM20A (FAM (4)), a gene set GC-2 for induction by GC during severe inflammation (GC-2), and gene modules for induction by either interferon gamma (IFN-G), or interferon alpha (IFN-A). Module expression values were plotted in ranges of 9 log 2 units and distributions compared within and between experiments and tentatively ordered according to deviation from healthy controls. Red arrows indicate maximal deviations from healthy control for each module. Decreases in basal module expression, as frequently seen in case of interferon gamma and alpha induction in severe inflammation, may occur because of shifts in cell percentages, and do not necessarily indicate gene repression. All experiments used whole blood except gse161918 (severe Covid-19) which used PBMCs (C. Liu et al., 2021). Asterisks indicate 2 experiments without healthy control group (gse157103 Covid-19 ICU group set arbitrarily at values for severe Covid-19 in gse171110, and gse106878 septic shock no GC usage group set arbitrarily at

values for septic shock group in gse66099). Datasets, different platforms, and supporting figure panels as shown.

Supporting information legends

S1 Figure

Differential expression of GC signature genes upon GC treatment *in vivo* and between circadian time points and correlation cluster analysis.

A) Ranking values for GC signature genes according to fold expression difference in each of 6 different experiments. Genes are listed according to their original rankings in GC signatures 1 and 2. Genes present in both signature 1 and 2 are indicated in bold, genes specific to signature 2 are listed from gene DAAM2 to gene HTRA1. Marker genes and marker gene sets for NK cells, neutrophils, T cells, B cells, monocytes, and immediate early gene expression added. NS, not significant, $p > 0.05$; NA, gene absent from platform or expression table. Marker gene rankings color coded from green (low rankings, up regulation), to red (high rankings, down regulation) for whole range in experiments. Rankings for GC signature genes shaded blue up till values reached by marker gene expression in NK cells or neutrophils, depending on individual experiment. gds3864, PBMC, intravenous GC, time series, 4 individuals (Carlet et al., 2010); gse67255, PBMC, intravenous hydrocortisone, time series, 18 individuals (Olnes et al., 2016); gds3704, PBMC, fatty acids consumption, 0h and 6h time points, 21 individuals (Bouwens et al., 2010); gse110160, whole blood, prednisolone, time series, 24 individuals (Hu et al., 2018); gse46743, whole blood, dexamethasone orally, 0h en 3h time points, 160 individuals (Arloth et al., 2015); gds2767, peripheral blood leukocytes, beverage consumption, time series, 4 times 6 individuals (Baty et al., 2006). **B**) Cluster analysis of GC signature 1 and 2 gene expression in PBMCs sampled with 6 h time difference. Hierarchical clustering of an expression correlation matrix of 53 GC signature 1 and 2 DEGs from circadian experiment gds3704, with 18 marker genes specifically expressed in different immune cells or early in cell activation as indicated. Signature genes were found in 4 larger clusters, broadly corresponding with lymphoid cells, myeloid cells, cortisol gene expression in lymphoids, and cortisol gene expressions in myeloid cells.

S2 Figure

Gene expression in separated monocytes and neutrophils in severe inflammation

A and **B**) hierarchical clustering of gene expression correlation matrices, each for 64 genes expressed in separated CD14 positive monocytes in severe inflammation, using CD14 samples sepsis and critically ill from RNAseq dataset gse133822 (Washburn et al., 2019). **A**) a selection of inducible genes involving interferon, genes expressed in non-classical monocytes and monocyte state 3 (MS3) in severe inflammation, genes expressed in classical monocytes, and genes downregulated in monocyte separations in severe inflammation. **B**) selection of genes upregulated in severe inflammation in monocyte states MS1 and MS3 including most GC inducible genes, and genes in the FAM20A group as well as several genes expressed in classical monocytes with relatively lower levels of upregulation in severe inflammation (eg CCR2). Genes present in GC signatures and in FAM20A group as indicated. Clusters corresponding to different cell types/states and inducible expression as shown for A and B. Inflammatory type indicates a cluster of genes generally upregulated in mild inflammation involving interferon (inflammation), and clusters of genes upregulated more specifically in severe inflammation (type severe inflammation). **C** and **D**) differential expression of several genes from figures A and B, respectively, comparing sepsis and healthy control CD14 samples from gse133822. **E**) hierarchical clustering of a gene expression correlation matrix of 112 genes expressed in separated granulocytes in severe inflammation, using samples sepsis and SIRS from dataset gse123729 (Coulibaly et al., 2019). Selected genes include genes generally upregulated in mild inflammation, involving induction by interferon (eg CASP1, TAP1) or not (eg IL1B), genes expressed in immature neutrophils, and a variety of genes upregulated in severe inflammation in neutrophils including genes in GC signatures, and genes in the FAM20A group. Clusters corresponding to myelocytes, metamyelocytes, inducible expression by GC and by interferon gamma, as shown, as well as corresponding inflammatory type. **F** and **G**) differential expression of several genes from figure E, comparing sepsis and SIRS with presurgical control samples in gse123729. X-axis values on log-2 scale (cpm in C an D), with interval of 13 log 2 units for each panel, shown are box plots with added binned dot plots.

S3 Figure

Expression correlation clustering of module genes and corresponding gene probes used in comparing module expression values between different inflammatory illnesses.

Hierarchical clustering of module genes in expression correlation matrices for 3 different datasets on severe inflammation, each from a different platform. Genes in module T cell (bias naive T cell, n= 13), SIM set (Severe Inflammatory Myeloid, n= 16), FAM20A module (n= 4), GC-2 module (n= 9), interferon gamma induced module (IFN gamma, n= 23), and interferon alpha induced module (IFN alpha, n= 8) as indicated. **A**) dataset gse66099, (Sweeney et al., 2015) , samples SIRS, sepsis and septic shock (n total = 229), gpl570, Affymetrix Human Genome U133 Plus 2.0 Array. **B**) dataset e-mtab-5273, (Burnham et al., 2017), samples sepsis (n total = 221), gpl10558, Illumina HumanHT-12 V4.0 expression beadchip. **C**) dataset gse154918, (Herwanto et al., 2021), samples sepsis, septic shock, and uncomplicated bacterial infection (n total = 65), gpl20301, Illumina HiSeq 4000 (Homo sapiens). Gene expression clusters corresponding to T cells and SIM set are well separated, with negative correlation. GC-2 clusters, corresponding to GC induced genes in severe inflammation, and genes from the SIM set are positively correlated, and well separated, while the existence of a cluster for FAM20A module genes, separate from other SIM genes, is not as clear from individual datasets. Gene expression clusters corresponding to either induction by interferon gamma, or interferon alpha are positively correlated and well separated. Experiment e-mtab-5273 only provided a subset of available probes for platform gpl10558 with 7 selected gene probes missing. The clustering results indicated that selected genes, and selected gene probes used for Affymetrix, Illumina, and RNAseq platforms (S12 Table) were generally adequate.

S4 Figure

Distribution of gene module expression in health and during inflammatory illnesses (Affymetrix)

GC-1 and GC-2 gene module expression in whole blood samples from sepsis, severe injury, systemic JIA, sarcoidosis, systemic sclerosis and rheumatoid arthritis patients. Included for comparison are expression values for gene modules T cell, severe inflammatory myeloid (SIM), FAM20A, (4 genes including FAM20A), interferon gamma (inf gamma), and interferon

alpha (inf alpha). All datasets are obtained using Affymetrix Human Genome U133 Plus 2.0 Array (GPL570), and identical probesets (S12 Table) were used to calculate module expression values for each dataset. **A**; gse66099 (Sweeney et al., 2015), healthy, SIRS, sepsis and septic shock (s-shock). **B**; gse36809 (Xiao et al., 2011), healthy, blunt trauma till 99 h (trauma<99h), from 99 h till 28 days (trauma>99h). **C**; gse77791 (Plassais et al., 2017), healthy, severe burn shock (1-5 days, excluding 7 days samples; b.shock), severe burn shock with hydrocortisone treatment (1-5 days, excluding 7 days samples; b.shock GC). **D**; gse80060 (Brachat et al., 2017), healthy, systemic juvenile idiopathic arthritis (SJIA),with or withour canakinumab (can.mab) treatment on day 3 (all samples batch 1). **E**; gse19314, (Koth et al., 2011), healthy and sarcoidosis. **F**; gse65336 (Guo et al., 2015) systemic sclerosis (SSc) before (SSC d0) and after 56 days of anifrolumab treatment (SSc anifrolumab, d56). **G**; gse93272 (Tasaki et al., 2018) healthy, and rheumatoid arthritis (both drugs treated and untreated; RA). X-axis values on log-2 scale, with interval of 9 log 2 units for each panel. Shown are box plots with added binned dot plots.

S5 Figure

Distribution of gene module expression in health and during inflammatory illnesses (Illumina)

GC-1 and GC-2 gene module expression in whole blood samples from patients with SIRS, sepsis, sepsis/ARDS, febrile bacterial and viral infection, Kawasaki disease, children's malaria, mild respiratory viral infection, and systemic lupus erythematosus (SLE), as well as from large healthy populations. Included for comparison are expression values for gene modules T cell, severe inflammatory myeloid (SIM), FAM20A, (4 genes including FAM20A), interferon gamma (inf gamma), and interferon alpha (inf alpha). All datasets are obtained using Illumina HumanHT-12 V4.0 or V3.0 expression beadchips (GPL10558 and GPL6947, respectively), and identical V4.0 probesets, which are also mostly present on V3.0, were used to calculate module expression values for each dataset (S12 Table). **A**; e-mtab-5273, gpl10558 (Burnham et al., 2017), healthy, sepsis due to pneumonia (pneumonia), sepsis due to faecal peritonitis (f. peritonitis). **B**; e-mtab-5273, gpl10558 (Burnham et al., 2017), healthy (none), sepsis response signature 1 (SRS1), sepsis response signature 2 (SRS2). **C**; gse32707, gpl10558 (Dolinay et al., 2012), SIRS day 0 (SIRS), sepsis + ARDS day 0 (se/ARDS), sepsis alone

day 0 (seps.), sepsis alone day 7 (seps.d7). **D**; gse72829, only gpl10558, (Herberg et al., 2016), febrile children with bacterial infection (bacterial), febrile childeren with viral infection (viral), febrile children with unknown infection (unknown). **E**; gse73463, gpl10558 (Wright et al., 2018), convalescent Kawasaki disease (kawasaki conv), acute Kawasaki disease (kawasaki acute). **F**: gse34404, gpl10558 (Idaghdour et al., 2012), children without symptomatic malaria (control), children with symptomatic *P. falciparum* malaria (Pf malaria). **G**; gse117613, gpl10558 (Nallandhighal et al., 2019), children without *P. falciparum* infection (no Pf), children with severe malarial anemia (m. anemia), children with cerebral malaria (c. malaria). **H**; gse138458, gpl10558 (Guthridge et al., 2020), SLE with low SLEDAI (SLE low), SLE with high SLEDAI (SLE high), control (control), (7 lower quality samples left out). **I**; gse83456, gpl10558 (Blankley et al., 2016), healthy control (healthy), sarcoidosis (Sarcoid), extra pulmonary TB (EPTB), pulmonary TB (PTB). **J**; gse42834, gpl10558 (Bloom et al., 2013), healthy control (healthy), non active Sarcoidosis (n act S), active Sarcoidosis (act Sarc), Tuberculosis (TB), lung cancer (lung Ca). **K**; gse135304, gpl10558 (Kossenkov et al., 2019), benign pulmonary nodules (N benign), malign pulmonary nodules (N malign). **L**; gse68310, gpl10558 (Zhai et al., 2015), healthy, mild respiratory influenza viral infection (ill). **M**; gse68310, gpl10558 (Zhai et al., 2015), healthy, mild respiratory non-influenza viral infection (ill). **N**; gse48348, gpl6947 (Westra et al., 2013), healthy individuals (n= 734). **O**; datasets e-mtab-1708, e-tabm-1036, and gse36382, each gpl6947 (Inouye et al., 2010; Mayerle et al., 2013; Schramm et al., 2014), healthy individuals (n= 993, 518, and 991, respectively), only box plot with outliers shown. X-axis values on log-2 scale, with interval of 9 log 2 units for each panel. Shown are box plots with added binned dot plots.

S6 Figure

Distribution of gene module expression in health and during inflammatory illnesses (RNAseq)

GC-2 gene module expression in whole blood samples from patients with SIRS, acute kidney injury, COVID-19, infectious diarrhea, brucellosis, leishmaniasis, adults malaria, inflammatory bowel disease (IBD), (systemic) juvenile idiopathic arthritis (SJIA and JIA), systemic lupus erythematosus (SLE), and mild respiratory viral infection, as well as from physically healthy populations. Included for comparison are expression values for gene modules T cell, severe inflammatory myeloid (SIM), FAM20A, (4 genes including FAM20A), interferon gamma (inf

gamma), and interferon alpha (inf alpha). All datasets are obtained using mRNA sequencing and all genes, as present in different datasets, were used to calculate module expression values for each dataset (S12 Table). **A**; gse67401 (Tsalik et al., 2015), SIRS, SIRS with acute kidney injury (SIRS-AKI), SIRS with hemodialysis (Hemodialysis), units 2 log rpm. **B**; gse157103 (Overmyer et al., 2021), non COVID-19 patients not in ICU (ill), or in ICU (ill ICU), COVID-19 patients not in ICU (C19), or in ICU (C19 ICU), units 2 log tpm. **C**; gse152641 (Thair et al., 2021), healthy control (healthy), Covid-19 hospital patients (S Covid-19), units 2 log cpm. **D**; gse69529 (DeBerg et al., 2018), healthy, infectious diarrhea with either bacterial (bact_drr), or rotaviral infection (rota_drr), units 2 log cpm. **E**; gse69597 (Dufort et al., 2016), healthy, brucellosis, leishmaniasis, units 2 log cpm. **F**; gse52166 (Tran et al., 2016), healthy adults (healthy), adults with febrile *Plasmodium falciparum* malaria (Pf malaria), units 2 log fpkm. **G**; gse112057 (Mo et al., 2018), healthy, ulcerative colitis (UC), Crohn disease (Crohn), juvenile idiopathic arthritis (JIA), systemic juvenile idiopathic arthritis (SJIA), units 2 log cpm. **H**; gse72509 (Hung et al., 2015), healthy, systemic lupus erythematosus (SLE), units 2 log rpkm. **I**; gse107994 (Singhania et al., 2018), control, LTBI (latent TB), LTBI Progressor (l prog TB), active TB, units 2 log cpm. **J;** gse107793 (Singhania et al., 2018), control, LTBI (latent TB), units 2 log cpm. **K**; gse97356 (Kuan et al., 2017), healthy and post traumatic stress disorder (PTSD), no PTSD, (no ptsd) , past PTSD (past ptsd), and actual PTSD (ptsd), units 2 log cpm. Shown are box plots with added binned dot plots.

S7 Figure

Distribution of gene module expression in health and during inflammatory illnesses (RNAseq and other platforms)

GC-1 and GC-2 gene module expression in whole blood samples from acute fungal, bacterial and viral infection, sepsis, Covid-19, rheumatoid arthritis, asthma, SLE, and IBD, and additionally, module expression also in PBMC samples for Covid-19. Included for comparison are expression values for gene modules T cell, severe inflammatory myeloid (SIM), FAM20A, (4 genes including FAM20A), interferon gamma (inf gamma), and interferon alpha (inf alpha) (S12 Table). **A**; gse176260, (Steinbrink et al., 2021), healthy control (Health), acute bacterial infection (Bact), acute candidemia (Cand), acute non infectious illness labeled SIRS (SIRS), acute viral infection (vir), units 2 log TMM normalized counts. **B**; gse60424 (Linsley et al.,

2014), diseases excluding sepsis patients and interferon treated MS patients (other), and sepsis patients (3 samples, sepsis), units 2 log TMM normalized counts. **C**; gse171110 (Lévy et al., 2021), healthy control (healthy), and severe Covid-19 patients (Sev. Covid-19), units 2 log cpm. **D**; gse117769 published by Goldberg and co-workers (2018), healthy control (healthy), rheumatoid arthritis without GC treatment (RA-GC), rheumatoid arthritis with GC treatment (RA+GC), units made 2 log cpm. **E**; gse115823 (Altman et al., 2019), asthmatic children with cold (cold), asthmatic children with cold, asthma exacerbation and systemic GC use (cold/asthmaX/GC), units made 2 log cpm. **F**; gse161918 (C. Liu et al., 2021), PBMC from healthy control (healthy), and severe Covid-19 patients (Sev. Covid-19), units made 2 log cpm. **G**; gse110169 (platform gpl13667 taking probesets with highest mean expression), batches 1 and 3 (Hu et al., 2018), healthy, RA without GC treatment (RA-GC), RA with GC treatment (RA+GC), SLE without GC treatment (SLE-GC), SLE with GC treatment (SLE+GC). **H**; gse110169 (platform gpl13667 taking probesets with highest mean expression), batches 2 and 4 (Hu et al., 2018), healthy, RA without GC treatment (RA-GC), RA with GC treatment (RA+GC), SLE without GC treatment (SLE-GC), SLE with GC treatment (SLE+GC). **I**; gse126124 (platform gpl6244, taking probes with highest mean expression) (Palmer et al., 2019), non inflammatory bowel disease (IBD) control (control), Crohn disease without GC use (Crohn), ulcerative colitis without GC use (UC). X-axis values on log-2 scale, with interval of 9 log 2 units for each panel. Shown are box plots with added binned dot plots.

S8 Figure

Graphical abstract

S1 Table

Sheet 1) average correlation results on programmatically selected datasets for circadian expressed, cortisol induced genes, DDIT4, TSC22D3, PER1, ZBTB16, KLF9, and IRS2, with ranks and rank of average rank. **Sheet 2**) average correlation results on programmatically selected datasets for cortisol induced genes in severe inflammation, ADAMTS2, VSIG4, OLAH, DAAM2, FLT3, ADORA3, CD163 with ranks and rank of average rank. Number indicates contributing profiles to the average value, which may be a bit more than the number of contributing datasets for a given gene, since a microarray dataset can have more than 1 adequate probeset per gene. Lists are cut off at 2000 genes.

S2 Table

Comparison of signature gene sets and 8 DEG sets of *in vitro* GC induction in immune cells.

Sheet 1) gene list for GC signatures 1 and 2. **Sheet 2**) GC induced DEGs in PBMCs (gse110156; (Hu et al., 2018)); **Sheet 3**) GC induced DEGs in monocyte derived macrophages (gse61880; (Jubb et al., 2016)), using time points corresponding with highest fold change as indicated. In bold genes taken as DEG set, in red log2 FC values not significant in comparing individual time points with untreated cells. **Sheets 4, and 5**) GC induced DEGs in monocyte derived macrophages and monocytes (gse109439; (Wang et al., 2019)). **Sheets 6, 7, 8, 9**) GC induced DEGs in monocytes, neutrophils, CD4 T cells, and B cells (gse112101; (Franco et al., 2019)). **Sheet 10**) presence of all signature genes and 8 DEG set genes in separate DEG sets, and frequency distribution for all signature and all 8 DEG set genes.

S3 Table

Cell type specific expression and *in vitro* induction by GC of cortisol signature genes.

Basal and upregulated gene expression by GC treatment of immune cells *in vitro*. gse60424 basal, relative base level expression for different immune cell types as a ratio of total expression in 6 cell types shown (B cell, CD4 T, CD8 T, monocyte, neutrophil, NK, excluding sepsis samples; gse60424, (Linsley et al., 2014). gse112101 basal, relative base level expression in 4 cell types shown (B cell, CD4 T, monocyte, neutrophil; gse112101, (Franco et al., 2019). gse112101 induced, differential expression upon GC treatment for different cell types in experiment gse112101 (4 cell types, 22.7 mM methylprednisolone, 2h and 6h, (Franco et al., 2019). gse109439 basal, relative base level gene expression in monocytes and macrophages (gse109439, (Wang et al., 2019). gse109439 induced, differential expression upon GC treatment of monocytes and macrophages (gse109439, 1 mM triamcinolone acetonide, 4h, (Wang et al., 2019). gse100521 induced, differential expression of M1 macrophages repolarized to M2 with methylprednisolone, 100nM, 24h (gse100521, (Gharib et al., 2019). Basal expression ratios are shaded blue. DEG values are log2 fold change of induced and base expression levels, with table cells shaded red (up regulation) and green (down regulation), accordingly. NS, not significant ($p > 0.05$); NA, gene not detected/absent

from platform, or absent p value. Log2 fold change, and unadjusted p values used for experiment gse109439 according to Wang et al., (2019). Genes from signature 1, signature 2 or both as indicated, marker genes (32) included as expression controls.

S4 Table

Analysis of gene expression correlation profiles from blood either in the absence, or in the presence of severe inflammation.

Sheet 1) GC signature 1 gene expression correlation in blood in the absence of severe inflammation. Ranking of marker gene (combinations) in gene expression correlation profiles obtained for GC signature 1 genes, (rows, n = 119), using a collection of 62 gene expression datasets on blood excluding severe inflammation, color coded in green. Marker gene (combinations) include GC1 ("core group" of GC induced genes), T cell (module), cytotoxic cell (module), NK (module), B cell (module), nucleosomal expression (module), ribosomal expression (module), mitochondrial expression (module), Fa (biogenesis module, mostly lymphoid), chrom. remod. (set of genes in chromatin remodeling), classical monocytes (module/set classical monocyte), non-classical monocytes (module), IFN gamma (module of interferon gamma induced genes), IFN alpha (module of interferon alpha induced genes), TNFAIP6 (marker for inflammation also involving interferon), IL1RN (marker for inflammation also involving interferon), IL1B (marker for inflammation), MME (old/mature neutrophil CD10), neutrophil (mature neutrophil, module), IL1R2 (marker for GC induced genes mainly in neutrophils), IRAK3, GYG1, Fb (biogenesis module with gene PAPOLA, mostly myeloid), and FOSB (marker for immediate early gene expression, mostly due to *in vitro* activation). Gene expression correlation profiles and gene marker (combinations) were ordered to indicate relevant gene groups. Visible groups correspond to genes expressed preferentially either in lymphoids or in neutrophils, genes strongly induced by cortisol, more generally, including DDIT4 and TSC22D3, genes induced by GC mostly in neutrophils including IL1R2, genes induced during inflammation (eg SOCS1 induced by interferon, and NFIL3), and genes expressed during biogenesis in myeloid cells (group Fb). A summary of correlation characteristics from evaluating individual profiles is included (description). Relatively strong circadian expression was seen for a number of GC signature 1 genes by plotting datasets gse73072 on mild respiratory viral infection (Liu et al., 2016), and gse56931 on sleep

deprivation (Arnardottir et al., 2014), best for DDIT4. Upregulation during mild inflammation was scored relative to upregulation of IL1B using dataset gse73072, and could be seen for several genes, best for SOCS1 (Visible DEGs). **Sheet 2**) Marker gene expression correlation in blood in the absence of severe inflammation. Ranking of marker gene (combinations) in gene expression correlation profiles obtained for selected genes, (rows, n = 329), using a collection of 62 gene expression datasets on blood excluding severe inflammation, color coded in green. Tested genes include GC-1 set ("core group" of 7 GC induced genes), genes that are preferentially expressed in different cell types such as monocytes and neutrophils in homeostasis, genes that are upregulated during inflammation such as induced by interferon, and other genes taken from relevant gene modules. A variety of marker genes and marker gene combinations was used to follow gene expression in homeostasis and inflammation. Shown marker genes and marker gene modules/sets include GC-1, ("core group" of GC induced genes taken together), HLA-DRA (in antigen presentation, mainly expressed in monocytes and B cells), CD86 (in co-stimulation, mainly expressed in monocytes), ALDH1A1, CCR2, and VCAN (all 3 expressed in classical monocytes), module/set classical monocyte, module non-classical monocyte, CDKN1C (non-classical monocyte), C1QABC (C1QA, B and C genes together, upregulated in non-classical monocyte in inflammation), MME (in module old/mature neutrophil CD10), module neutrophil mature/base, IL1B (upregulated in inflammation), GK (upregulated in inflammation), module/set gk-11 (genes upregulated in inflammation, co-expressed with GK), IL1RN, TNFAIP6, and CASP1 (upregulated in inflammation also involving interferon), FCGR1AB (FCGR1A, and B genes together, upregulated in inflammation also involving interferon), IFN gamma (module of genes induced by interferon gamma), IFN alpha (module of genes induced by interferon alpha), IRAK3 (upregulated in severe inflammation), gyg1-4 (module of 4 co-expressed genes highly upregulated in severe inflammation including GYG1), rhog-zyx, (RHOG and ZYX together, co-expressed genes, functionally in actin dynamics), ppp (module indicating increased presence of pentose phosphate pathway), Fb (biogenesis module with gene PAPOLA, mostly myeloid), PAPOLA, Fa (biogenesis module, mostly lymphoid), gene EVI2A, evi2a-20 (gene module, includes EVI2A , also TXN and GLRX, mostly myeloid), and additional marker gene (combinations) for different cell types and cell proliferation, as indicated. Gene expression correlation profiles and gene marker (combinations) were ordered to indicate relevant gene groups. Different groups are shown of genes that are variably expressed in homeostasis, and

of genes that are regulated during inflammation. Several groups, mainly derived from homeostasis, correspond to different cell types such as monocytes, neutrophils, and lymphoid cells, and to cellular activities such as biogenesis and induction by GC. Inflammation related gene groups corresponded to inflammatory monocytes (genes upregulated in monocytes, often involving induction by interferon, eg C2 and C1QA/B/C genes, red box 1), inflammatory myeloid cells (upregulation not involving interferon, eg IL1B and GK, as well as induction involving interferon, eg IL1RN and TNFAIP6, red box 2), and another group corresponding with inflammatory myeloid cells (both with gene induction involving interferon, and induction by interferon gamma and alpha more exclusively, red box 3). An interesting group of genes with EVI2A, is also highlighted (dark-green box). Number of datasets and correlations shows number of times a gene was present in the dataset collection (with gene, maximally 62), the approximate number of positive datasets (selected for consistent, similar correlations) contributing to the profiles for a given gene (appr. positive), and the approximate correlation values of the top 10 ranking genes in the profile (appr. correlation). Genes with mixed expression in different cell types, and genes that are only expressed during severe inflammation had lower numbers of positive datasets and lower correlation values, for example in case of ADAMTS2 for which no reliable profile could be obtained from the collection (only 2 false positive datasets). Gene PER3 had very few positive datasets, likely because of mostly inadequate probesets, instead. Added for comparison are corresponding differential gene expression data for whole blood during inflammation in mild respiratory viral infection gse68310, (Zhai et al., 2015), gse30550, (Huang et al., 2011), gse73072, (Liu et al., 2016), and data for expression peaks unrelated to viral infection and inflammation, marked by upregulation of genes EVI2A, CD3D, FCER1A, etc (gse73072), which resembled differential expression in PBMCs at 2 days after high altitude transfer (gse46480, (Johnson et al., 2014)). Also added are data on basal and interferon induced expression in different immune cells after interferon beta treatment of MS (gse60424, (Linsley et al., 2014)), and differential expression in sepsis for monocytes and neutrophils (gse60424), to compare with expression in severe inflammation. Inflammation related gene groups as visible in correlation, were upregulated in mild respiratory viral infection, with genes expressed in inflammatory monocytes more upregulated in influenza, than in other respiratory viral infection, as shown (comparisons DEGs mild respiratory viral infection, and DEGs mild influenza, red boxes). Genes in a group with EVI2A, as visible in

correlation, were upregulated in expression peaks marked by EVI2A in whole blood, and also at 2 days at high altitude in PBMCs (gene group shown in brown). Genes expressed in non-classical monocytes, as well as in inflammation related gene group 1 (monocyte), both as visible in correlation, were upregulated by i*n vivo* interferon treatment (interferon beta treatment of MS, blue box 1). Genes in inflammation related group 3 (myeloid), as visible in correlation, were upregulated by *in vivo* interferon treatment, mainly in neutrophils (blue box 2). Additionally, genes IL1RN and TNFAIP6 were also induced by interferon *in vivo*. In contrast, differential gene expression in monocytes and neutrophils in sepsis (DEGs SEPSIS mono and neutro), did not correspond well with differential expression in mild inflammation, nor with differential expression in interferon treatment, nor with patterns of correlated gene expression in blood in the absence of severe inflammation. Differential expression given as log2 fold change (log2FC), color coded in red to green for upregulation, and downregulation, respectively. Values are denoted NS, for not significant ($p > 0.05$). Very small p values ($p < 1e-20$) in experiment altitude are shown in yellow. Ratios of gene expression values between different cell types color coded in blue. The main source of expression in blood, as judged by correlation characteristics and differential expression, is tentatively summarized for each gene (description). **Sheet 3)** GC signature 2 gene expression correlation in blood in the presence of severe inflammation. Ranking of marker gene (combinations) in gene expression correlation profiles obtained for GC signature 2 genes, (rows, n = 135), using a collection of 38 gene expression datasets on blood excluding severe inflammation, color coded in green. A variety of genes and marker gene combinations was used to follow gene expression of GC signature 2 genes, using marker genes that are specifically expressed in different monocyte states, and in neutrophils during severe inflammation. Shown marker genes and marker gene modules/sets include HLA-DRA (in antigen presentation, downregulated in monocytes in severe inflammation), CD86 (in co-stimulation, mainly expressed in monocytes), CCR2 and VCAN (classical monocyte and monocyte state MS1, according to Reyes et al. (2020), in severe inflammation), ANG-7, (module with gene ANG, expressed in monocytes), PPARG (marker for M2 monocytes), MERTK (functional marker for efferocytosis), C1QABC (induced in non-classical monocyte and monocyte state MS3, according to Reyes et al., (2020), with C1Q (module/set co-expressed with C1Q genes in severe inflammation, includes NR1H3), EDNRB (expressed in monocytes in severe inflammation, possibly GC induced), LYVE1 (expressed in monocytes in

severe inflammation, likely GC induced), VSIG4 (expressed in monocytes in severe inflammation, GC induced), GC-2 (set of genes highly induced by GC in myeloid cells in severe inflammation), TSC22D3 (GC induced, less related to inflammation), GC-1 (set of genes induced by GC, and co-expressed in the absence of severe inflammation), neutrophil mature/base (mature neutrophil, module), IL18R1-IL18RAP (both genes taken together, upregulated in neutrophils in severe inflammation, likely GC induced), ARG1 (upregulated mainly in neutrophils in severe inflammation, likely GC induced), SIMgr (set of genes highly upregulated in myeloid cells in severe inflammation, unrelated to induction by GC), GYG1 (highly upregulated in severe inflammation, mainly in neutrophil), LDHA (highly upregulated in severe inflammation mainly in neutrophil), CD177 (highly upregulated in severe inflammation in neutrophil, possibly in immature neutrophil). GC signature 2 expression correlation profiles and gene marker (combinations) were ordered to indicate relevant gene groups. Visible gene groups corresponded to monocytes, neutrophils, or both. Genes expressed in monocytes, could be grouped depending on relative strength of induction by GC, and expression clusters were visible with gene ANG, and with C1QA/B/C including TCN2. Genes preferentially expressed in neutrophils could also be grouped according to relative strength of induction by GC, strength of association with severe inflammation (eg SIMgr variable), and an expression cluster was visible with genes IL18R1 and IL18RAP. Added for comparison are corresponding differential gene expression data for whole blood in sepsis (gse66099, (Sweeney et al., 2015)), expression ratios for different immune cells in sepsis (gse60424, (Linsley et al., 2014)), data for differential expression in CD14 monocytes and granulocytes in sepsis (gse133822, (Washburn et al., 2019), gse123729, (Coulibaly et al., 2019)), and visible upregulation during mild inflammation as determined for datasets gse73072 and gse68310 on experimental and prospective respiratory viral infection (Liu et al., 2016; Zhai et al., 2015). Increased expression in whole blood in sepsis was observed for most GC signature 2 genes, which might more generally reflect general upshifts in myeloid cell percentages. Genes in the monocyte group, as visible in correlation, were also expressed at high ratios in monocytes compared to neutrophils in sepsis, and several were upregulated in sepsis monocytes (eg ADAMTS2 and VSIG4, but not ALOX15B, LPL and CPM), and not in sepsis granulocytes, compared to controls. C1Q genes were also upregulated in sepsis CD14 monocytes, possibly indicating the presence of intermediary monocytes or contaminating cells. Genes IL18R1, IL18RAP, and ARG1, used as marker genes in correlation profiling, were

much more expressed in neutrophils than in monocytes in sepsis, and highly upregulated in neutrophils. Comparing gene expression in whole blood in sepsis, and in mild inflammation during respiratory viral infection indicated an absence of upregulation of VSIG4 and OLAH in mild inflammation, for example. In contrast, C1Q and TCN2 genes, expressed in non-classical monocytes, and also in MS4 cells in severe inflammation, were upregulated in both mild and severe inflammation. Differential expression given as log2 fold change (log2FC), color coded in red to green for upregulation, and downregulation, respectively. Corresponding p values are shown in grey, or expression values denoted NS, for not significant ($p > 0.05$). Ratios of gene expression values between different cell types color coded in blue. A summary of correlation characteristics from evaluating individual gene expression correlation profiles is also included (description) **Sheet 4**) Marker gene expression correlation in severe inflammation. Ranking of marker gene (combinations) in gene expression correlation profiles obtained for selected genes, most of which are expressed in monocytes and neutrophils (rows, n = 138), using a collection of 38 gene expression datasets on blood in the presence of severe inflammation, color coded in green. Tested genes are in set GC-1 ("core group" of GC induced genes seen in the absence of severe inflammation), set GC-2 (GC induced genes especially in severe inflammation), set SIM (selection of genes highly upregulated in myeloid cells in severe inflammation), and set FAM20A (n= 4), and include other relevant genes for grouping, such as expressed in inflammation, or in different cell types. Marker gene (combinations) include a set named "with HLA-DRA" (monocyte expressed genes downregulated in severe inflammation in correlation with HLA-DRA), CD86 (in co-expression cluster with with HLA-DRA), ALDH1A1 (expressed in classical monocytes and downregulated in severe inflammation in correlation with HLA-DRA), CCR2 (classical monocyte and monocyte state MS1 in severe inflammation), VCAN (classical monocyte and monocyte state MS1 in severe inflammation), CDKN1C (non classical monocyte), module neutrophil mature/base (genes expressed more generally in neutrophils), MME (neutrophil, strongly decreased expression in severe inflammation), IL1B, TNF, and CASP1 (3 genes upregulated in inflammation), interferon gamma induced genes, interferon alpha induced genes, BLVRA (induction involving interferon, mainly monocyte), GYG1 and LDHA (both highly upregulated in severe inflammation), SIM set (contains 16 genes highly upregulated in severe inflammation including GYG1 and LDHA), set FAM20A group extended (9 genes expressed in correlation with FAM20A), HP (potentially indicating STAT3 dependent gene expression in

severe inflammation), GC-2 set (induction by GC in severe inflammation), VSIG4 (induced by GC in monocytes in severe inflammation), CD163 (induced by GC in monocytes and neutrophils in severe inflammation), band 1, band 2, and proliferation (3 gene modules together indicating immature neutrophils in severe inflammation), T cells (T naive), MERTK (upregulated in neutrophil and monocyte in severe inflammation, functionally indicative for efferocytosis), PPARG (highly upregulated, mainly in M2 monocytes in severe inflammation), MAFB, HMOX1, and MARCO (mainy expressed in monocytes, upregulated in severe inflammation), C1QABC (C1QA, B and C genes, upregulated expression in inflammation in non-classical monocytes, and in monocyte state MS3 in severe inflammation), a set named "with C1Q " (4 genes expressed in correlation with C1Qs in severe inflammation including NR1H3). Rankings of several of these marker genes, and of ARG1 (induction by GC in neutrophil in severe inflammation) were also determined for gene expression profiles specifically obtained to indicate negative correlation, using adequate probesets with highest negative correlation, and are color coded in red. Gene expression correlation profiles and gene marker (combinations) were ordered to indicate relevant gene groups. Visible groups corresponded to induction involving interferon in monocytes, genes expressed with C1QA, B, and C in severe inflammation, pro-inflammatory expression ("inflammation"), severe inflammation (in different combinations with FAM20A, HP, or GC induction), induction by interferon gamma and alpha, immature neutrophils, and T cells. Negative expression correlation was visible, more generally between groups of genes that were either upregulated or down regulated during severe inflammation, for example between marker genes GYG1 and MME, and between "SIM" genes and genes expressed in naive T cells. Clusters of tighter co-expression (modules), as seen in meta analysis, include "antigen presentation" (cluster with HLA-DRA), a cluster with PEA15, a cluster with MME (mature neutrophil CD-10), a cluster with CASP1 (inflammation involving induction by interferon), a cluster with GYG1 (mainly from neutrophil in severe inflammation), a smaller cluster with FAM20A, and a cluster of GC induced genes in severe inflammation (GC-2) as indicated. <u>Added for comparison</u> are corresponding differential gene expression data for whole blood in burn shock (gse77791, microarray (Plassais et al., 2017)), sepsis (gse66099, microarray (Sweeney et al., 2015)), sepsis (gse154918, RNA seq (Herwanto et al., 2021)), differential expression in sepsis, and in i*n vivo* interferon treatment for monocytes and neutrophils (gse60424, RNA seq (Linsley et al., 2014)), differential gene expression data for whole blood

in mild respiratory viral infection (gse68310, beadchip array (Zhai et al., 2015)), and differential expression for isolated monocyte and dendritic cell types in health (gse35457, beadchip array (Haniffa et al., 2012)). In case of experiment gse68310, differential expression is shown separately for influenza, or for respiratory viral infection not involving influenza. Upregulation during inflammation in mild respiratory viral infection, as visible by plotting, was scored to take into account the variable background signals of different probes for a given gene. Only probes with highest expression values in experiments gse68310 and gse3547 were used for DEG analysis, except for a few preferred probes indicated in bold. DEG profiles from burn shock and sepsis showed a difference with respect to induction by interferon, which was absent in burn shock, but variably present in sepsis. In contrast, *in vivo* interferon treatment, and mild respiratory viral infection mainly indicated genes that are upregulated by interferon, or by both interferon and interleukins. DEG profiles from blood in severe inflammation, and from monocytes and neutrophils in sepsis, broadly agreed with patterns of correlated gene expression. Differential expression given as log2 fold change (log2FC), color coded in red to green for upregulation, and downregulation, respectively. Corresponding p values in grey for insignificant ($p > 0.05$). Ratios of gene expression values between different cell types color coded in blue. The main source of expression in blood, as judged by correlation characteristics and differential expression, is tentatively summarized for each gene (description). **Sheet 5)** List of datasets in 2 collections used for gene expression correlation profiling, either in the absence or presence of severe inflammation. **Sheet 6)** Overview of gene modules and sets used as markers in correlation analysis. **Sheet 7)** Overview of datasets used in comparisons with correlation patterns, and dataset sample groups used for differential gene expression analys

S5 Table

Differential expression of GC signature genes upon GC treatment *in vivo* and between circadian time points, fold increase and p values.

Unpaired differential expression was calculated for 6 experiments, and unpaired t tests were performed to determine significance. **gds3864**, PBMC, intravenous GC, time series, 4 individuals (Carlet et al., 2010), DEGs, 2h and 6h versus 0h and 24h time points. **gse67255**, PBMC, intravenous hydrocortisone, time series, 18 individuals (Olnes et al., 2016), DEGs, 1h

and 4h versus 0h, 12h, and 24h time points excluding S021 samples. **gds3704**, PBMC, fatty acids consumption, 0h and 6h time points, 21 individuals (Bouwens et al., 2010). **gse110160**, whole blood, prednisolone, time series, 24 individuals (Hu et al., 2018), DEGs 4h GC versus rest of samples excluding 2h GC and 8h GC. **gse46743**, whole blood, dexamethasone orally, 0h and 3h time points, 160 individuals (Arloth et al., 2015). **gds2767**, peripheral blood leukocytes, beverage consumption, time series, 4 times 6 individuals (Baty et al., 2006), DEGs, 12h versus 0h, 1h, 2h, and 4h time points excluding MBGrap samples. **Sheet 1**) DEG rankings in 6 different experiments with corresponding p values for differential expression. Genes are listed according to their original rankings in GC signatures 1 and 2 with marker genes and marker gene sets added. **Sheets 2-7**) GC signature 1 and 2 genes, marker genes, and marker gene sets ranked according to differential expression of all probesets on each experiment platform. Genes and the specific probesets (ID_REF) used, genes present in GC signatures or genes used as marker, log 2 fold change values (Log2FC), P values, and DEG rankings as indicated for different experiments. **Sheet 8**) genes in the marker gene sets used in this analysis for T cells, B cells, neutrophils, monocytes , NK cells, and early gene expression.

S6 Table

Immune cell and tissue specific gene expression correlation profiles.

Gene expression datasets of 6 different immune cell types, and tissues muscle, skin, and fat were edited as required and put in 9 separate collections. Genes were ranked by average expression correlation with a query gene for a given dataset collection. Similar results for selected query genes were averaged to obtain a ranked gene list for each collection. **Sheets 1-15)** included in separate sheets are the top 2000 ranking genes in 15 gene expression correlation profiles. Correlation with expression of GC induced genes in different immune cells (CD4, CD8, NK, B cell, neutrophil not from severe inflammation, and monocyte not from severe inflammation), and tissues (muscle GC, skin GC, fat GC), correlation with clock driven genes in tissues (circadian, muscle, skin, fat), and correlation with antiphasic ARNTL gene expression in tissues (circadian ARNTL, muscle, skin, fat). Note, a marked inflammation signal in muscle, and inflammatory neutrophil infiltration in fat tissue from obese patients, in agreement with immunohistochemical data (Shah et al., 2010), occurred at the time of

upregulated ARNTL mRNA in the circadian evening. Separate rankings in correlation profiles corresponding to each query gene used to obtain the final profiles are also included. **Sheet 16**) overview of datasets and subsets in the separate collections, dataset editing, number of samples of each dataset/subset in a collection, the number of query genes used to obtain each gene expression correlation profile, and the total number of genes in the profiles.

S7 Table

Go analysis of immune cell and tissue specific gene expression correlation profiles.

Sheet 1) GO term enrichment analysis performed for biological process on the top 1000 genes of each GC correlation profile obtained for separated immune cells and tissues, as well as on CLOCK, and gene ARNTL profiles for tissues only (S6 Table) with a FDR (false discovery rate) of < 0.05. Shown are related GO terms recurring in different profiles. **Sheet 2**) related GO terms boxed, significantly enriched values color coded in green.

S8 Table

Analysis of gene expression correlation profiles obtained for separated cells and tissues

Comparison of GC driven gene expression correlation profiles obtained for separated immune cells and tissues, using the top 200 ranking genes in each GC profile in S6 Table, and corresponding gene regulation by GC treatment assayed *in vitro*. Presence of profile genes in GC signatures 1 and 2 as indicated, gene rankings in profiles color coded in green. # N/A denotes a ranking above 2000 in profile, or more rarely, gene absent in profile. DEGs from in *in vitro* GC treatment of primary human cell types (gse112101, (Franco et al., 2019)). Log2 fold change of GC treated cell samples and corresponding control samples, color coded in red (up regulation) and green (down regulation), corresponding p values (paired t test, FDR adjusted) color coded in green, basal expression ratios color coded in blue.

S9 Table

Analysis of gene expression correlation profiles from monocytes, and neutrophils, either in the absence, or in the presence of severe inflammation.

Gene markers (columns) and gene profiles (rows) tentatively ordered to indicate relevant groups of gene expression such as corresponding to cell type, inflammation, and GC induction. **Sheet 1**) Ranking of marker gene (combinations) in gene expression correlation profiles obtained for relevant genes (rows, n = 183), using datasets on monocytes in the absence of severe inflammation, color coded in green. Marker gene (combinations) include immediate early genes (eg FOSB), genes upregulated during mild inflammation (eg MCL1), interferon gamma induced genes, interferon alpha induced genes, gene induction involving interferon in non-classical / intermediary monocytes (IFI27, C2, C1QA/B/C), FCER1A (marker for myeloid dendritic cells in monocyte separations), CDKN1C (non-classical monocytes), VCAN, and CCR2 (both classical monocyte), and GC induced genes (GC1 set, TSC22D3, DDIT4). Visible groups correspond to *in vitro* activation, mild inflammation involving interferon, antigen presentation, myeloid dendritic cells including VSIG4, non-classical monocytes, distinct groups with either VCAN or CCR2, and induction by GC. Added for comparison are data (gse60424) showing *in vitro* activation caused by monocyte separation from whole blood, and gene induction in monocytes by interferon treatment *in vivo,* color coded in red to green for upregulation and downregulation, respectively. In case of comparing monocytes with blood, color white was set at approximate enrichment level for monocyte expressed gene VCAN. Samples used for differential gene expression in gse60424 (Linsley et al., 2014)are monocytes (n = 14, excluding sepsis and interferon treatment) versus blood (n = 14, excluding sepsis and interferon treatment), to indicate *in vitro* activation, and monocytes after interferon treatment (n =3), versus monocytes (n = 14, excluding sepsis and interferon treatment), to indicate induction by interferon treatment *in vivo*. **Sheet 2**) Ranking of marker gene (combinations) in gene expression correlation profiles obtained for selected genes (rows, n = 365), using datasets on monocytes in the presence of severe inflammation, color coded in green. Genes tested include the top 200 ranking genes from a gene expression correlation profile obtained for monocytes in severe inflammation (S10 Table, sheet 8), several GC signature genes, and additional relevant genes for grouping. Marker gene (combinations) include FOSB (immediate early expression), interferon gamma induction, interferon alpha induction, CDKN1C (non-classical monocyte), FCER1A (a marker for mDCs in monocyte separations), VCAN (classical monocyte), CD86 (to indicate co-expression with HLA-DRA, which is downregulated in severe inflammation), a set of genes co-expressed with FAM20A, 3 C1Q genes, induction by GC (sets GC-2 and GC-1), and genes

used as controls to indicate gene expression correlation profiles mainly originating from contaminating neutrophils, NK cells, and platelets. Visible groups correspond to *in vitro* activation, a group of genes upregulated in mild inflammation, possibly *in vivo*, a group similar to mild inflammation involving interferon, non-classical monocytes, a small group for myeloid dendritic cells, a group of downregulated genes such as HLA-DRA, a large group of upregulated genes co-expresssed with VCAN in severe inflammation, a group of genes with FAM20A including HP and RETN, a distinct group of upregulated genes with C1QA/B/C such as VSIG4 and LYVE1, induction by GC, and groups of contaminating cells. Added for comparison are data (gse60424 (Linsley et al., 2014)) showing expression ratios between monocytes, and neutrophils, in controls in the absence of sepsis or interferon treatment (n = 14 each), and in sepsis (n = 3 each). Also added for comparison, differential gene expression between monocytes from sepsis patients and healthy people (gse133822(Washburn et al., 2019)), and data for induction by GC treatment of monocytes from healthy people *in vitro* (gse112101(Franco et al., 2019)), both color coded in red to green for upregulation and downregulation, respectively. Corresponding p values (paired t test, in case of DEGs from gse112101) color coded white for significant, and grey for insignificant ($p > 0.05$). **Sheet 3**) Ranking of marker gene (combinations) in gene expression correlation profiles obtained for relevant genes (rows, n = 158), using datasets on neutrophils in the absence of severe inflammation, color coded in green. Marker gene combinations include immediate early genes (eg FOSB), genes upregulated in mild inflammation (GK), interferon gamma induced genes, interferon alpha induced genes, neutrophil primary granules, (band 1), neutrophil non primary granules (band 2), induction by GC (gene sets GC NA and GC NB), eosinophil, and monocyte (VCAN, MARCO). Visible groups correspond to *in vitro* activation, mild inflammation without interferon, mild inflammation involving interferon, neutrophil bands, basal/mature neutrophil, induction by GC, eosinophils, and contaminating monocytes. Added for comparison are data (gse60424(Linsley et al., 2014)) showing *in vitro* activation caused by neutrophil separation from whole blood (EARLY in vitro), and gene induction *in vivo* in neutrophils by interferon treatment of MS patients (IFN MS in vivo), color coded in red to green for upregulation and downregulation, respectively. In case of comparing neutrophils with blood, color white was set at approximate enrichment level for neutrophil expressed gene TNFRSF10C. Samples used for differential gene expression in gse60424 are neutrophils (n = 14, excluding sepsis and interferon treatment) versus blood (n = 14,

excluding sepsis and interferon treatment), to indicate *in vitro* activation, and neutrophils after interferon treatment (n =3), versus neutrophils (n = 14, excluding sepsis and interferon treatment), to indicate induction by interferon treatment *in vivo*. Log2 fold change shown, NA, gene absent from experiment, none, no detection in samples. **Sheet 4**) Ranking of marker gene (combinations) in gene expression correlation profiles obtained for selected genes (rows, n = 436), using datasets on neutrophils in the presence of severe inflammation, color coded in green. Genes tested include the top 200 ranking genes from a gene expression correlation profile obtained for neutrophils in severe inflammation (similar to S10 Table, sheet 9), several GC signature genes, and additional relevant genes for grouping. Marker gene (combinations) include immediate early genes (eg FOSB), genes upregulated in mild inflammation (ICAM1, SOD2), interferon gamma induced genes, interferon alpha induced genes, neutrophil primary granules, (band 1), neutrophil non primary granules (band 2), genes MME and GYG1 with strong negative expression correlation in neutrophils in severe inflammation, a larger set of genes upregulated in severe inflammation including GYG1 (SIMgr), a set of genes co-expressed with FAM20A, and 2 gene sets to indicate induction by GC (GC NC, and GC ND). Visible groups correspond to *in vitro* activation, a group similar to mild inflammation with IL1B, a group similar to mild inflammation involving interferon, basal/mature neutrophil, immature neutophil, immature/severe inflammatory neutrophil expressing MMP8, RETN and HP, severe inflammatory neutrophil expressing GYG1 and other "SIM" genes, a small group with FAM20A, and several groups of induction by GC (eg group nr1 with gene markers for severe inflammation including OLAH, and group nr4 without, including FLT3). Added for comparison are data (gse60424) showing expression ratios between monocytes, and neutrophils, in controls in the absence of sepsis or interferon treatment (n = 14 each), and in sepsis (n = 3 each). Also added for comparison, differential gene expression between granulocytes from septic shock patients and presurgical controls (gse123729(Coulibaly et al., 2019)), and data for induction by GC treatment of neutrophils from healthy people *in vitro* (gse112101(Franco et al., 2019)), both color coded in red to green for upregulation, and downregulation, respectively. Corresponding p values (paired t test, in case of DEGs from gse112101) color coded white for significant, and grey for insignificant ($p > 0.05$). **Sheets 5-9**) Reciprocal ranking in gene expression correlation profiles (rows) obtained using 5 collections of datasets on separated monocyte and neutrophils, with or without severe inflammation. Genes listed in same order in all 5 sheets for easy

comparison, in rows and in columns. Profile rankings color coded in green from 1 (high) to 500 (low). Tested genes in profiles include all genes shown in figures 11 (overview of gene induction by GC in homeostasis, and during severe inflammation), and 12 (overview of gene expression in homeostasis, inflammation, and during severe inflammation), and additional marker genes for different (contaminating) cell types, and early *in vitro* activation. Groups of profiles mainly originating from different contaminating cell types color coded in grey (column IMPURE), groups of profiles mainly originating from induction by GC color coded in darkgreen (strong) and light green (weaker) (column GC), groups of profiles mainly originating from gene expression in severe inflammation color coded in purple (column SEVERE). Mean correlation coefficients of highest ranking 10 genes (excluding profile query gene) in profiles color coded from red (higher) to blue (lower) (column COR-10), Number of supporting datasets for each profile as given and as color coded (column SETS). Note, some profiles originating from severe inflammation can also be found in collections of datasets on control separated cells, due to low frequency presence of corresponding contaminating samples. Such profiles can be recognized by the presence of marker genes for severe inflammation, and / or by lower mean correlation coefficients in top ranking genes. **Sheet 5**) using collection of datasets on monocytes in the absence of severe inflammation, collection same as in sheet 1. **Sheet 6**) using another collection of 4 datasets on monocytes in the absence of severe inflammation. **Sheet 7**) using collection of datasets on monocytes in severe inflammation, collection same as in sheet 2. **Sheet 8**) using collection of datasets on neutrophils in the absence of severe inflammation, collection same as in sheet 3. **Sheet 9**) using collection of datasets on neutrophils in the presence of severe inflammation, collection same as in sheet 4. **Sheet 10**) Overview of dataset collections used in gene expression correlation analysis, and datasets used for comparison of differential expression. **Sheet 11**) Overview of gene sets used as marker gene combinations in sheets 1-4.

S10 Table

Gene expression correlation profiles of GC induced genes in blood, monocytes, and neutrophils either in the absence or in the presence of severe inflammation

Sheet 1) Correlation profile with a bias for gene expression originating from NK cells and other lymphocytes, obtained by using gene DDIT4 as a query, on selected datasets from a

collection of 62 blood datasets excluding severe inflammation. **Sheet 2**) Correlation profile with a bias for gene expression in neutrophils, obtained by using 3 query genes, as indicated, on a collection of 62 blood datasets excluding severe inflammation. **Sheet 3**) Correlation profile also with a bias for gene expression in neutrophils, obtained by using 3 query genes, as indicated, on selected datasets from a collection of 62 blood datasets excluding severe inflammation. **Sheet 4**) Correlation profile with a bias for gene expression in monocytes in severe inflammation, obtained by using 4 query genes, as indicated, on a collection of 38 blood datasets on severe inflammation. **Sheet 5**) Correlation profile with a bias for gene expression in neutrophils in severe inflammation, obtained by using 4 query genes, as indicated, on a collection of 38 blood datasets on severe inflammation. **Sheet 6**) Correlation profile obtained by using 9 query genes, as indicated, on a large dataset for isolated monocytes from MESA participants (gse56045, (Reynolds et al., 2014)), and 4 subsets thereof. **Sheet 7**) Correlation profile obtained by using 8 query genes, as indicated, on a collection of datasets (n = 5) on isolated neutrophils from healthy people. **Sheet 8**) Correlation profile obtained by using 6 query genes, as indicated, on a collection of datasets (n = 7) on monocytes and PBMCs in severe inflammation **Sheet 9**) Correlation profile obtained by using 7 query genes, as indicated, on a collection of datasets (n = 6) on neutrophils and granulocytes in severe inflammation. **Sheet 10**) Comparison 1. High ranking genes from expression correlation profiles of GC induction, in neutrophils, and monocytes, either in the presence or absence of severe inflammation, as well as genes present in GC signatures 1 and 2, were compared across profiles. A selection of 778 genes was tested which included several duplo's due to the presence of gene aliases on different platforms. HUGO approved gene symbols for aliases and for previous gene symbols are provided where necessary (Tweedie et al., 2021). Gene expression correlation profiles used in comparison include profiles provided in sheets 1-9, gene expression profiles corresponding with GC signatures 1 and 2 (S1 Table), as well as gene expression profiles obtained earlier for lymphoid cells, myeloid cells, and tissues (S6 Table). Gene rankings (1-200) in different profiles are color coded in green. Of note, GC induced genes may "drop down" in correlation profiles from separated cells due to the presence of contaminating cells or due to *in vitro* gene activation. **Sheet 11**) Comparison 2. Same 778 genes tested for basal expression and inducibility by GC *in vitro* in B cells, CD4 T cells, monocytes, and neutrophils (gse112101, (Franco et al., 2019)), and for expression in B cells, CD4 T cells, monocytes, neutrophils, and

NK cells in the absence of severe inflammation, as well as in monocytes and neutrophils during sepsis (gse60424, (Linsley et al., 2014)). Many high ranking genes in expression correlation profiles are GC inducible *in vitro.* Basal expression ratio's between B cells (B contr.), CD4 T cells (CD4 contr.), monocytes (M contr.), and neutrophils (N contr.) color coded in blue. Log2 fold change in GC treatment compared with controls in B cells (log B GC/-), CD4 T cells (log CD4 GC/-), monocytes (log M GC/-), and neutrophils (log N GC/-) color coded in red (upregulation) to green (downregulation). Corresponding p values given for paired two sided t-tests, color coded in green for $p < 0.05$. Additional basal expression ratio's of 778 genes between different immune cell controls in the absence of severe inflammation in experiment gse60424 (controls include healthy, type 1 diabetes, amyotrophic lateral sclerosis, and multiple sclerosis excluding interferon beta treatment). Expression ratio's between B cells (B contr.), CD4 T cells (CD4 contr.), CD8 T cells (CD8 contr.), monocytes (M contr.), neutrophils (N contr.), and natural killer cells (NK contr.) color coded in blue. Expression of many genes, especially from GC signature 2, is upregulated in monocytes and neutrophil samples isolated from sepsis patients (3 samples each). Log2 fold change between sepsis samples and controls color coded in red (upregulation) to green (downregulation) for monocytes (log M seps/M contr.) and neutrophils (log N seps/N contr.). Genes with detectable expression only in sepsis or only in control samples (value #DIV/0!) color coded brown and green, respectively. Differential expression between monocytes and neutrophils broadly corresponds with different ranking of genes in corresponding expression correlation profiles. Log2 of expression ratio's between monocytes and neutrophils in control samples (log M contr./ N contr.) and in sepsis samples (log M seps/N seps), color coded from yellow (more in monocytes) to blue (more in neutrophils). Genes with detectable expression only in monocytes or only in neutrophils (value #DIV/0!) color coded yellow and blue, respectively. **Sheet 12**) Ranking of GC induced marker gene (combinations) in a total of 939 gene expression correlation profiles obtained on 6 different dataset collections of monocytes, neutrophils, and blood, either in the absence, or in the presence of severe inflammation. The total number of 939 genes were selected as top ranking genes present in several GC driven gene expression correlation profiles (see below). Not all 939 genes were used for expression correlation profiling with each of the 6 dataset collections, due to computing time limitations. Instead, genes were only used on the dataset collection in which they had been present as top ranking genes in the earlier profiles. Gene expression

profiles obtained on the 6 different dataset collections were put in one table for comparison. Ranking of marker gene (combinations) in different gene expression correlation profiles was visualized in green using identical cut offs for shading in case of marker gene and marker gene combinations used multiple times. NA denotes missing values for genes that were not found as top ranking genes in GC driven gene expression profiles using the corresponding dataset collection, and therefore not tested.

The following is an overview of the selection of top ranking genes (total unique = 939) from several different gene expression correlation profiles, the dataset collections used for obtaining new gene expression correlation profiles in turn, and of marker gene (combinations) for which a ranking in the new profiles was determined.

Genes (final n = 335) for correlation expression profiling using a collection of large dataset gse56045 (MESA study, (Reynolds et al., 2014)) and 4 subsets thereof, on control monocytes (n= 5), were selected as the top 200 ranking genes from gene expression correlation profile 1a (S10 Table, sheet 6, COR monocyte non severe), obtained on the same collection (n = 5), as well as the top 200 ranking genes from profile 2a (S6 Table , sheet 6, mono not severe GC) obtained on a different dataset collection of control monocytes (n = 4). The ranking of 5 marker gene (combinations) in different profiles was visualized in green. Marker gene combinations include the GC1 set, and combinations GC MA , and GC MB, as used to obtain gene expression correlation profiles 2a and 1a, respectively.

Genes (final n = 302) for correlation expression profiling using a collection of datasets on monocytes in severe inflammation (n = 7) were selected as the top ranking 200 genes in each of 2 gene expression correlation profiles 1b (S10 Table, sheet 8, COR mono severe), and 2b, which used another set of GC induced marker genes (KLF9, ZBTB16, IRS2, PER1), both obtained on the same collection of 7 datasets. The ranking of 5 marker gene (combinations) in different profiles was visualized in green. Marker gene combinations include the GC1 and GC2 sets, and a 6 gene combination GC MC, as used to obtain gene expression correlation profile 1b.

Genes (final n = 100) for correlation expression profiling using a collection of datasets on control neutrophils (n= 5) were selected from 2 gene expression correlation profiles 1c (S10 Table, sheet 7, COR neutrophil non severe), and 2c (S6 Table , sheet 5, neutro not severe GC)

obtained on the same collection of 5 datasets. The ranking of 5 marker gene (combinations) in different profiles was visualized in green. Marker gene combinations include the GC1 set, and combinations GC NA ,and GC NB, as used to obtain gene expression correlation profiles 2c and 1c, respectively.

Genes (final n = 196) for correlation expression profiling using a collection of datasets on neutrophils in severe inflammation (n = 6) were selected as the top ranking 200 genes from a single gene expression correlation profile similar to 1d (S10 Table, sheet 9, COR neutro severe), obtained on the same dataset collection. The ranking of 6 marker gene (combinations) in different profiles was visualized in green. Marker gene combinations include the GC1 and GC2 sets, combination GC NC as used to obtain gene expression correlation profile 1d, and a combination GC ND (IL1R1, IL1R2, IL18R1, IL18RAP).

Genes (final n = 232) for correlation expression profiling using a collection of blood datasets excluding severe inflammation (n = 62), included all genes from GC signature 1, as well as the top ranking 50 genes in each of 4 gene expression correlation profiles, 1e (control monocytes, S10 Table, sheet 6), 2e (control monocytes, S6 Table, sheet 6), 3e (control neutrophils, S10 Table, sheet 7), and 4e (control neutrophils, S6 Table, sheet 5), and also 13 genes recurring in different profiles. The ranking of 8 marker gene (combinations) in different profiles was visualized in green. Marker gene combinations include the GC1, and GC2 sets, and a combination of 2 genes PIK3IP1 and FBXO32 (GC T bias), which was used to indicate gene expression correlation profiles with relatively strong contribution from T cells. Genes SPON2, CLEC4E, and GPER1 (GPER) were used to indicate gene profiles with relatively strong contribution from NK cells, neutrophils, and monocytes, respectively.

Genes (final n = 410) for correlation expression profiling using a collection of blood datasets on severe inflammation (n = 38), included all genes from GC signature 2, as well as the top 200 genes in each of 4 gene expression correlation profiles, 1f (blood severe, S10 Table, sheet 4, bias monocyte), 2f (blood severe, S10 Table, sheet 5, bias neutrophil), 3f (monocytes severe S10 Table, sheet 8), and 4f (neutrophils severe S10 Table, sheet 9). The ranking of 10 marker gene (combinations) in different profiles was visualized in green. Marker gene combinations include the GC1, and GC2 sets, and 4 gene combinations GC M bias (n = 4), C1Q (n = 3), GC N bias (n = 4), and GC ND (n = 4). Gene combinations GC M bias and GC N bias as used to obtain profiles 1f and 2f, respectively, on the same collection of 38

datasets on severe inflammation. Gene combination GC M bias (ADAMTS2, VSIG4, FLT3, RNASE1) was used to indicate gene expression profiles more generally originating from monocytes present during severe inflammation. Gene combination C1Q (C1QA, C1QB, and C1QC) was used to indicate gene expression profiles mostly originating from C1Q positive monocytes (monocytes MS3) present during severe inflammation. Gene LYVE1 was also included as a potentially interesting monocyte marker in severe inflammation. Overlapping gene combinations GC N bias (IL18R1, IL18RAP, OLAH, ARG1), GC ND (IL1R1, IL1R2, IL18R1, IL18RAP), and gene ARG1, were used to indicate gene expression profiles mainly originating from neutrophils present during severe inflammation. **Sheet 13**) Overview of 6 dataset collections used in gene expression correlation analysis of GC induction. **Sheet 14**) Overview of GC1 and GC2 gene sets, and other GC gene marker combinations used for analysis.

S11 Table

GC treatment induced DEGs in septic shock and burn shock

Sheet 1) DEGs in PBMCs at 0h and 6h time points after fatty acid consumption (GDS3704, 84 samples, dietary unsaturated and saturated fatty acid consumption, (Bouwens et al., 2010)), experiment added to compare DEGs induced by circadian GC in health, and by GC treatment in shock. Expression of circadian, GC induced genes is higher at 0h time point in the experiment. Log2 fold change and P values given for unpaired and paired two-sided t-tests of highest 2000 upregulated DEGs. **Sheet 2**) Upregulated DEGs in whole blood of septic shock patients beween either 24h GC or 24h placebo treatment (gse106878, sequential hydrocortisone injections, 24 GC treated patients, 23 placebo treated patients, (Kolte, 2020)). Log2 fold change and P values given for unpaired two sided t-tests of highest 2000 upregulated DEGs. **Sheet 3**) Upregulated DEGs in whole blood of burn shock patients treated with GC, comparing one day and 120h time points with placebo treatment at one day and at 120h time points (gse77791, priming dose and continuous infusion of hydrocortisone, time series, 15 GC treated individuals, 15 placebo treated individuals, (Plassais et al., 2017)). Log2 fold change and P values given for unpaired two sided t-tests of highest 2000 upregulated DEGs. **Sheet 4**) Upregulated and downregulated DEGs in whole blood of GC treated pediatric septic shock. Differentially expressed Affymetrix probe sets with provided gene annotation (256) after corticosteroid treatment of pediatric septic shock (Wong et al., 2014).

Probe sets corresponding with GC 1 and 2 signature genes as indicated. DEGs present in GC signatures 1 and 2 marked in red, DEGs also present in gse106878 and gse77791 marked in orange. **Sheet 5**) A comparison of GC treatment induced DEGs in septic shock (gse106878, (Kolte, 2020)), and in burn shock (gse77791, (Plassais et al., 2017)). The highest 2000 upregulated DEGs in GC treatment of either septic shock or burn shock, with P values less than 0.05, were profiled together for expression in monocytes and neutrophils during sepsis (gse60424, (Linsley et al., 2014)), inducibility by GC *in vitro* in monocytes and neutrophils (gse112101, (Franco et al., 2019)), as well as for gene expression correlation characteristics. A large proportion of DEGs are shared between both experiments, including several genes with different gene symbols on both platforms (eg OLAH and THEDC1). HUGO approved gene symbols are provided where necessary. Log2 fold change (log GC/-) and corresponding P values given for unpaired two sided t-tests. Several highly induced genes in GC treatment of septic shock and burn shock are also upregulated in monocytes, neutrophils or in both cell types during sepsis (3 samples for each cell type) compared with controls (healthy, type 1 diabetes, amyotrophic lateral sclerosis, and multiple sclerosis excluding interferon beta treatment, 14 samples for each cell type in total) in experiment gse60424 (Linsley et al., 2014). Ratios of gene expression in monocytes (M) and neutrophils (N) in controls and sepsis as indicated, and color coded in blue. Log2 of gene expression ratio between monocytes and neutrophils during sepsis added separately (log M seps N seps), and color coded from yellow (more in monocytes) to blue (more in neutrophils). Gene inducibility by GC *in vitro* in monocytes and in neutrophils isolated from healthy people (GSE112101, (Franco et al., 2019)) broadly agrees with a direct effect of GC on DEGs seen *in vivo*. Log2 of gene expression ratio between GC treated monocytes and GC treated neutrophils (log M GC/N GC) color coded from yellow (more in monocytes) to blue (more in neutrophils). Log2 fold change and P values given for unpaired and paired two sided t-tests of differential expression in monocytes (MGC) and neutrophils (NGC). Gene expression correlation profiles indicate induction by endogenous and/or exogenous GC during severe inflammation, in broad agreement with DEGs seen *in vivo* in GC treated shock. Correlation profiles for DDIT4, TSC22D3, and IRS2 obtained on a collection of 62 datasets excluding severe inflammation added for comparison with correlation profiles obtained on a collection of 38 data sets on severe inflammation. IL18R1 and OLAH profiles with bias for expression originating from neutrophils, and ADAMTS2 and VSIG4 from monocytes. Gene expression correlation profiles

obtained on collections of datasets on separated monocytes (7) and neutrophils (6) in severe inflammation, using suitable GC induced marker gene sets GCa and GCb. Of note, GC induced genes may "drop down" in correlation profiles from separated cells due to the presence of contaminating cells or due to *in vitro* gene activation. Rankings in correlation profiles color coded in green. **Sheet 6**) Overview of dataset collections used in gene expression correlation analysis of GC induction. **Sheet 7**) Two sets of GC induced genes, used as markers in gene expression correlation analysis of monocytes and neutrophils in severe inflammation, specifically in this comparison.

S12 Table

Gene modules and gene probe identifiers used in screening different illnesses

Gene composition for modules T cell, SIM (severe inflammatory myeloid), FAM20A cluster, GC-2, GC-1, interferon gamma, and interferon alpha as provided. For determining module expression values in microarray experiments, module genes were represented by a single adequate probe identifier chosen for microarray platforms GPL570 (Affymetrix Human Genome U133 Plus 2.0 array), GPL10558 (Illumina HumanHT-12 V4.0 expression beadchip), and GPL6947 (Illumina HumanHT-12 V3.0 expression beadchip) as given. Illumina platforms GPL10558 and GPL6947 share probe identifiers, but with a small number of specific gene probes absent from GPL6947 compared to GPL10558. Gene module expression values were calculated according to methods.

REFERENCES

Abdelaziz, M. H., Abdelwahab, S. F., Wan, J., Cai, W., Huixuan, W., Jianjun, C., . . . Xu, H. (2020). Alternatively activated macrophages; a double-edged sword in allergic asthma. *J Transl Med*, *18*(1), 58. https://doi.org/10.1186/s12967-020-02251-w

Ackermann, K., Revell, V. L., Lao, O., Rombouts, E. J., Skene, D. J., & Kayser, M. (2012). Diurnal rhythms in blood cell populations and the effect of acute sleep deprivation in healthy young men. *Sleep*, *35*(7), 933-940. https://doi.org/10.5665/sleep.1954

Alder, M. N., Opoka, A. M., & Wong, H. R. (2018). The glucocorticoid receptor and cortisol levels in pediatric septic shock. *Critical Care*, *22*(1). https://doi.org/10.1186/s13054-018-2177-8

Alexander, R. A. (1990). A note on averaging correlations. *Bulletin of the Psychonomic Society*, *28*(4). https://doi.org/10.3758/BF03334037

Altman, M. C., Gill, M. A., Whalen, E., Babineau, D. C., Shao, B., Liu, A. H., . . . Jackson, D. J. (2019). Transcriptome networks identify mechanisms of viral and nonviral asthma exacerbations in children. *Nature Immunology*, *20*(5). https://doi.org/10.1038/s41590-019-0347-8

Altman, M. C., Rinchai, D., Baldwin, N., Toufiq, M., Whalen, E., Garand, M., . . . Chaussabel, D. (2021). Development of a fixed module repertoire for the analysis and interpretation of blood transcriptome data. *Nature Communications*, *12*(1). https://doi.org/10.1038/s41467-021-24584-w

Altonsy, M. O., Sasse, S. K., Phang, T. L., & Gerber, A. N. (2014). Context-dependent cooperation between nuclear factor κB (NF-κB) and the glucocorticoid receptor at a TNFAIP3 intronic enhancer: A mechanism to maintain negative feedback control of inflammation. *Journal of Biological Chemistry*, *289*(12). https://doi.org/10.1074/jbc.M113.545178

Annane, D., Pastores, S. M., Rochwerg, B., Arlt, W., Balk, R. A., Beishuizen, A., . . . Van Den Berghe, G. (2017). Guidelines for the diagnosis and management of Critical Illness-Related Corticosteroid Insufficiency (CIRCI) in critically ill patients (Part I): Society of Critical Care Medicine (SCCM) and European Society of Intensive Care Medicine (ESICM) 2017. *Critical Care Medicine*, *45*(12). https://doi.org/10.1097/CCM.0000000000002737

Arloth, J., Bogdan, R., Weber, P., Frishman, G., Menke, A., Wagner, K. V., . . . Binder, E. B. (2015). Genetic Differences in the Immediate Transcriptome Response to Stress Predict Risk-Related Brain Function and Psychiatric Disorders. *Neuron*, *86*(5). https://doi.org/10.1016/j.neuron.2015.05.034

Arnardottir, E. S., Nikonova, E. V., Shockley, K. R., Podtelezhnikov, A. A., Anafi, R. C., Tanis, K. Q., . . . Pack, A. I. (2014). Blood-gene expression reveals reduced circadian rhythmicity in individuals resistant to sleep deprivation. *Sleep*, *37*(10). https://doi.org/10.5665/sleep.4064

Aschenbrenner, A. C., Mouktaroudi, M., Krämer, B., Oestreich, M., Antonakos, N., Nuesch-Germano, M., . . . Ulas, T. (2021). Disease severity-specific neutrophil signatures in blood transcriptomes stratify COVID-19 patients. *Genome medicine*, *13*(1). https://doi.org/10.1186/s13073-020-00823-5

Athar, A., Füllgrabe, A., George, N., Iqbal, H., Huerta, L., Ali, A., . . . Brazma, A. (2019). ArrayExpress update - From bulk to single-cell expression data. *Nucleic Acids Research*, *47*(D1). https://doi.org/10.1093/nar/gky964

Auguie, B., Antonov, A., Auguie, M. B., & Robinson, D. (2017). *Package 'gridExtra'* (Miscellaneous Functions for "Grid" Graphics, Issue.

Avendaño-Ortiz, J., Maroun-Eid, C., Martín-Quirós, A., Toledano, V., Cubillos-Zapata, C., Gómez-Campelo, P., . . . López-Collazo, E. (2018). PD-L1 Overexpression During Endotoxin Tolerance Impairs the Adaptive Immune Response in Septic Patients via HIF1α. *J Infect Dis*, *217*(3), 393-404. https://doi.org/10.1093/infdis/jix279

Banchereau, R., Jordan-Villegas, A., Ardura, M., Mejias, A., Baldwin, N., Xu, H., . . . Ramilo, O. (2012). Host immune transcriptional profiles reflect the variability in clinical disease manifestations in patients with Staphylococcus aureus infections. *PLoS One*, *7*(4), e34390. https://doi.org/10.1371/journal.pone.0034390

Barrett, T., Wilhite, S. E., Ledoux, P., Evangelista, C., Kim, I. F., Tomashevsky, M., . . . Soboleva, A. (2013). NCBI GEO: Archive for functional genomics data sets - Update. *Nucleic Acids Research*, *41*(D1). https://doi.org/10.1093/nar/gks1193

Baty, F., Facompré, M., Wiegand, J., Schwager, J., & Brutsche, M. H. (2006). Analysis with respect to instrumental variables for the exploration of microarray data structures. *BMC Bioinformatics*, *7*. https://doi.org/10.1186/1471-2105-7-422

Binkowska, A. M., Michalak, G., & Slotwiński, R. (2015). Current views on the mechanisms of immune responses to trauma and infection. In *Central European Journal of Immunology* (Vol. 40).

Blankley, S., Graham, C. M., Turner, J., Berry, M. P. R., Bloom, C. I., Xu, Z., . . . O'Garra, A. (2016). The transcriptional signature of active tuberculosis reflects symptom status in extra-pulmonary

and pulmonary tuberculosis. *PLoS ONE*, *11*(10). https://doi.org/10.1371/journal.pone.0162220

Bloom, C. I., Graham, C. M., Berry, M. P. R., Rozakeas, F., Redford, P. S., Wang, Y., . . . O'Garra, A. (2013). Transcriptional Blood Signatures Distinguish Pulmonary Tuberculosis, Pulmonary Sarcoidosis, Pneumonias and Lung Cancers. *PLoS ONE*, *8*(8). https://doi.org/10.1371/journal.pone.0070630

Bone, R. C. (1996). Sir Isaac Newton, sepsis, SIRS, and CARS. In *Critical Care Medicine* (Vol. 24).

Bouhlel, M. A., Derudas, B., Rigamonti, E., Dièvart, R., Brozek, J., Haulon, S., . . . Chinetti-Gbaguidi, G. (2007). PPARγ Activation Primes Human Monocytes into Alternative M2 Macrophages with Anti-inflammatory Properties. *Cell Metabolism*, *6*(2). https://doi.org/10.1016/j.cmet.2007.06.010

Bouwens, M., Bromhaar, M. G., Jansen, J., Müller, M., & Afman, L. A. (2010). Postprandial dietary lipid-specific effects on human peripheral blood mononuclear cell gene expression profiles. *American Journal of Clinical Nutrition*, *91*(1). https://doi.org/10.3945/ajcn.2009.28586

Brachat, A. H., Grom, A. A., Wulffraat, N., Brunner, H. I., Quartier, P., Brik, R., . . . Morris, P. (2017). Early changes in gene expression and inflammatory proteins in systemic juvenile idiopathic arthritis patients on canakinumab therapy. *Arthritis Research and Therapy*, *19*(1). https://doi.org/10.1186/s13075-016-1212-x

Braschi, B., Denny, P., Gray, K., Jones, T., Seal, R., Tweedie, S., . . . Bruford, E. (2019). Genenames.org: The HGNC and VGNC resources in 2019. *Nucleic Acids Research*, *47*(D1). https://doi.org/10.1093/nar/gky930

Braun, D. A., Fribourg, M., & Sealfon, S. C. (2013). Cytokine response is determined by duration of receptor and signal transducers and activators of transcription 3 (STAT3) activation. *Journal of Biological Chemistry*, *288*(5). https://doi.org/10.1074/jbc.M112.386573

Braun, R., Kath, W. L., Iwanaszko, M., Kula-Eversole, E., Abbott, S. M., Reid, K. J., . . . Allada, R. (2018). Universal method for robust detection of circadian state from gene expression. *Proceedings of the National Academy of Sciences of the United States of America*, *115*(39). https://doi.org/10.1073/pnas.1800314115

Briegel, J., Huge, V., & Möhnle, P. (2018). Hydrocortisone in septic shock: All the questions answered? In *Journal of Thoracic Disease* (Vol. 10).

Burnham, K. L., Davenport, E. E., Radhakrishnan, J., Humburg, P., Gordon, A. C., Hutton, P., . . . Knight, J. C. (2017). Shared and distinct aspects of the sepsis transcriptomic response to fecal peritonitis and pneumonia. *American Journal of Respiratory and Critical Care Medicine*, *196*(3). https://doi.org/10.1164/rccm.201608-1685OC

Buttgereit, F. (2021). Glucocorticoids: surprising new findings on their mechanisms of actions. In *Annals of the Rheumatic Diseases* (Vol. 80).

Carlet, J., Payen, D., & Opal, S. M. (2020). Steroids for sepsis and ARDS: this eternal controversy remains with COVID-19. *Lancet*, *396*(10259), e61-e62. https://doi.org/10.1016/s0140-6736(20)32132-2

Carlet, M., Janjetovic, K., Rainer, J., Schmidt, S., Panzer-Grümayer, R., Mann, G., . . . Kofler, R. (2010). Expression, regulation and function of phosphofructo-kinase/fructose-biphosphatases (PFKFBs) in glucocorticoid-induced apoptosis of acute lymphoblastic leukemia cells. *BMC Cancer*, *10*. https://doi.org/10.1186/1471-2407-10-638

Cazalis, M. A., Lepape, A., Venet, F., Frager, F., Mougin, B., Vallin, H., . . . Monneret, G. (2014). Early and dynamic changes in gene expression in septic shock patients: a genome-wide approach. *Intensive Care Medicine Experimental*, *2*(1). https://doi.org/10.1186/s40635-014-0020-3

Chan, E. D., Chan, M. M., Chan, M. M., & Marik, P. E. (2020). Use of glucocorticoids in the critical care setting: Science and clinical evidence. In *Pharmacology and Therapeutics* (Vol. 206).

Chantzichristos, D., Svensson, P. A., Garner, T., Glad, C. A. M., Walker, B. R., Bergthorsdottir, R., . . . Johannsson, G. (2021). Identification of human glucocorticoid response markers using integrated multi-omic analysis from a randomized crossover trial. *eLife*, *10*. https://doi.org/10.7554/ELIFE.62236

Chaussabel, D., & Baldwin, N. (2014). Democratizing systems immunology with modular transcriptional repertoire analyses. In *Nat Rev Immunol* (Vol. 14, pp. 271-280). https://doi.org/10.1038/nri3642

Chaussabel, D., Quinn, C., Shen, J., Patel, P., Glaser, C., Baldwin, N., . . . Pascual, V. (2008). A modular analysis framework for blood genomics studies: application to systemic lupus erythematosus. *Immunity*, *29*(1), 150-164. https://doi.org/10.1016/j.immuni.2008.05.012

Chen, P., Li, J., Barnes, J., Kokkonen, G. C., Lee, J. C., & Liu, Y. (2002). Restraint of Proinflammatory Cytokine Biosynthesis by Mitogen-Activated Protein Kinase Phosphatase-1 in Lipopolysaccharide-Stimulated Macrophages. *The Journal of Immunology*, *169*(11). https://doi.org/10.4049/jimmunol.169.11.6408

Coulibaly, A., Velásquez, S. Y., Sticht, C., Figueiredo, A. S., Himmelhan, B. S., Schulte, J., . . . Lindner, H. A. (2019). AKIRIN1: A potential new reference gene in human natural killer cells and granulocytes in sepsis. *International Journal of Molecular Sciences*, *20*(9). https://doi.org/10.3390/ijms20092290

Cox, K. H., & Takahashi, J. S. (2019). Circadian clock genes and the transcriptional architecture of the clock mechanism. *Journal of Molecular Endocrinology*, *63*(4). https://doi.org/10.1530/JME-19-0153

Dankers, W., Northcott, M., Bennett, T., D'Cruz, A., Sherlock, R., Gearing, L. J., . . . Jones, S. A. (2022). Type 1 interferon suppresses expression and glucocorticoid induction of glucocorticoid-induced leucine zipper (GILZ). *Front Immunol*, *13*, 1034880. https://doi.org/10.3389/fimmu.2022.1034880

Darcy, C. J., Minigo, G., Piera, K. A., Davis, J. S., McNeil, Y. R., Chen, Y., . . . Woodberry, T. (2014). Neutrophils with myeloid derived suppressor function deplete arginine and constrain T cell function in septic shock patients. *Critical Care*, *18*(4). https://doi.org/10.1186/cc14003

de Kleijn, S., Kox, M., Sama, I. E., Pillay, J., van Diepen, A., Huijnen, M. A., . . . Pickkers, P. (2012). Transcriptome kinetics of circulating neutrophils during human experimental endotoxemia. *PLoS ONE*, *7*(6). https://doi.org/10.1371/journal.pone.0038255

De Lucena, D. D., & Rangel, É. B. (2018). Glucocorticoids use in kidney transplant setting. In *Expert Opinion on Drug Metabolism and Toxicology* (Vol. 14).

DeBerg, H. A., Zaidi, M. B., Altman, M. C., Khaenam, P., Gersuk, V. H., Campos, F. D., . . . Linsley, P. S. (2018). Shared and organism-specific host responses to childhood diarrheal diseases revealed by whole blood transcript profiling. *PLoS ONE*, *13*(1). https://doi.org/10.1371/journal.pone.0192082

Demaret, J., Venet, F., Friggeri, A., Cazalis, M.-A., Plassais, J., Jallades, L., . . . Monneret, G. (2015). Marked alterations of neutrophil functions during sepsis-induced immunosuppression. *Journal of Leukocyte Biology*, *98*(6). https://doi.org/10.1189/jlb.4a0415-168rr

Desgeorges, T., Caratti, G., Mounier, R., Tuckermann, J., & Chazaud, B. (2019). Glucocorticoids shape macrophage phenotype for tissue repair. In *Frontiers in Immunology* (Vol. 10).

Dolinay, T., Kim, Y. S., Howrylak, J., Hunninghake, G. M., An, C. H., Fredenburgh, L., . . . Choi, A. M. K. (2012). Inflammasome-regulated cytokines are critical mediators of acute lung injury. *American Journal of Respiratory and Critical Care Medicine*, *185*(11). https://doi.org/10.1164/rccm.201201-0003OC

Dragulescu, A. A. (2012). Package ' xlsx '. *Cell*, *9*.

Dubois-Camacho, K., Ottum, P. A., Franco-Muñoz, D., De La Fuente, M., Torres-Riquelme, A., Díaz-Jiménez, D., . . . Hermoso, M. A. (2017). Glucocorticosteroid therapy in inflammatory bowel diseases: From clinical practice to molecular biology. In *World Journal of Gastroenterology* (Vol. 23).

Dufort, M. J., Hanniffy, S., Conde-Álvarez, R., Arce-Gorvel, V., Altman, M. C., Khaenam, P., . . . Gorvel, J.-P. (2016). Gene expression profiles predict treatment outcomes in Brucellosis. *the Journal of Immunology*, *196*. https://doi.org/https://doi.org/10.4049/jimmunol.196.Supp.66.21

Ehrchen, J., Steinmüller, L., Barczyk, K., Tenbrock, K., Nacken, W., Eisenacher, M., . . . Roth, J. (2007). Glucocorticoids induce differentiation of a specifically activated, anti-inflammatory subtype of human monocytes. *Blood*, *109*(3). https://doi.org/10.1182/blood-2006-02-001115

Ehrchen, J. M., Roth, J., & Barczyk-Kahlert, K. (2019). More than suppression: Glucocorticoid action on monocytes and macrophages. In *Frontiers in Immunology* (Vol. 10).

ElTanbouly, M. A., Zhao, Y., Schaafsma, E., Burns, C. M., Mabaera, R., Cheng, C., & Noelle, R. J. (2021). VISTA: A Target to Manage the Innate Cytokine Storm. *Frontiers in Immunology*, *11*. https://doi.org/10.3389/fimmu.2020.595950

Enwonwu, C. O., Afolabi, B. M., Salako, L. A., Idigbe, E. O., Al-Hassan, H., & Rabiu, R. A. (1999). Hyperphenylalaninaemia in children with falciparum malaria. *QJM - Monthly Journal of the Association of Physicians*, *92*(9). https://doi.org/10.1093/qjmed/92.9.495

Escoter-Torres, L., Caratti, G., Mechtidou, A., Tuckermann, J., Uhlenhaut, N. H., & Vettorazzi, S. (2019). Fighting the fire: Mechanisms of inflammatory gene regulation by the glucocorticoid receptor. In *Frontiers in Immunology* (Vol. 10).

Estupiñán-Moreno, E., Ortiz-Fernández, L., Li, T., Hernández-Rodríguez, J., Ciudad, L., Andrés-León, E., . . . Martín, J. (2022). Methylome and transcriptome profiling of giant cell arteritis monocytes reveals novel pathways involved in disease pathogenesis and molecular response to glucocorticoids. *Ann Rheum Dis*, *81*(9), 1290-1300. https://doi.org/10.1136/annrheumdis-2022-222156

Field, A. P. (2005). Is the meta-analysis of correlation coefficients accurate when population correlations vary? *Psychological Methods*, *10*(4). https://doi.org/10.1037/1082-989X.10.4.444

Fleuriet, J., Heming, N., Meziani, F., Reignier, J., Declerq, P. L., Mercier, E., . . . Annane, D. (2023). Rapid rEcognition of COrticosteRoiD resistant or sensitive Sepsis (RECORDS): study protocol for a multicentre, placebo-controlled, biomarker-guided, adaptive Bayesian design basket trial. *BMJ Open*, *13*(3), e066496. https://doi.org/10.1136/bmjopen-2022-066496

Franco, L. M., Gadkari, M., Howe, K. N., Sun, J., Kardava, L., Kumar, P., . . . Germain, R. N. (2019). Immune regulation by glucocorticoids can be linked to cell type–dependent transcriptional responses. *Journal of Experimental Medicine*, *216*(2). https://doi.org/10.1084/jem.20180595

Galvan, M. D., Hulsebus, H., Heitker, T., Zeng, E., & Bohlson, S. S. (2014). Complement protein C1q and adiponectin stimulate mer tyrosine kinase-dependent engulfment of apoptotic cells through a shared pathway. *Journal of Innate Immunity*, *6*(6). https://doi.org/10.1159/000363295

Gentile, L. F., Cuenca, A. G., Efron, P. A., Ang, D., Bihorac, A., McKinley, B. A., . . . Moore, F. A. (2012). Persistent inflammation and immunosuppression: A common syndrome and new horizon for surgical intensive care. In *Journal of Trauma and Acute Care Surgery* (Vol. 72).

Gerber, A. N., Newton, R., & Sasse, S. K. (2021). Repression of transcription by the glucocorticoid receptor: A parsimonious model for the genomics. *Journal of Biological Chemistry*, *296*. https://doi.org/10.1016/j.jbc.2021.100687

Gharib, S. A., McMahan, R. S., Eddy, W. E., Long, M. E., Parks, W. C., Aitken, M. L., & Manicone, A. M. (2019). Transcriptional and functional diversity of human macrophage repolarization. *Journal of Allergy and Clinical Immunology*, *143*(4). https://doi.org/10.1016/j.jaci.2018.10.046

Gorgani, N. N., Thathaisong, U., Mukaro, V. R. S., Poungpair, O., Tirimacco, A., Hii, C. S. T., & Ferrante, A. (2011). Regulation of CRIg expression and phagocytosis in human macrophages by arachidonate, dexamethasone, and cytokines. *American Journal of Pathology*, *179*(3). https://doi.org/10.1016/j.ajpath.2011.05.021

Groselj-Grenc, M., Ihan, A., & Derganc, M. (2008). Neutrophil and monocyte CD64 and CD163 expression in critically ill neonates and children with sepsis: Comparison of fluorescence intensities and calculated indexes. *Mediators of Inflammation*, *2008*. https://doi.org/10.1155/2008/202646

Grzywa, T. M., Sosnowska, A., Matryba, P., Rydzynska, Z., Jasinski, M., Nowis, D., & Golab, J. (2020). Myeloid Cell-Derived Arginase in Cancer Immune Response. In *Frontiers in Immunology* (Vol. 11).

Guignant, C., Venet, F., Planel, S., Demaret, J., Gouel-Chéron, A., Nougier, C., . . . Monneret, G. (2013). Increased MerTK expression in circulating innate immune cells of patients with septic shock. *Intensive Care Medicine*, *39*(9). https://doi.org/10.1007/s00134-013-3006-9

Guo, B., Huang, X., Cooper, S., & Broxmeyer, H. E. (2017). Glucocorticoid hormone-induced chromatin remodeling enhances human hematopoietic stem cell homing and engraftment. *Nature Medicine*, *23*(4). https://doi.org/10.1038/nm.4298

Guo, X., Higgs, B. W., Bay-Jensen, A. C., Karsdal, M. A., Yao, Y., Roskos, L. K., & White, W. I. (2015). Suppression of T Cell Activation and Collagen Accumulation by an Anti-IFNAR1 mAb, Anifrolumab, in Adult Patients with Systemic Sclerosis. *Journal of Investigative Dermatology*, *135*(10). https://doi.org/10.1038/jid.2015.188

Gupta, S., Jain, A., Syed, S. N., Snodgrass, R. G., Pflüger-Müller, B., Leisegang, M. S., . . . Namgaladze, D. (2018). IL-6 augments IL-4-induced polarization of primary human macrophages through synergy of STAT3, STAT6 and BATF transcription factors. *OncoImmunology*, *7*(10). https://doi.org/10.1080/2162402X.2018.1494110

Gustafson, M. P., DiCostanzo, A. C., Wheatley, C. M., Kim, C. H., Bornschlegl, S., Gastineau, D. A., . . . Dietz, A. B. (2017). A systems biology approach to investigating the influence of exercise and fitness on the composition of leukocytes in peripheral blood. *J Immunother Cancer*, *5*, 30. https://doi.org/10.1186/s40425-017-0231-8

Guthridge, J. M., Lu, R., Tran, L. T. H., Arriens, C., Aberle, T., Kamp, S., . . . James, J. A. (2020). Adults with systemic lupus exhibit distinct molecular phenotypes in a cross-sectional study. *EClinicalMedicine*, *20*. https://doi.org/10.1016/j.eclinm.2020.100291

Haniffa, M., Shin, A., Bigley, V., McGovern, N., Teo, P., See, P., . . . Ginhoux, F. (2012). Human tissues contain CD141hi cross-presenting dendritic cells with functional homology to mouse CD103+ nonlymphoid dendritic cells. *Immunity*, *37*(1), 60-73. https://doi.org/10.1016/j.immuni.2012.04.012

He, Y. J., Xu, J. Q., Sun, M. M., Fang, X. Z., Peng, Z. K., Pan, S. W., . . . Shang, Y. (2020). Glucocorticoid-Induced Leucine Zipper: A Promising Marker for Monitoring and Treating Sepsis. *Front Immunol*, *11*, 606649. https://doi.org/10.3389/fimmu.2020.606649

Heideveld, E., Hampton-O'Neil, L. A., Cross, S. J., van Alphen, F. P. J., van den Biggelaar, M., Toye, A. M., & van den Akker, E. (2018). Glucocorticoids induce differentiation of monocytes towards macrophages that share functional and phenotypical aspects with erythroblastic island macrophages. *Haematologica*, *103*(3), 395-405. https://doi.org/10.3324/haematol.2017.179341

Hellebrekers, P., Vrisekoop, N., & Koenderman, L. (2018). Neutrophil phenotypes in health and disease. In *European Journal of Clinical Investigation* (Vol. 48).

Herberg, J. A., Kaforou, M., Wright, V. J., Shailes, H., Eleftherohorinou, H., Hoggart, C. J., . . . Levin, M. (2016). Diagnostic test accuracy of a 2-transcript host RNA signature for discriminating bacterial vs viral infection in febrile children. *JAMA - Journal of the American Medical Association*, *316*(8). https://doi.org/10.1001/jama.2016.11236

Herwanto, V., Tang, B., Wang, Y., Shojaei, M., Nalos, M., Shetty, A., . . . Schughart, K. (2021). Blood transcriptome analysis of patients with uncomplicated bacterial infection and sepsis. *BMC Research Notes*, *14*(1). https://doi.org/10.1186/s13104-021-05488-w

Hesselink, L., Spijkerman, R., Van Wessem, K. J. P., Koenderman, L., Leenen, L. P. H., Huber-Lang, M., & Hietbrink, F. (2019). Neutrophil heterogeneity and its role in infectious complications after severe trauma. In *World Journal of Emergency Surgery* (Vol. 14).

Hibbert, J. E., Currie, A., & Strunk, T. (2018). Sepsis-Induced Immunosuppression in Neonates. *Front Pediatr*, *6*, 357. https://doi.org/10.3389/fped.2018.00357

Hofer, T. P. J., Frankenberger, M., Mages, J., Lang, R., Hoffmann, R., Colige, A., & Ziegler-Heitbrock, L. (2008). Tissue-specific induction of ADAMTS2 in monocytes and macrophages by

glucocorticoids. *Journal of Molecular Medicine*, *86*(3). https://doi.org/10.1007/s00109-007-0284-0

Hoffman, J. A., Trotter, K. W., Day, C. R., Ward, J. M., Rodriguez, J., & Archer, T. K. (2021). Differential Activity and Utilization of Glucocorticoid Receptor Binding Sites Yields Transcriptional Heterogeneity. *Journal of the Endocrine Society*, *5*(Supplement_1). https://doi.org/10.1210/jendso/bvab048.1021

Hotchkiss, R. S., Moldawer, L. L., Opal, S. M., Reinhart, K., Turnbull, I. R., & Vincent, J. L. (2016). Sepsis and septic shock. In *Nature Reviews Disease Primers* (Vol. 2).

Hu, Y., Carman, J. A., Holloway, D., Kansal, S., Fan, L., Goldstine, C., . . . Nadler, S. G. (2018). Development of a Molecular Signature to Monitor Pharmacodynamic Responses Mediated by In Vivo Administration of Glucocorticoids. *Arthritis and Rheumatology*, *70*(8). https://doi.org/10.1002/art.40476

Huang, Y., Zaas, A. K., Rao, A., Dobigeon, N., Woolf, P. J., Veldman, T., . . . Hero, A. O., 3rd. (2011). Temporal dynamics of host molecular responses differentiate symptomatic and asymptomatic influenza a infection. *PLoS Genet*, *7*(8), e1002234. https://doi.org/10.1371/journal.pgen.1002234

Huber, W., Carey, V. J., Gentleman, R., Anders, S., Carlson, M., Carvalho, B. S., . . . Morgan, M. (2015). Orchestrating high-throughput genomic analysis with Bioconductor. *Nature Methods*, *12*(2). https://doi.org/10.1038/nmeth.3252

Huber-Lang, M., Lambris, J. D., & Ward, P. A. (2018). Innate immune responses to trauma review-article. In *Nature Immunology* (Vol. 19).

Hughey, J. J. (2017). Machine learning identifies a compact gene set for monitoring the circadian clock in human blood. *Genome Medicine*, *9*(1). https://doi.org/10.1186/s13073-017-0406-4

Hung, T., Pratt, G. A., Sundararaman, B., Townsend, M. J., Chaivorapol, C., Bhangale, T., . . . Behrens, T. W. (2015). The Ro60 autoantigen binds endogenous retroelements and regulates inflammatory gene expression. *Science*, *350*(6259), 455-459. https://doi.org/10.1126/science.aac7442

Idaghdour, Y., Quinlan, J., Goulet, J. P., Berghout, J., Gbeha, E., Bruat, V., . . . Awadalla, P. (2012). Evidence for additive and interaction effects of host genotype and infection in malaria. *Proceedings of the National Academy of Sciences of the United States of America*, *109*(42). https://doi.org/10.1073/pnas.1204945109

Ince, L. M., Weber, J., & Scheiermann, C. (2019). Control of leukocyte trafficking by stress-associated hormones. In *Frontiers in Immunology* (Vol. 10).

Inouye, M., Silander, K., Hamalainen, E., Salomaa, V., Harald, K., Jousilahti, P., . . . Peltonen, L. (2010). An immune response network associated with blood lipid levels. *PLoS Genetics*, *6*(9). https://doi.org/10.1371/journal.pgen.1001113

Jarczak, D., Kluge, S., & Nierhaus, A. (2021). Sepsis—Pathophysiology and Therapeutic Concepts. In *Frontiers in Medicine* (Vol. 8).

Jiang, Y., Rosborough, B. R., Chen, J., Das, S., Kitsios, G. D., McVerry, B. J., . . . Ray, P. (2020). Single cell RNA sequencing identifies an early monocyte gene signature in acute respiratory distress syndrome. *JCI Insight*, *5*(13). https://doi.org/10.1172/jci.insight.135678

Johannsson, G., Falorni, A., Skrtic, S., Lennernäs, H., Quinkler, M., Monson, J. P., & Stewart, P. M. (2015). Adrenal insufficiency: Review of clinical outcomes with current glucocorticoid replacement therapy. In *Clinical Endocrinology* (Vol. 82).

Johnson, B., Herman, N., Grill, D., Anderson, P., Miller, A., Johnson, J., . . . Ceridon Richert, M. (2014). Peripheral blood mononuclear cell gene expression in healthy adults rapidly transported to high altitude. *Advances in Genomics and Genetics*. https://doi.org/10.2147/agg.s66784

Johnson, T. A., Paakinaho, V., Kim, S., Hager, G. L., & Presman, D. M. (2021). Genome-wide binding potential and regulatory activity of the glucocorticoid receptor's monomeric and dimeric forms. *Nature Communications*, *12*(1). https://doi.org/10.1038/s41467-021-22234-9

Jubb, A. W., Young, R. S., Hume, D. A., & Bickmore, W. A. (2016). Enhancer Turnover Is Associated with a Divergent Transcriptional Response to Glucocorticoid in Mouse and Human

Macrophages. *The Journal of Immunology*, *196*(2). https://doi.org/10.4049/jimmunol.1502009

Juss, J. K., House, D., Amour, A., Begg, M., Herre, J., Storisteanu, D. M. L., . . . Chilvers, E. R. (2016). Acute respiratory distress syndrome neutrophils have a distinct phenotype and are resistant to phosphoinositide 3-kinase inhibition. *American Journal of Respiratory and Critical Care Medicine*, *194*(8). https://doi.org/10.1164/rccm.201509-1818OC

Kalinski, P. (2012). Regulation of Immune Responses by Prostaglandin E 2. *The Journal of Immunology*, *188*(1). https://doi.org/10.4049/jimmunol.1101029

Kim, H., & Baumann, H. (1997). The carboxyl-terminal region of STAT3 controls gene induction by the mouse haptoglobin promoter. *Journal of Biological Chemistry*, *272*(23). https://doi.org/10.1074/jbc.272.23.14571

Kim, O. Y., Monsel, A., Bertrand, M., Coriat, P., Cavaillon, J. M., & Adib-Conquy, M. (2010). Differential down-regulation of HLA-DR on monocyte subpopulations during systemic inflammation. *Critical Care*, *14*(2). https://doi.org/10.1186/cc8959

Kolde, R. (2019). Package 'pheatmap': Pretty heatmaps. *Version 1.0.12*.

Kolte, A. (2020). Improving the outcome of the critically ill with cortico- and sex-steroids employing clinico-transcriptomics approaches. In. Jena: Digitale Bibliothek Thueringen.

Komorowski, M., Green, A., Tatham, K. C., Seymour, C., & Antcliffe, D. (2022). Sepsis biomarkers and diagnostic tools with a focus on machine learning. *EBioMedicine*, *86*, 104394. https://doi.org/10.1016/j.ebiom.2022.104394

Kossenkov, A. V., Qureshi, R., Dawany, N. B., Wickramasinghe, J., Liu, Q., Majumdar, R. S., . . . Showe, L. C. (2019). A Gene Expression Classifier from Whole Blood Distinguishes Benign from Malignant Lung Nodules Detected by Low-Dose CT. *Cancer Res*, *79*(1), 263-273. https://doi.org/10.1158/0008-5472.can-18-2032

Koth, L. L., Solberg, O. D., Peng, J. C., Bhakta, N. R., Nguyen, C. P., & Woodruff, P. G. (2011). Sarcoidosis blood transcriptome reflects lung inflammation and overlaps with tuberculosis. *American Journal of Respiratory and Critical Care Medicine*, *184*(10). https://doi.org/10.1164/rccm.201106-1143OC

Kovtun, A., Messerer, D. A. C., Scharffetter-Kochanek, K., Huber-Lang, M., & Ignatius, A. (2018). Neutrophils in tissue trauma of the skin, bone, and lung: Two sides of the same coin. In *Journal of Immunology Research* (Vol. 2018).

Kuan, P. F., Waszczuk, M. A., Kotov, R., Clouston, S., Yang, X., Singh, P. K., . . . Luft, B. J. (2017). Gene expression associated with PTSD in World Trade Center responders: An RNA sequencing study. *Translational Psychiatry*, *7*(12). https://doi.org/10.1038/s41398-017-0050-1

Kwok, I., Becht, E., Xia, Y., Ng, M., Teh, Y. C., Tan, L., . . . Ng, L. G. (2020). Combinatorial Single-Cell Analyses of Granulocyte-Monocyte Progenitor Heterogeneity Reveals an Early Uni-potent Neutrophil Progenitor. *Journal of Cleaner Production*. https://doi.org/10.1016/j.immuni.2020.06.005

König, R., Kolte, A., Ahlers, O., Oswald, M., Krauss, V., Roell, D., . . . Bauer, M. (2021). Use of IFNγ/IL10 Ratio for Stratification of Hydrocortisone Therapy in Patients With Septic Shock. *Frontiers in Immunology*, *12*. https://doi.org/10.3389/fimmu.2021.607217

Labrecque, N., & Cermakian, N. (2015). Circadian clocks in the immune system. In *Journal of Biological Rhythms* (Vol. 30).

Laing, E. E., Möller-Levet, C. S., Poh, N., Santhi, N., Archer, S. N., & Dijk, D. J. (2017). Blood transcriptome based biomarkers for human circadian phase. *eLife*, *6*. https://doi.org/10.7554/eLife.20214

Langfelder, P., & Horvath, S. (2008). WGCNA: an R package for weighted correlation network analysis. *BMC Bioinformatics*, *9*, 559. https://doi.org/10.1186/1471-2105-9-559

Lauber, K., Keppeler, H., Munoz, L. E., Koppe, U., Schröder, K., Yamaguchi, H., . . . Herrmann, M. (2013). Milk fat globule-EGF factor 8 mediates the enhancement of apoptotic cell clearance by glucocorticoids. *Cell Death and Differentiation*, *20*(9). https://doi.org/10.1038/cdd.2013.82

Lei, W., Liu, D., Sun, M., Lu, C., Yang, W., Wang, C., . . . Yang, Y. (2021). Targeting STAT3: A crucial modulator of sepsis. In *Journal of Cellular Physiology* (Vol. 236).

Leliefeld, P. H. C., Wessels, C. M., Leenen, L. P. H., Koenderman, L., & Pillay, J. (2016). The role of neutrophils in immune dysfunction during severe inflammation. In *Critical Care* (Vol. 20).

Leligdowicz, A., & Matthay, M. A. (2019). Heterogeneity in sepsis: New biological evidence with clinical applications. In *Critical Care* (Vol. 23).

Liepelt, A., Hohlstein, P., Gussen, H., Xue, J., Aschenbrenner, A. C., Ulas, T., . . . Tacke, F. (2020). Differential Gene Expression in Circulating CD14(+) Monocytes Indicates the Prognosis of Critically Ill Patients with Sepsis. *J Clin Med*, *9*(1). https://doi.org/10.3390/jcm9010127

Linsley, P. S., Speake, C., Whalen, E., & Chaussabel, D. (2014). Copy number loss of the interferon gene cluster in melanomas is linked to reduced T cell infiltrate and poor patient prognosis. *PLoS ONE*, *9*(10). https://doi.org/10.1371/journal.pone.0109760

Liu, C., Martins, A. J., Lau, W. W., Rachmaninoff, N., Chen, J., Imberti, L., . . . Tsang, J. S. (2021). Time-resolved systems immunology reveals a late juncture linked to fatal COVID-19. *Cell*, *184*(7). https://doi.org/10.1016/j.cell.2021.02.018

Liu, D., Huang, S. Y., Sun, J. H., Zhang, H. C., Cai, Q. L., Gao, C., . . . Zeng, L. (2022). Sepsis-induced immunosuppression: mechanisms, diagnosis and current treatment options. *Mil Med Res*, *9*(1), 56. https://doi.org/10.1186/s40779-022-00422-y

Liu, N., Jiang, C., Cai, P., Shen, Z., Sun, W., Xu, H., . . . Qu, K. (2021). Single-cell analysis of COVID-19, sepsis, and HIV infection reveals hyperinflammatory and immunosuppressive signatures in monocytes. *Cell Reports*, *37*(1). https://doi.org/10.1016/j.celrep.2021.109793

Liu, T. Y., Burke, T., Park, L. P., Woods, C. W., Zaas, A. K., Ginsburg, G. S., & Hero, A. O. (2016). An individualized predictor of health and disease using paired reference and target samples. *BMC Bioinformatics*, *17*(1). https://doi.org/10.1186/s12859-016-0889-9

Loboda, A., Kraft, W. K., Fine, B., Joseph, J., Nebozhyn, M., Zhang, C., . . . Lum, P. Y. (2009). Diurnal variation of the human adipose transcriptome and the link to metabolic disease. *BMC Med Genomics*, *2*, 7. https://doi.org/10.1186/1755-8794-2-7

Lundell, L. S., Parr, E. B., Devlin, B. L., Ingerslev, L. R., Altıntaş, A., Sato, S., . . . Hawley, J. A. (2020). Time-restricted feeding alters lipid and amino acid metabolite rhythmicity without perturbing clock gene expression. *Nat Commun*, *11*(1), 4643. https://doi.org/10.1038/s41467-020-18412-w

Lurier, E. B., Dalton, D., Dampier, W., Raman, P., Nassiri, S., Ferraro, N. M., . . . Spiller, K. L. (2017). Transcriptome analysis of IL-10-stimulated (M2c) macrophages by next-generation sequencing. *Immunobiology*, *222*(7). https://doi.org/10.1016/j.imbio.2017.02.006

Lévy, Y., Wiedemann, A., Hejblum, B. P., Durand, M., Lefebvre, C., Surénaud, M., . . . Thiébaut, R. (2021). CD177, a specific marker of neutrophil activation, is associated with coronavirus disease 2019 severity and death. *iScience*, *24*(7). https://doi.org/10.1016/j.isci.2021.102711

Lützner, N., Kalbacher, H., Krones-Herzig, A., & Rösl, F. (2012). FOXO3 is a glucocorticoid receptor target and regulates LKB1 and its own expression based on cellular AMP levels via a positive autoregulatory loop. *PLoS ONE*, *7*(7). https://doi.org/10.1371/journal.pone.0042166

Mayerle, J., Den Hoed, C. M., Schurmann, C., Stolk, L., Homuth, G., Peters, M. J., . . . Kuipers, E. (2013). Identification of genetic loci associated with Helicobacter pylori serologic status. *JAMA*, *309*(18). https://doi.org/10.1001/jama.2013.4350

Melo, R. C. N., & Weller, P. F. (2016). Lipid droplets in leukocytes: Organelles linked to inflammatory responses. In *Experimental Cell Research* (Vol. 340).

Mengos, A. E., Gastineau, D. A., & Gustafson, M. P. (2019). The CD14+HLA-DrlO/NEG monocyte: An immunosuppressive phenotype that restrains responses to cancer immunotherapy. In *Frontiers in Immunology* (Vol. 10).

Mo, A., Marigorta, U. M., Arafat, D., Chan, L. H. K., Ponder, L., Jang, S. R., . . . Gibson, G. (2018). Disease-specific regulation of gene expression in a comparative analysis of juvenile idiopathic arthritis and inflammatory bowel disease. *Genome Medicine*, *10*(1). https://doi.org/10.1186/s13073-018-0558-x

Monneret, G., & Venet, F. (2014). Monocyte HLA-DR in sepsis: shall we stop following the flow? *Crit Care*, *18*(1), 102. https://doi.org/10.1186/cc13179

Mortaz, E., Alipoor, S. D., Adcock, I. M., Mumby, S., & Koenderman, L. (2018). Update on neutrophil function in severe inflammation. In *Frontiers in Immunology* (Vol. 9).

Mostafa, M. M., Bansal, A., Michi, A. N., Sasse, S. K., Proud, D., Gerber, A. N., & Newton, R. (2021). Genomic determinants implicated in the glucocorticoid-mediated induction of KLF9 in pulmonary epithelial cells. *Journal of Biological Chemistry*, *296*. https://doi.org/10.1074/jbc.RA120.015755

Murrell, P. (2002). The \pkg{grid} Graphics Package. *\proglang{R} News*, *2*(2).

Nallandhighal, S., Park, G. S., Ho, Y. Y., Opoka, R. O., John, C. C., & Tran, T. M. (2019). Whole-blood transcriptional signatures composed of erythropoietic and NRF2-Regulated genes differ between cerebral malaria and severe malarial anemia. *Journal of Infectious Diseases*, *219*(1). https://doi.org/10.1093/infdis/jiy468

Northcott, M., Gearing, L. J., Nim, H. T., Nataraja, C., Hertzog, P., Jones, S. A., & Morand, E. F. (2021). Glucocorticoid gene signatures in systemic lupus erythematosus and the effects of type I interferon: a cross-sectional and in-vitro study. *The Lancet Rheumatology*, *3*(5). https://doi.org/10.1016/S2665-9913(21)00006-0

Okun, J. G., Conway, S., Schmidt, K. V., Schumacher, J., Wang, X., de Guia, R., . . . Rose, A. J. (2015). Molecular regulation of urea cycle function by the liver glucocorticoid receptor. *Molecular Metabolism*, *4*(10). https://doi.org/10.1016/j.molmet.2015.07.006

Olnes, M. J., Kotliarov, Y., Biancotto, A., Cheung, F., Chen, J., Shi, R., . . . Nussenblatt, R. (2016). Effects of Systemically Administered Hydrocortisone on the Human Immunome. *Sci Rep*, *6*, 23002. https://doi.org/10.1038/srep23002

Ono, S., Tsujimoto, H., Hiraki, S., & Aosasa, S. (2018). Mechanisms of sepsis-induced immunosuppression and immunological modification therapies for sepsis. *Ann Gastroenterol Surg*, *2*(5), 351-358. https://doi.org/10.1002/ags3.12194

Oster, H., Challet, E., Ott, V., Arvat, E., de Kloet, E. R., Dijk, D. J., . . . Van Cauter, E. (2017). The Functional and Clinical Significance of the 24-Hour Rhythm of Circulating Glucocorticoids. *Endocr Rev*, *38*(1), 3-45. https://doi.org/10.1210/er.2015-1080

Overmyer, K. A., Shishkova, E., Miller, I. J., Balnis, J., Bernstein, M. N., Peters-Clarke, T. M., . . . Jaitovich, A. (2021). Large-Scale Multi-omic Analysis of COVID-19 Severity. *Cell Systems*, *12*(1). https://doi.org/10.1016/j.cels.2020.10.003

Pakos-Zebrucka, K., Koryga, I., Mnich, K., Ljujic, M., Samali, A., & Gorman, A. M. (2016). The integrated stress response. *EMBO reports*, *17*(10). https://doi.org/10.15252/embr.201642195

Palmer, N. P., Silvester, J. A., Lee, J. J., Beam, A. L., Fried, I., Valtchinov, V. I., . . . Kohane, I. S. (2019). Concordance between gene expression in peripheral whole blood and colonic tissue in children with inflammatory bowel disease. *PLoS ONE*, *14*(10). https://doi.org/10.1371/journal.pone.0222952

Pan, T., Sun, S., Chen, Y., Tian, R., Chen, E., Tan, R., . . . Qu, H. (2022). Immune effects of PI3K/Akt/HIF-1α-regulated glycolysis in polymorphonuclear neutrophils during sepsis. *Critical Care*, *26*(1). https://doi.org/10.1186/s13054-022-03893-6

Perrin, L., Loizides-Mangold, U., Chanon, S., Gobet, C., Hulo, N., Isenegger, L., . . . Dibner, C. (2018). Transcriptomic analyses reveal rhythmic and CLOCK-driven pathways in human skeletal muscle. *Elife*, *7*. https://doi.org/10.7554/eLife.34114

Petta, I., Dejager, L., Ballegeer, M., Lievens, S., Tavernier, J., De Bosscher, K., & Libert, C. (2016). The Interactome of the Glucocorticoid Receptor and Its Influence on the Actions of Glucocorticoids in Combatting Inflammatory and Infectious Diseases. *Microbiology and Molecular Biology Reviews*, *80*(2). https://doi.org/10.1128/mmbr.00064-15

Pillay, J., Kamp, V. M., Van Hoffen, E., Visser, T., Tak, T., Lammers, J. W., . . . Koenderman, L. (2012). A subset of neutrophils in human systemic inflammation inhibits T cell responses through Mac-1. *Journal of Clinical Investigation*, *122*(1). https://doi.org/10.1172/JCI57990

Plassais, J., Venet, F., Cazalis, M. A., Le Quang, D., Pachot, A., Monneret, G., . . . Textoris, J. (2017). Transcriptome modulation by hydrocortisone in severe burn shock: Ancillary analysis of a prospective randomized trial. *Critical Care*, *21*(1). https://doi.org/10.1186/s13054-017-1743-9

Pottecher, J., Meyer, A., Wenceslau, C. F., Timmermans, K., Hauser, C. J., & Land, W. G. (2019). Editorial: Trauma-induced, DAMP-mediated remote organ injury, and immunosuppression in the acutely Ill patient. In *Frontiers in Immunology* (Vol. 10).

Prekovic, S., Schuurman, K., Mayayo-Peralta, I., Manjón, A. G., Buijs, M., Yavuz, S., . . . Zwart, W. (2021). Glucocorticoid receptor triggers a reversible drug-tolerant dormancy state with acquired therapeutic vulnerabilities in lung cancer. *Nature Communications*, *12*(1). https://doi.org/10.1038/s41467-021-24537-3

Quatrini, L., & Ugolini, S. (2021). New insights into the cell- and tissue-specificity of glucocorticoid actions. In *Cellular and Molecular Immunology* (Vol. 18).

Radom-Aizik, S., Zaldivar, F., Leu, S. Y., & Cooper, D. M. (2009a). A brief bout of exercise alters gene expression and distinct gene pathways in peripheral blood mononuclear cells of early- and late-pubertal females. *Journal of Applied Physiology*, *107*(1). https://doi.org/10.1152/japplphysiol.00121.2009

Radom-Aizik, S., Zaldivar, F., Leu, S. Y., & Cooper, D. M. (2009b). Brief bout of exercise alters gene expression in peripheral blood mononuclear cells of early- and late-pubertal males. *Pediatric Research*, *65*(4). https://doi.org/10.1203/PDR.0b013e3181993473

Raymond, S. L., Holden, D. C., Mira, J. C., Stortz, J. A., Loftus, T. J., Mohr, A. M., . . . Efron, P. A. (2017). Microbial recognition and danger signals in sepsis and trauma. *Biochim Biophys Acta Mol Basis Dis*, *1863*(10 Pt B), 2564-2573. https://doi.org/10.1016/j.bbadis.2017.01.013

Recovery. (2021). Dexamethasone in Hospitalized Patients with Covid-19 - The RECOVERY Collaborative Group. *New England Journal of Medicine*, *384*(8).

Relja, B., & Land, W. G. (2020). Damage-associated molecular patterns in trauma. *Eur J Trauma Emerg Surg*, *46*(4), 751-775. https://doi.org/10.1007/s00068-019-01235-w

Reusch, N., De Domenico, E., Bonaguro, L., Schulte-Schrepping, J., Baßler, K., Schultze, J. L., & Aschenbrenner, A. C. (2021). Neutrophils in COVID-19. In *Frontiers in Immunology* (Vol. 12).

Reyes, M., Filbin, M. R., Bhattacharyya, R. P., Billman, K., Eisenhaure, T., Hung, D. T., . . . Hacohen, N. (2020). An immune-cell signature of bacterial sepsis. In *Nature Medicine* (Vol. 26).

Reyes, M., Filbin, M. R., Bhattacharyya, R. P., Sonny, A., Mehta, A., Billman, K., . . . Hacohen, N. (2021). Plasma from patients with bacterial sepsis or severe COVID-19 induces suppressive myeloid cell production from hematopoietic progenitors in vitro. *Science Translational Medicine*, *13*(598). https://doi.org/10.1126/scitranslmed.abe9599

Reynolds, L. M., Taylor, J. R., Ding, J., Lohman, K., Johnson, C., Siscovick, D., . . . Liu, Y. (2014). Age-related variations in the methylome associated with gene expression in human monocytes and T cells. *Nat Commun*, *5*, 5366. https://doi.org/10.1038/ncomms6366

Rinchai, D., Altman, M. C., Konza, O., Hässler, S., Martina, F., Toufiq, M., . . . Chaussabel, D. (2020). Definition of erythroid cell-positive blood transcriptome phenotypes associated with severe respiratory syncytial virus infection. *Clin Transl Med*, *10*(8), e244. https://doi.org/10.1002/ctm2.244

Ritchie, M. K., Johnson, L. C., Clodfelter, J. E., Pemble, C. W., Fulp, B. E., Furdui, C. M., . . . Lowther, W. T. (2016). Crystal structure and substrate specificity of human thioesterase 2: Insights into the molecular basis for the modulation of fatty acid synthase. *Journal of Biological Chemistry*, *291*(7). https://doi.org/10.1074/jbc.M115.702597

Ronchetti, S., Ricci, E., Migliorati, G., Gentili, M., & Riccardi, C. (2018). How glucocorticoids affect the neutrophil life. In *International Journal of Molecular Sciences* (Vol. 19).

Roszer, T. (2015). Understanding the mysterious M2 macrophage through activation markers and effector mechanisms. In *Mediators of Inflammation* (Vol. 2015).

Russell, J. A. (2018). When and how to use predictive biomarkers for corticosteroid treatment of septic shock. In *Critical Care* (Vol. 22).

Saelens, W., Cannoodt, R., & Saeys, Y. (2018). A comprehensive evaluation of module detection methods for gene expression data. *Nat Commun*, *9*(1), 1090. https://doi.org/10.1038/s41467-018-03424-4

Sano, S., Nakagawa, Y., Iwashima, S., Ishikawa, T., Satake, E., Matsushita, R., . . . Ohzeki, T. (2010). Dynamics of endogenous glucocorticoid secretion and its metabolism in Kawasaki disease. *Steroids*, *75*(12). https://doi.org/10.1016/j.steroids.2010.06.006

Sautron, V., Terenina, E., Gress, L., Lippi, Y., Billon, Y., Larzul, C., . . . Mormède, P. (2015). Time course of the response to ACTH in pig: Biological and transcriptomic study. *BMC Genomics*, *16*(1). https://doi.org/10.1186/s12864-015-2118-8

Schramm, K., Marzi, C., Schurmann, C., Carstensen, M., Reinmaa, E., Biffar, R., . . . Prokisch, H. (2014). Mapping the genetic architecture of gene regulation in whole blood. *PLoS ONE*, *9*(4). https://doi.org/10.1371/journal.pone.0093844

Schrijver, I. T., Théroude, C., & Roger, T. (2019). Myeloid derived suppressor cells sepsis. In *Frontiers in Immunology* (Vol. 10).

Schulte-Schrepping, J., Reusch, N., Paclik, D., Baßler, K., Schlickeiser, S., Zhang, B., . . . Ziebuhr, J. (2020). Severe COVID-19 Is Marked by a Dysregulated Myeloid Cell Compartment. *Cell*, *182*(6). https://doi.org/10.1016/j.cell.2020.08.001

Scicluna, B. P., Klein Klouwenberg, P. M. C., Van Vught, L. A., Wiewel, M. A., Ong, D. S. Y., Zwinderman, A. H., . . . Van Der Poll, T. (2015). A molecular biomarker to diagnose community-acquired pneumonia on intensive care unit admission. *American Journal of Respiratory and Critical Care Medicine*, *192*(7). https://doi.org/10.1164/rccm.201502-0355OC

Sean, D., & Meltzer, P. S. (2007). GEOquery: A bridge between the Gene Expression Omnibus (GEO) and BioConductor. *Bioinformatics*, *23*(14). https://doi.org/10.1093/bioinformatics/btm254

Shah, T. J., Leik, C. E., & Walsh, S. W. (2010). Neutrophil infiltration and systemic vascular inflammation in obese women. *Reprod Sci*, *17*(2), 116-124. https://doi.org/10.1177/1933719109348252

Shalova, I. N., Lim, J. Y., Chittezhath, M., Zinkernagel, A. S., Beasley, F., Hernández-Jiménez, E., . . . Biswas, S. K. (2015). Human monocytes undergo functional re-programming during sepsis mediated by hypoxia-inducible factor-1α. *Immunity*, *42*(3). https://doi.org/10.1016/j.immuni.2015.02.001

Shen, X. F., Cao, K., Jiang, J. P., Guan, W. X., & Du, J. F. (2017). Neutrophil dysregulation during sepsis: an overview and update. In *Journal of Cellular and Molecular Medicine* (Vol. 21).

Shimba, A., & Ikuta, K. (2020). Glucocorticoids Regulate Circadian Rhythm of Innate and Adaptive Immunity. In *Frontiers in Immunology* (Vol. 11).

Silvestre-Roig, C., Fridlender, Z. G., Glogauer, M., & Scapini, P. (2019). Neutrophil Diversity in Health and Disease. *Trends Immunol*, *40*(7), 565-583. https://doi.org/10.1016/j.it.2019.04.012

Singer, M., Deutschman, C. S., Seymour, C., Shankar-Hari, M., Annane, D., Bauer, M., . . . Angus, D. C. (2016). The third international consensus definitions for sepsis and septic shock (sepsis-3). In *JAMA - Journal of the American Medical Association* (Vol. 315).

Singhania, A., Verma, R., Graham, C. M., Lee, J., Tran, T., Richardson, M., . . . O'Garra, A. (2018). A modular transcriptional signature identifies phenotypic heterogeneity of human tuberculosis infection. *Nature Communications*, *9*(1). https://doi.org/10.1038/s41467-018-04579-w

Sinha, S., Rosin, N. L., Arora, R., Labit, E., Jaffer, A., Cao, L., . . . Biernaskie, J. (2022). Dexamethasone modulates immature neutrophils and interferon programming in severe COVID-19. *Nat Med*, *28*(1), 201-211. https://doi.org/10.1038/s41591-021-01576-3

So, A. Y. L., Bernal, T. U., Pillsbury, M. L., Yamamoto, K. R., & Feldman, B. J. (2009). Glucocorticoid regulation of the circadian clock modulates glucose homeostasis. *Proceedings of the National Academy of Sciences of the United States of America*, *106*(41). https://doi.org/10.1073/pnas.0909733106

Steinbrink, J. M., Myers, R. A., Hua, K., Johnson, M. D., Seidelman, J. L., Tsalik, E. L., . . . McClain, M. T. (2021). The host transcriptional response to Candidemia is dominated by neutrophil

activation and heme biosynthesis and supports novel diagnostic approaches. *Genome Medicine*, *13*(1). https://doi.org/10.1186/s13073-021-00924-9

Strehl, C., Ehlers, L., Gaber, T., & Buttgereit, F. (2019). Glucocorticoids-All-Rounders Tackling the Versatile Players of the Immune System. In *Frontiers in immunology* (Vol. 10).

Strickland, B. A., Ansari, S. A., Dantoft, W., & Uhlenhaut, N. H. (2022). How to tame your genes: mechanisms of inflammatory gene repression by glucocorticoids. *FEBS Lett*, *596*(20), 2596-2616. https://doi.org/10.1002/1873-3468.14409

Sweeney, T. E., Shidham, A., Wong, H. R., & Khatri, P. (2015). A comprehensive time-course-based multicohort analysis of sepsis and sterile inflammation reveals a robust diagnostic gene set. *Science Translational Medicine*, *7*(287). https://doi.org/10.1126/scitranslmed.aaa5993

Sweeney, T. E., & Wong, H. R. (2021). Transcriptional markers in response to hydrocortisone in sepsis in ADRENAL: a step toward precision medicine. In *Intensive Care Med* (Vol. 47, pp. 1011-1013). https://doi.org/10.1007/s00134-021-06504-0

Sævik, Å. B., Wolff, A. B., Björnsdottir, S., Simunkova, K., Hynne, M. S., Dolan, D. W. P., . . . Øksnes, M. (2021). Potential Transcriptional Biomarkers to Guide Glucocorticoid Replacement in Autoimmune Addison's Disease. *Journal of the Endocrine Society*, *5*(3). https://doi.org/10.1210/jendso/bvaa202

Take, Y., Koizumi, S., & Nagahisa, A. (2020). Prostaglandin E Receptor 4 Antagonist in Cancer Immunotherapy: Mechanisms of Action. In *Frontiers in Immunology* (Vol. 11).

Talker, S. C., Barut, G. T., Lischer, H. E. L., Rufener, R., von Münchow, L., Bruggmann, R., & Summerfield, A. (2022). Monocyte biology conserved across species: Functional insights from cattle. *Front Immunol*, *13*, 889175. https://doi.org/10.3389/fimmu.2022.889175

Tan, T., Khoo, B., Mills, E. G., Phylactou, M., Patel, B., Eng, P. C., . . . Dhillo, W. S. (2020). Association between high serum total cortisol concentrations and mortality from COVID-19. In *The Lancet Diabetes and Endocrinology* (Vol. 8).

Tang, B. M. P., McLean, A. S., Dawes, I. W., Huang, S. J., & Lin, R. C. Y. (2009). Gene-expression profiling of peripheral blood mononuclear cells in sepsis. *Critical Care Medicine*, *37*(3). https://doi.org/10.1097/CCM.0b013e31819b52fd

Tasaki, S., Suzuki, K., Kassai, Y., Takeshita, M., Murota, A., Kondo, Y., . . . Takeuchi, T. (2018). Multi-omics monitoring of drug response in rheumatoid arthritis in pursuit of molecular remission. *Nature Communications*, *9*(1). https://doi.org/10.1038/s41467-018-05044-4

Thair, S. A., He, Y. D., Hasin-Brumshtein, Y., Sakaram, S., Pandya, R., Toh, J., . . . Sweeney, T. E. (2021). Transcriptomic similarities and differences in host response between SARS-CoV-2 and other viral infections. *iScience*, *24*(1), 101947. https://doi.org/10.1016/j.isci.2020.101947

Thielens, N. M., Tedesco, F., Bohlson, S. S., Gaboriaud, C., & Tenner, A. J. (2017). C1q: A fresh look upon an old molecule. In *Molecular Immunology* (Vol. 89).

Timmermans, S., Souffriau, J., & Libert, C. (2019). A general introduction to glucocorticoid biology. In *Frontiers in Immunology* (Vol. 10).

Torres, L. K., Pickkers, P., & van der Poll, T. (2022). Sepsis-Induced Immunosuppression. *Annu Rev Physiol*, *84*, 157-181. https://doi.org/10.1146/annurev-physiol-061121-040214

Tran, T. M., Jones, M. B., Ongoiba, A., Bijker, E. M., Schats, R., Venepally, P., . . . Crompton, P. D. (2016). Transcriptomic evidence for modulation of host inflammatory responses during febrile Plasmodium falciparum malaria. *Scientific Reports*, *6*. https://doi.org/10.1038/srep31291

Tsakiroglou, M., Evans, A., & Pirmohamed, M. (2023). Leveraging transcriptomics for precision diagnosis: Lessons learned from cancer and sepsis. *Frontiers in Genetics*, *14*. https://doi.org/https://doi.org/10.3389/fgene.2023.1100352

Tsalik, E. L., Willig, L. K., Rice, B. J., Van Velkinburgh, J. C., Mohney, R. P., McDunn, J. E., . . . Langley, R. J. (2015). Renal systems biology of patients with systemic inflammatory response syndrome. *Kidney International*, *88*(4). https://doi.org/10.1038/ki.2015.150

Tulzo, Y. L., Pangault, C., Amiot, L., Guilloux, V., Tribut, O., Arvieux, C., . . . Drénou, B. (2004). Monocyte human leukocyte antigen-DR transcriptional downregulation by cortisol during

septic shock. *American Journal of Respiratory and Critical Care Medicine*, *169*(10). https://doi.org/10.1164/rccm.200309-1329oc

Tweedie, S., Braschi, B., Gray, K., Jones, T. E. M., Seal, R. L., Yates, B., & Bruford, E. A. (2021). Genenames.org: The HGNC and VGNC resources in 2021. *Nucleic Acids Research*, *49*(D1). https://doi.org/10.1093/nar/gkaa980

Uhel, F., Azzaoui, I., Grégoire, M., Pangault, C., Dulong, J., Tadié, J. M., . . . Tarte, K. (2017). Early expansion of circulating granulocytic myeloid-derived suppressor cells predicts development of nosocomial infections in patients with sepsis. *American Journal of Respiratory and Critical Care Medicine*, *196*(3). https://doi.org/10.1164/rccm.201606-1143OC

van Dam, S., Võsa, U., van der Graaf, A., Franke, L., & de Magalhães, J. P. (2018). Gene co-expression analysis for functional classification and gene-disease predictions. *Briefings in Bioinformatics*, *19*(4). https://doi.org/10.1093/bib/bbw139

Van den Berghe, G., Téblick, A., Langouche, L., & Gunst, J. (2022). The hypothalamus-pituitary-adrenal axis in sepsis- and hyperinflammation-induced critical illness: Gaps in current knowledge and future translational research directions. *EBioMedicine*, *84*, 104284. https://doi.org/10.1016/j.ebiom.2022.104284

van der Poll, T., Shankar-Hari, M., & Wiersinga, W. J. (2021). The immunology of sepsis. In *Immunity* (Vol. 54).

Van Der Poll, T., Van De Veerdonk, F. L., Scicluna, B. P., & Netea, M. G. (2017). The immunopathology of sepsis and potential therapeutic targets. In *Nature Reviews Immunology* (Vol. 17).

Vandewalle, J., & Libert, C. (2020). Glucocorticoids in Sepsis: To Be or Not to Be. *Front Immunol*, *11*, 1318. https://doi.org/10.3389/fimmu.2020.01318

Vangeti, S., Falck-Jones, S., Yu, M., Österberg, B., Liu, S., Asghar, M., . . . Smed-Sörensen, A. (2023). Human influenza virus infection elicits distinct patterns of monocyte and dendritic cell mobilization in blood and the nasopharynx. *Elife*, *12*. https://doi.org/10.7554/eLife.77345

Venet, F., Demaret, J., Gossez, M., & Monneret, G. (2021). Myeloid cells in sepsis-acquired immunodeficiency. *Ann N Y Acad Sci*, *1499*(1), 3-17. https://doi.org/10.1111/nyas.14333

Venet, F., & Monneret, G. (2018). Advances in the understanding and treatment of sepsis-induced immunosuppression. *Nat Rev Nephrol*, *14*(2), 121-137. https://doi.org/10.1038/nrneph.2017.165

Venet, F., Plassais, J., Textoris, J., Cazalis, M. A., Pachot, A., Bertin-Maghit, M., . . . Tissot, S. (2015). Low-dose hydrocortisone reduces norepinephrine duration in severe burn patients: A randomized clinical trial. *Critical Care*, *19*(1). https://doi.org/10.1186/s13054-015-0740-0

Vettorazzi, S., Nalbantoglu, D., Gebhardt, J. C. M., & Tuckermann, J. (2021). A guide to changing paradigms of glucocorticoid receptor function—a model system for genome regulation and physiology. *FEBS Journal*. https://doi.org/10.1111/febs.16100

Vieira Da Silva Pellegrina, D., Severino, P., Barbeiro, H. V., Andreghetto, F. M., Velasco, I. T., Possolo De Souza, H., . . . Pinheiro Da Silva, F. (2015). Septic shock in advanced age: Transcriptome analysis reveals altered molecular signatures in neutrophil granulocytes. *PLoS ONE*, *10*(6). https://doi.org/10.1371/journal.pone.0128341

Vihervaara, A., Duarte, F. M., & Lis, J. T. (2018). Molecular mechanisms driving transcriptional stress responses. In *Nature Reviews Genetics* (Vol. 19).

Wang, C., Nanni, L., Novakovic, B., Megchelenbrink, W., Kuznetsova, T., Stunnenberg, H. G., . . . Logie, C. (2019). Extensive epigenomic integration of the glucocorticoid response in primary human monocytes and in vitro derived macrophages. *Scientific Reports*, *9*(1). https://doi.org/10.1038/s41598-019-39395-9

Wang, T., Zhang, X., Liu, Z., Yao, T., Zheng, D., Gan, J., . . . Sun, J. (2021). Single-cell RNA sequencing reveals the sustained immune cell dysfunction in the pathogenesis of sepsis secondary to bacterial pneumonia. *Genomics*, *113*(3). https://doi.org/10.1016/j.ygeno.2021.01.026

Wang, Y., Schughart, K., Pelaia, T. M., Chew, T., Kim, K., Karvunidis, T., . . . Shojaei, M. (2022). Blood transcriptome responses in patients correlate with severity of COVID-19 disease. *Front Immunol*, *13*, 1043219. https://doi.org/10.3389/fimmu.2022.1043219

Ward, N. S., Casserly, B., & Ayala, A. (2008). The Compensatory Anti-inflammatory Response Syndrome (CARS) in Critically Ill Patients. In *Clinics in Chest Medicine* (Vol. 29).

Washburn, M. L., Wang, Z., Walton, A. H., Goedegebuure, S. P., Figueroa, D. J., Van Horn, S., . . . Hotchkiss, R. S. (2019). T Cell– and Monocyte-Specific RNA-Sequencing Analysis in Septic and Nonseptic Critically Ill Patients and in Patients with Cancer. *The Journal of Immunology*, *203*(7). https://doi.org/10.4049/jimmunol.1900560

Weller, P. F. (2016). LEUKOCYTE LIPID BODIES - STRUCTURE AND FUNCTION AS "EICOSASOMES". *Transactions of the American Clinical and Climatological Association*, *127*.

Wen, M., Cai, G., Ye, J., Liu, X., Ding, H., & Zeng, H. (2020). Single-cell transcriptomics reveals the alteration of peripheral blood mononuclear cells driven by sepsis. *Annals of Translational Medicine*, *8*(4). https://doi.org/10.21037/atm.2020.02.35

Westman, J., Grinstein, S., & Marques, P. E. (2020). Phagocytosis of Necrotic Debris at Sites of Injury and Inflammation. In *Frontiers in Immunology* (Vol. 10).

Westra, H. J., Peters, M. J., Esko, T., Yaghootkar, H., Schurmann, C., Kettunen, J., . . . Franke, L. (2013). Systematic identification of trans eQTLs as putative drivers of known disease associations. *Nature Genetics*, *45*(10). https://doi.org/10.1038/ng.2756

Wickham, H. (2016). *ggplot2: Elegant Graphics for Data Analysis. Springer-Verlag New York* (Vol. 35).

Wickham, H., Bryan, J., Rstudio, Kalicinski, M., Valery, K., Leitienne, C., . . . Miller, E. (2019). readxl: Read Excel files. R package version 1.3.1. In *https://CRAN.R-project.org/package=readxl*.

Wittenbrink, N., Ananthasubramaniam, B., Münch, M., Koller, B., Maier, B., Weschke, C., . . . Kramer, A. (2018). High-accuracy determination of internal circadian time from a single blood sample. *Journal of Clinical Investigation*, *128*(9). https://doi.org/10.1172/JCI120874

Wong, H. R., Cvijanovich, N. Z., Allen, G. L., Thomas, N. J., Freishtat, R. J., Anas, N., . . . Zimmerman, J. J. (2014). Corticosteroids are associated with repression of adaptive immunity gene programs in pediatric septic shock. *American Journal of Respiratory and Critical Care Medicine*, *189*(8). https://doi.org/10.1164/rccm.201401-0171OC

Wong, K. L., Tai, J. J. Y., Wong, W. C., Han, H., Sem, X., Yeap, W. H., . . . Wong, S. C. (2011). Gene expression profiling reveals the defining features of the classical, intermediate,and nonclassical human monocyte subsets. *Blood*, *118*(5). https://doi.org/10.1182/blood-2010-12-326355

Wright, V. J., Herberg, J. A., Kaforou, M., Shimizu, C., Eleftherohorinou, H., Shailes, H., . . . Levin, M. (2018). Diagnosis of Kawasaki Disease Using a Minimal Whole-Blood Gene Expression Signature. *JAMA Pediatrics*, *172*(10). https://doi.org/10.1001/jamapediatrics.2018.2293

Wu, G., Ruben, M. D., Schmidt, R. E., Francey, L. J., Smith, D. F., Anafi, R. C., . . . Hogenesch, J. B. (2018). Population-level rhythms in human skin with implications for circadian medicine. *Proceedings of the National Academy of Sciences of the United States of America*, *115*(48). https://doi.org/10.1073/pnas.1809442115

Xavier, A. M., Anunciato, A. K. O., Rosenstock, T. R., & Glezer, I. (2016). Gene expression control by glucocorticoid receptors during innate immune responses. In *Frontiers in Endocrinology* (Vol. 7).

Xiao, W., Mindrinos, M. N., Seok, J., Cuschieri, J., Cuenca, A. G., Gao, H., . . . Wong, W. H. (2011). A genomic storm in critically injured humans. *Journal of Experimental Medicine*, *208*(13). https://doi.org/10.1084/jem.20111354

Yan, J., Wang, H., Liu, Y., & Shao, C. (2008). Analysis of gene regulatory networks in the mammalian circadian rhythm. *PLoS Computational Biology*, *4*(10). https://doi.org/10.1371/journal.pcbi.1000193

Zhai, Y., Franco, L. M., Atmar, R. L., Quarles, J. M., Arden, N., Bucasas, K. L., . . . Couch, R. B. (2015). Host Transcriptional Response to Influenza and Other Acute Respiratory Viral Infections – A Prospective Cohort Study. *PLoS Pathogens*, *11*(6). https://doi.org/10.1371/journal.ppat.1004869

Zhao, J., Brault, J. J., Schild, A., Cao, P., Sandri, M., Schiaffino, S., . . . Goldberg, A. L. (2007). FoxO3 Coordinately Activates Protein Degradation by the Autophagic/Lysosomal and Proteasomal

Pathways in Atrophying Muscle Cells. *Cell Metabolism*, *6*(6).
https://doi.org/10.1016/j.cmet.2007.11.004

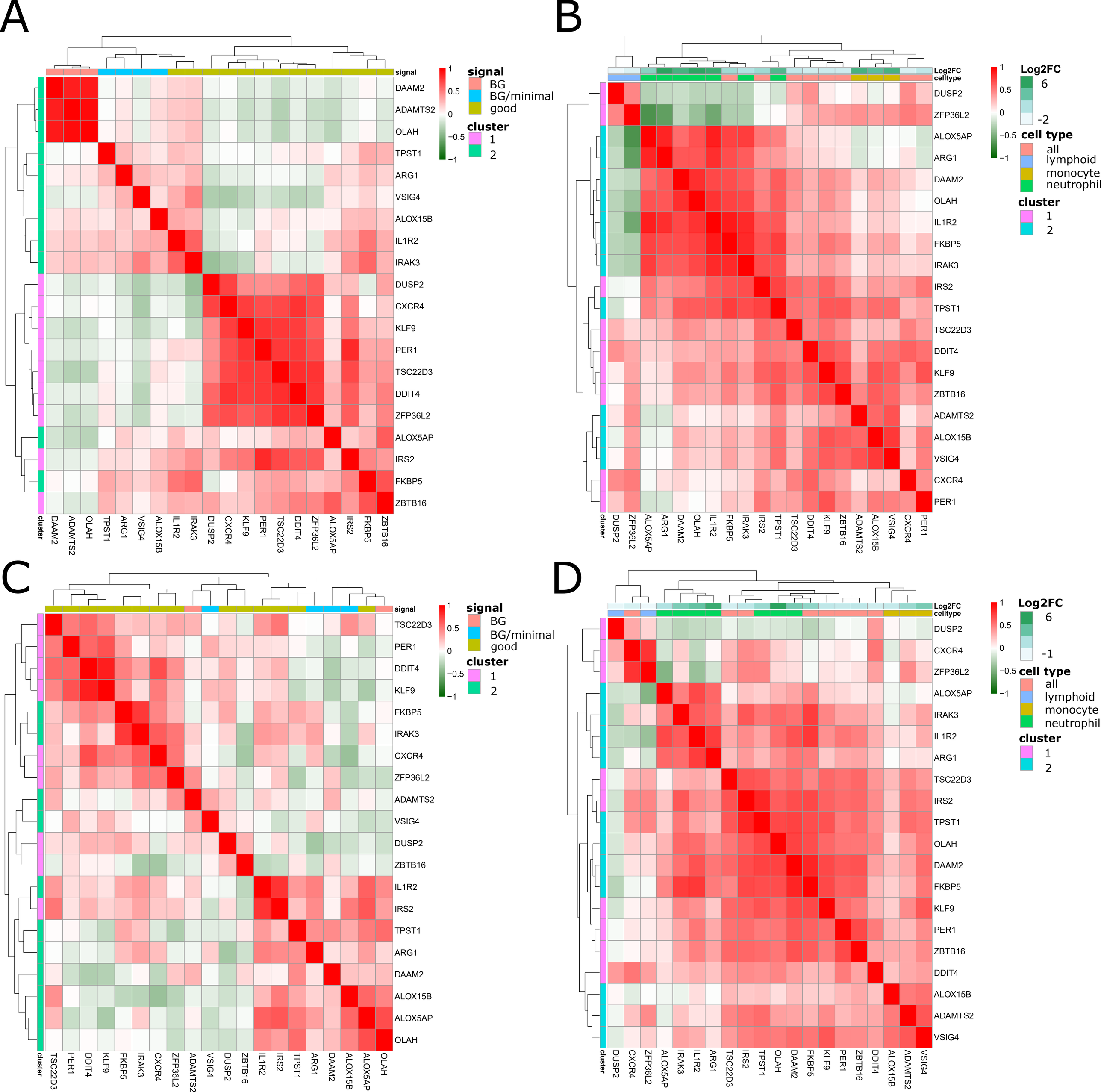
A
signal
cluster
DAAM2
ADAMTS2
OLAH
TPST1
ARG1
VSIG4
ALOX15B
IL1R2
IRAK3
DUSP2
CXCR4
KLF9
PER1
TSC22D3
DDIT4
ZFP36L2
ALOX5AP
IRS2
FKBP5
ZBTB16
1
0.5
0
−0.5
−1
signal
BG
BG/minimal
good
cluster
1
2
B
Log2FC
celltype
DUSP2
ZFP36L2
ALOX5AP
ARG1
DAAM2
OLAH
IL1R2
FKBP5
IRAK3
IRS2
TPST1
TSC22D3
DDIT4
KLF9
ZBTB16
ADAMTS2
ALOX15B
VSIG4
CXCR4
PER1
Log2FC
6
-2
cell type
all
lymphoid
monocyte
neutrophil
cluster
1
2
C
TSC22D3
PER1
DDIT4
KLF9
FKBP5
IRAK3
CXCR4
ZFP36L2
ADAMTS2
VSIG4
DUSP2
ZBTB16
IL1R2
IRS2
TPST1
ARG1
DAAM2
ALOX15B
ALOX5AP
OLAH
D
DUSP2
CXCR4
ZFP36L2
ALOX5AP
IRAK3
IL1R2
ARG1
TSC22D3
IRS2
TPST1
OLAH
DAAM2
FKBP5
KLF9
PER1
ZBTB16
DDIT4
ALOX15B
ADAMTS2
VSIG4
Log2FC
6
-1

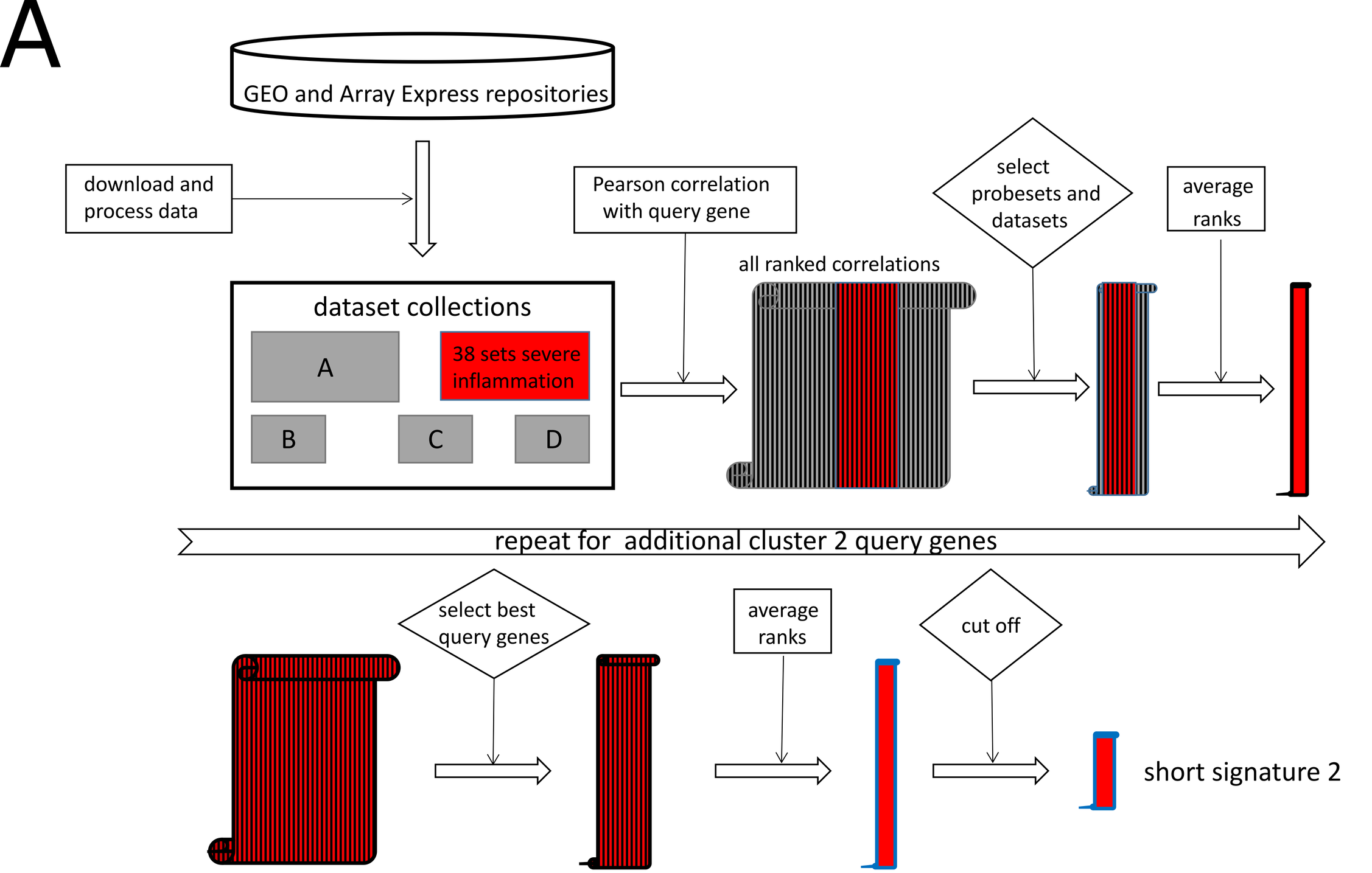
A
GEO and Array Express repositories
download and process data
dataset collections
A
38 sets severe inflammation
B
C
D
Pearson correlation with query gene
all ranked correlations
select probesets and datasets
average ranks
repeat for additional cluster 2 query genes
select best query genes
average ranks
cut off
short signature 2

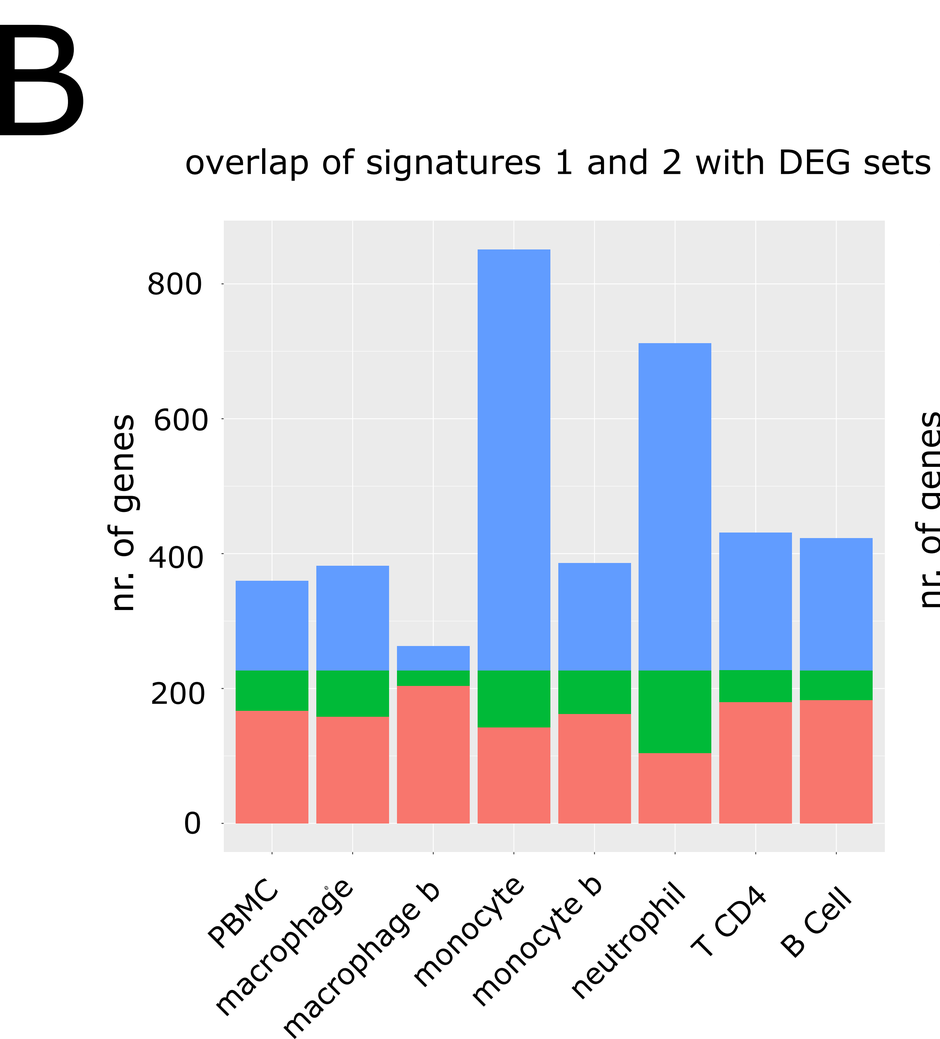
B
overlap of signatures 1 and 2 with DEG sets
nr. of genes
0
200
400
600
800
PBMC
macrophage
macrophage b
monocyte
monocyte b
neutrophil
T CD4
B Cell

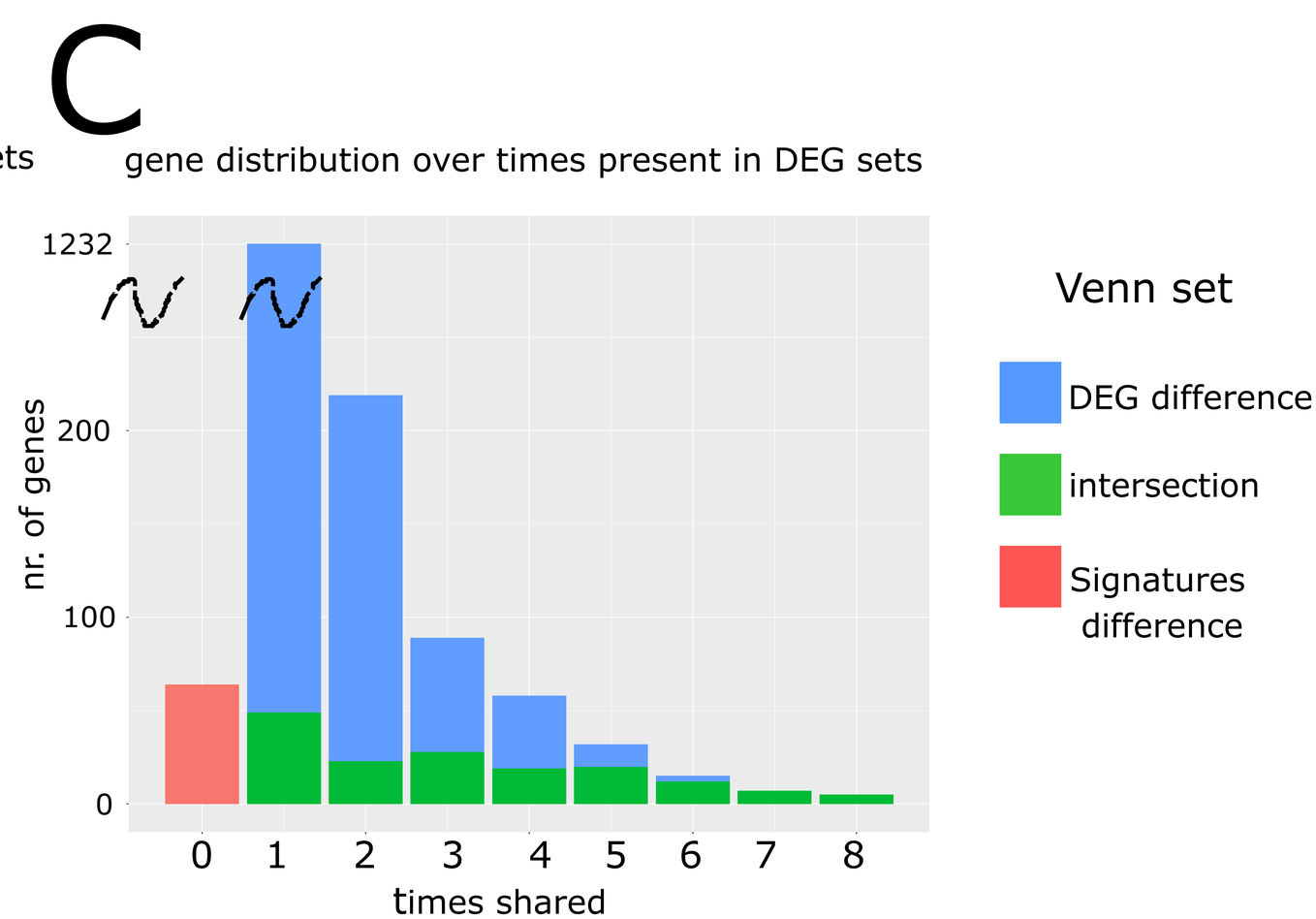
C
gene distribution over times present in DEG sets
nr. of genes
0
100
200
1232
0
1
2
3
4
5
6
7
8
times shared
Venn set
DEG difference
intersection
Signatures difference

				basal				induced				basal		induced		
query	signature	GC-set	gene	B	T	M	N	B	T	M	N	M	Mf	M	Mf	protein / function
1	1 and 2	GC-1	ZBTB16 (PLZF)	0,75	0,11	0,03	0,11	2,11	4,37	6,83	6,3	0,81	0,19	8,13	NA	transcription factor
1	1 and 2	GC-1	KLF9	0,26	0,34	0,37	0,03	1,47	1,56	1,84	3,76	0,55	0,45	1,91	0,87	transcription factor
1	1	GC-1	DDIT4 (REDD1)	0,1	0,16	0,41	0,34	2,2	3	0,66	2,23	0,92	0,08	1,11	1,23	inhibitory in mTOR signaling
1	1	GC-1	TSC22D3 (GILZ)	0,14	0,11	0,04	0,71	1,71	2,28	3,03	2,5	0,8	0,2	3,4	3,21	inhibitory in NF-kB and MAPK signaling
1	1	GC-1	PER1	0,1	0,15	0,21	0,54	0,99	1,89	2,42	4,01	0,77	0,23	2,69	1,6	repression of transcription by CLOCK/BMAL1
1	1 and 2	GC-1	IRS2	0,03	0,03	0,1	0,83	0,85	NS	1,29	1,81	0,77	0,23	1,79	0,92	signaling adaptor
	1	GC-1	CXCR4	0,18	0,04	0,04	0,75	0,37	1,34	0,6	0,57	0,92	0,08	1,1	NS	CXCL12 GPCR, chemotaxis
	1 and 2		FKBP5 (FKBP51)	0,08	0,61	0,26	0,05	3,25	2,1	3,77	7,79	0,59	0,41	4,24	2,56	GC receptor complex component
	2		HPGD	0,01	0,59	0,34	0,06	2,51	2,27	2,55	3,16	0,24	0,76	1,16	0,73	15- hydroxyprostaglandin dehydrogenase
2	2	GC-2	ADAMTS2	0,03	0,04	0,86	0,07	NS	NS	2,47	NS	0,76	0,24	2,27	NA	procollagen proteinase
2	1 and 2	GC-2	FLT3	0,25	0,02	0,47	0,27	1,22	NS	2,43	3,33	0,87	0,13	3,03	0,9	receptor tyrosine kinase
2	2		CD163	0	0	1	0	2,58	NS	2,05	3,91	0,17	0,83	4,54	1,19	scavenger receptor
2	2	GC-2	VSIG4 (CRig)	0	0	1	0	NS	1,6	NS	NS	0,03	0,97	2,12	0,64	C3b receptor
	2		ALOX15B (15-LOX-B)	0,01	0	0,99	0	NS	NS	4,2	Inf	0,04	0,96	3,84	1,58	arachidonate 15-lipoxygenase B, SPM?
	2	GC-2	MAOA	0	0,01	0,95	0,04	NS	-2,07	NS	3,84	0,13	0,87	NS	NS	monoamine oxidase A
	2	GC-2	AMPH	0	0,07	0,79	0,14	NS	NS	NS	3,94	0,5	0,5	5,53	NS	amphiphysin
2	1 and 2	GC-2	ADORA3	0,01	0	0,63	0,35	NS	NS	3,16	4,61	0,1	0,9	6,29	0,81	adenosine GPCR, Gi coupled
	2	GC-2	MACIR (C5orf30)	0,19	0,18	0,17	0,46	NS	NS	0,62	1,64	0,52	0,48	NS	NS	macrophage immunometabolism regulator
2	2	GC-2	OLAH	0,05	0,02	0,16	0,77	6,31	9,14	5,28	5,45	0,65	0,35	1,17	NS	thioesterase 2
2	2	GC-2	DAAM2	0	0	0,01	0,99	1,35	NS	4,37	4,42	0,22	0,78	1,76	NA	actin nucleation
	2		ALOX5AP (FLAP)	0,02	0,02	0,09	0,87	NS	NS	NS	1,05	0,79	0,21	1,34	0,81	arachidonate 5-lipoxygenase activation, LTB4
	2		ARG1	0	0,03	0	0,97	NS	1,38	NS	2,8	0,74	0,26	NS	NS	arginase 1

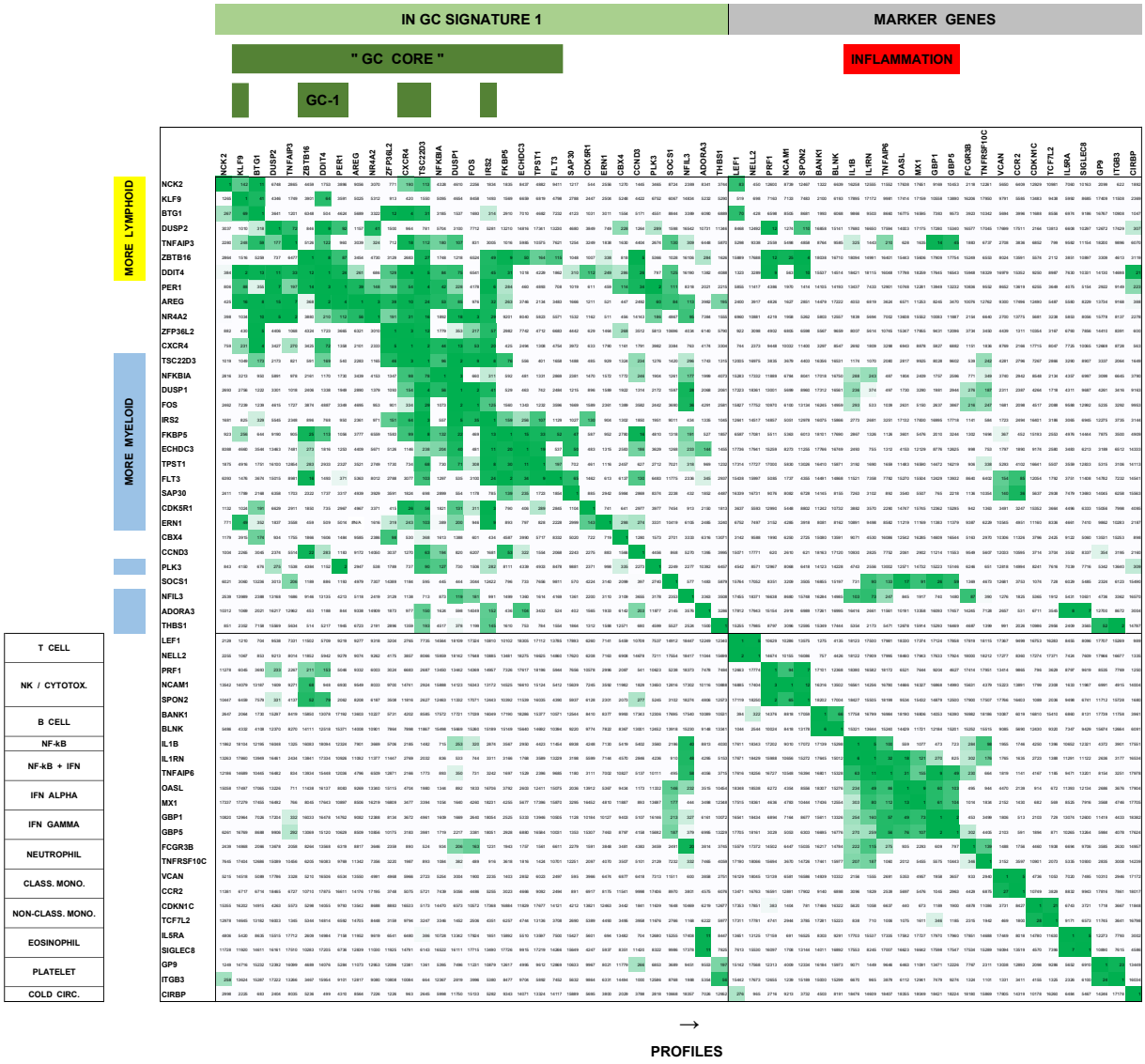

MODULE / SET GC-1 : KLF9, ZBTB16, DDIT4, PER1, CXCR4, TSC22D3, IRS2

A

groups: GC

	KLF9	DDIT4	ZBTB16	CXCR4	TSC22D3	IRS2	PER1	PER2	NR1D2	CRY2	DBP	TEF
KLF9	1	64	3901	420	1550	1493	3591	2109	329	6818	7457	9292
DDIT4	2	1	12	6	5	45	24	1841	669	1231	1684	2398
ZBTB16	1516	8	1	2683	27	49	87	2322	13505	2275	1379	1609
CXCR4	231	72	3425	1	2	20	1358	2223	1757	10475	11646	9146
TSC22D3	1049	169	591	3	1	8	540	3412	7770	14341	11800	4254
IRS2	825	768	896	64	3	1	950	1596	4913	16463	14969	6130
PER1	88	3	14	54	4	6	1	1770	8501	343	1247	598
PER2	684	3977	6799	2132	3736	2500	6543	1	631	3320	6809	9875
NR1D2	754	4516	8198	3742	6118	8109	7705	2887	1	4887	4931	8388
CRY2	6719	4704	4808	8496	5200	16956	3758	3790	4512	1	55	1449
DBP	7981	4698	4185	11973	5805	15476	4413	5838	3707	72	1	1710
TEF	7314	2375	1780	4341	1972	6332	1603	5207	6266	54	261	1

B

groups: GC, CLOCK

	KLF9	DDIT4	ZBTB16	CXCR4	TSC22D3	IRS2	PER1	PER2	NR1D2	CRY2	DBP	TEF
KLF9	1	7	5	14	4	2	3	39	1968	528	252	105
DDIT4	4	1	16	2	9	5	7	699	1990	67	446	900
ZBTB16	7	48	1	36	11	3	4	52	270	2959	170	71
CXCR4	6	3	12	1	2	5	4	55	451	554	284	2799
TSC22D3	4	18	10	6	1	2	3	52	599	97	391	242
IRS2	2	12	5	8	4	1	3	42	3234	2465	1188	281
PER1	4	9	5	6	3	2	1	23	95	240	61	22
PER2	142	5014	333	716	191	46	184	1	1305	2293	472	1651
NR1D2	4152	5327	2811	3704	2907	5074	2103	2146	1	7031	3708	2817
CRY2	1684	1907	4872	3387	713	4122	2140	2356	8806	1	346	2913
DBP	1580	3775	2154	3081	2025	2873	1303	1166	3423	842	1	137
TEF	489	4029	739	4930	665	791	192	1548	1809	2585	14	1

ranking of DBP in PER1 profile

ranking of PER1 in DBP profile

C

groups: GC, CLOCK

	KLF9	DDIT4	ZBTB16	CXCR4	TSC22D3	IRS2	PER1	PER2	NR1D2	CRY2	DBP	TEF
KLF9	1	201	20	18609	479	128	41	1172	135	1262	4655	976
DDIT4	123	1	671	14319	17	80	12	5482	7685	411	7057	788
ZBTB16	44	850	1	19017	1321	129	148	178	2538	68	3569	1190
CXCR4	19031	15733	19083	1	11414	16756	16260	17097	16710	18993	12766	15547
TSC22D3	587	24	1640	11121	1	1310	44	3983	2862	2549	3070	111
IRS2	324	309	152	15597	1802	1	68	124	4008	962	8138	6298
PER1	318	225	521	14410	381	213	1	23	1133	181	10	7
PER2	1379	4446	74	16863	2996	37	3	1	9	41	86	8
NR1D2	458	5192	3154	14836	2490	3013	616	52	1	4134	195	107
CRY2	3096	1722	276	18875	3613	1727	247	409	5761	1	2296	138
DBP	7328	6577	5792	11177	3502	7881	5	267	115	1629	1	2
TEF	2579	2129	2610	15279	452	7085	4	41	112	55	2	1

D

signature	gene	CD4	CD8	NK	B cell	Mono	Neutro
1	TSC22D3 (GILZ)	3	3	4	1	1	229
1	DDIT4 (REDD1)	11	109	6	666	216	110
1 and 2	KLF9	15	21	971	12	11	189
1	CXCR4	2	4	27	24	3	798
no	FOXO3	926	57	>2000	>2000	15	20
no	PTGER4 (EP4)	21	10	78	149	>2000	>2000
1	PIK3IP1	83	293	7	3	>2000	>2000
1	FBXO32 (MAFbx / atrogin 1)	12	66	>2000	>2000	>2000	>2000
no	PIK3R1 (P85)	192	37	69	1903	342	>2000
1 and 2	IL1R2	>2000	>2000	>2000	>2000	10	1
no	PICK1	>2000	>2000	>2000	>2000	20	>2000
1 and 2	VSIR (VISTA / C10orf54)	>2000	>2000	>2000	>2000	>2000	17

GC profiles

↓

A

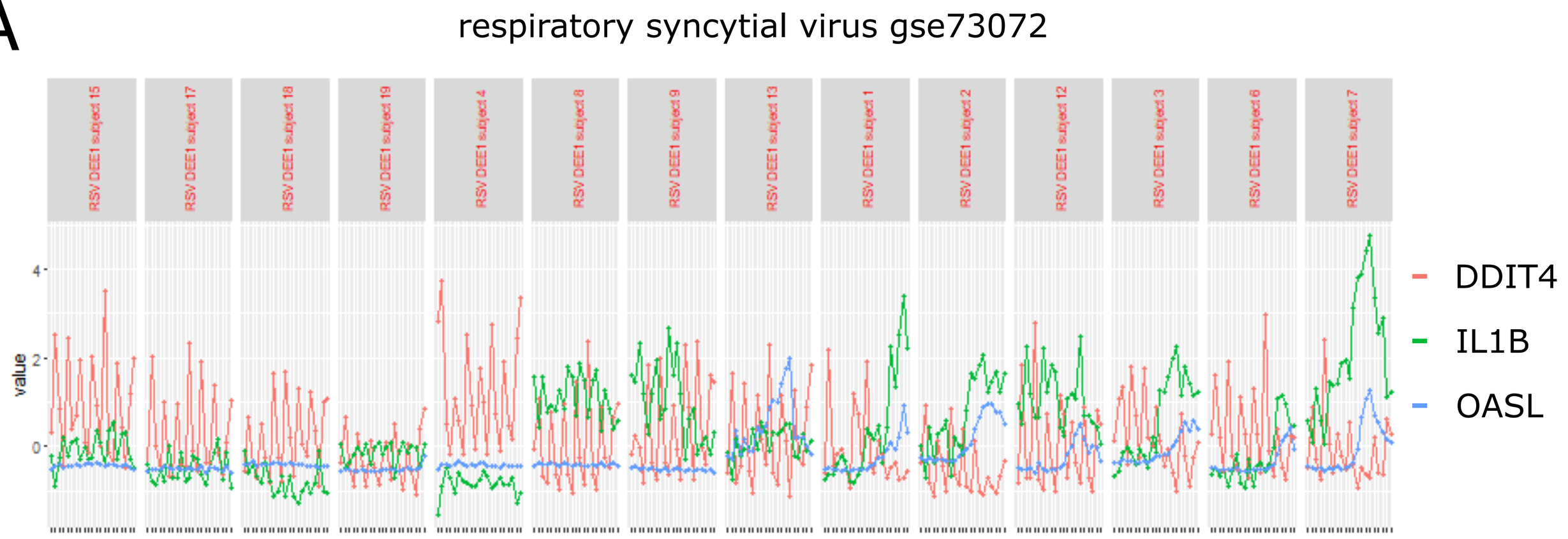
respiratory syncytial virus gse73072
value
DDIT4
IL1B
OASL

B

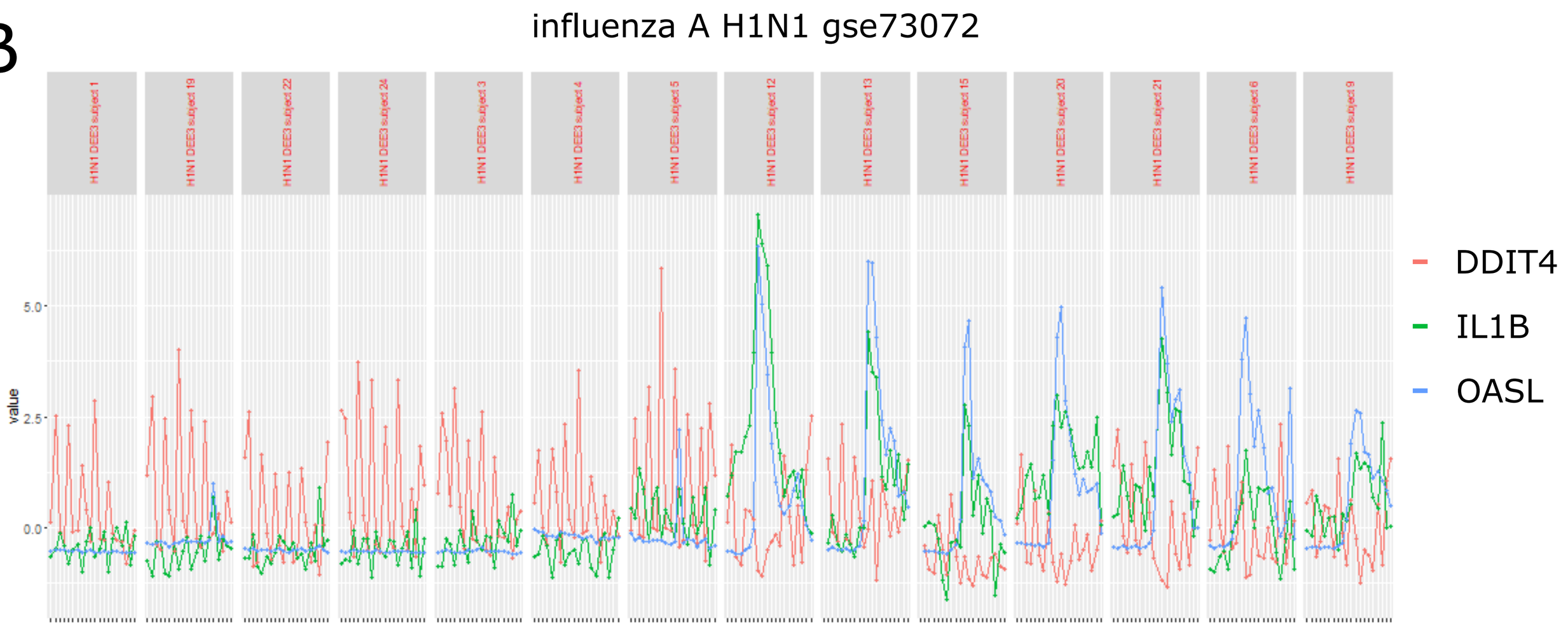
influenza A H1N1 gse73072
value
DDIT4
IL1B
OASL

C

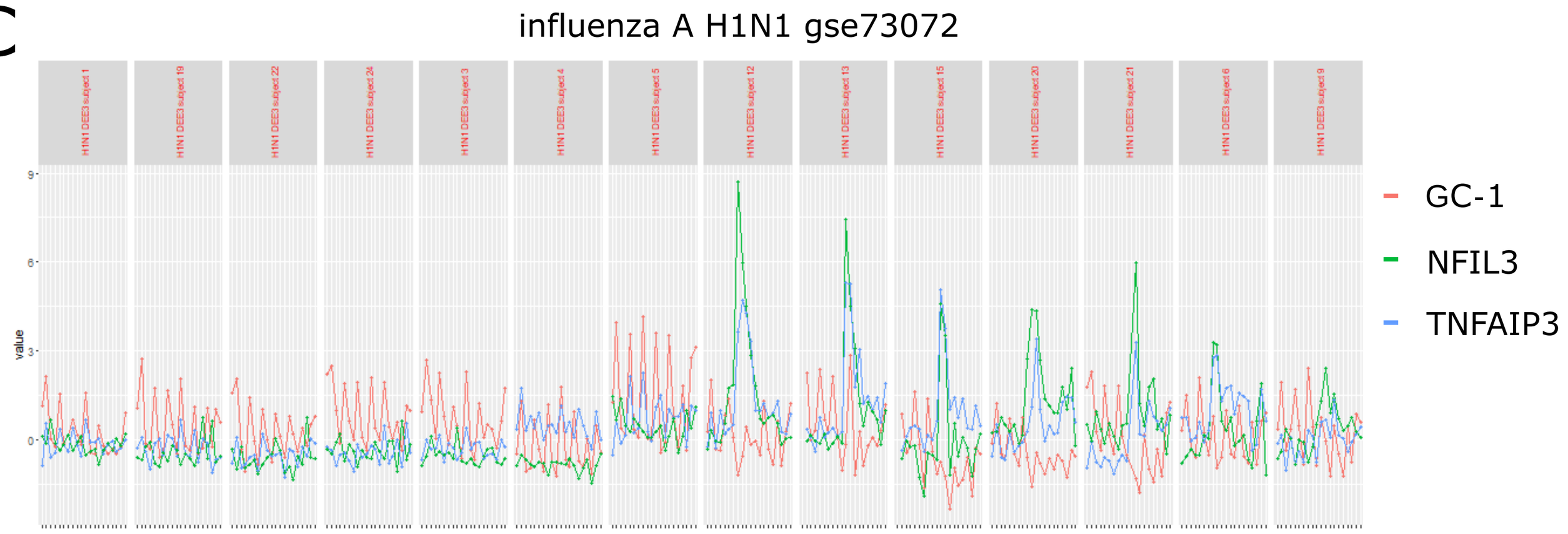
influenza A H1N1 gse73072
value
GC-1
NFIL3
TNFAIP3

D

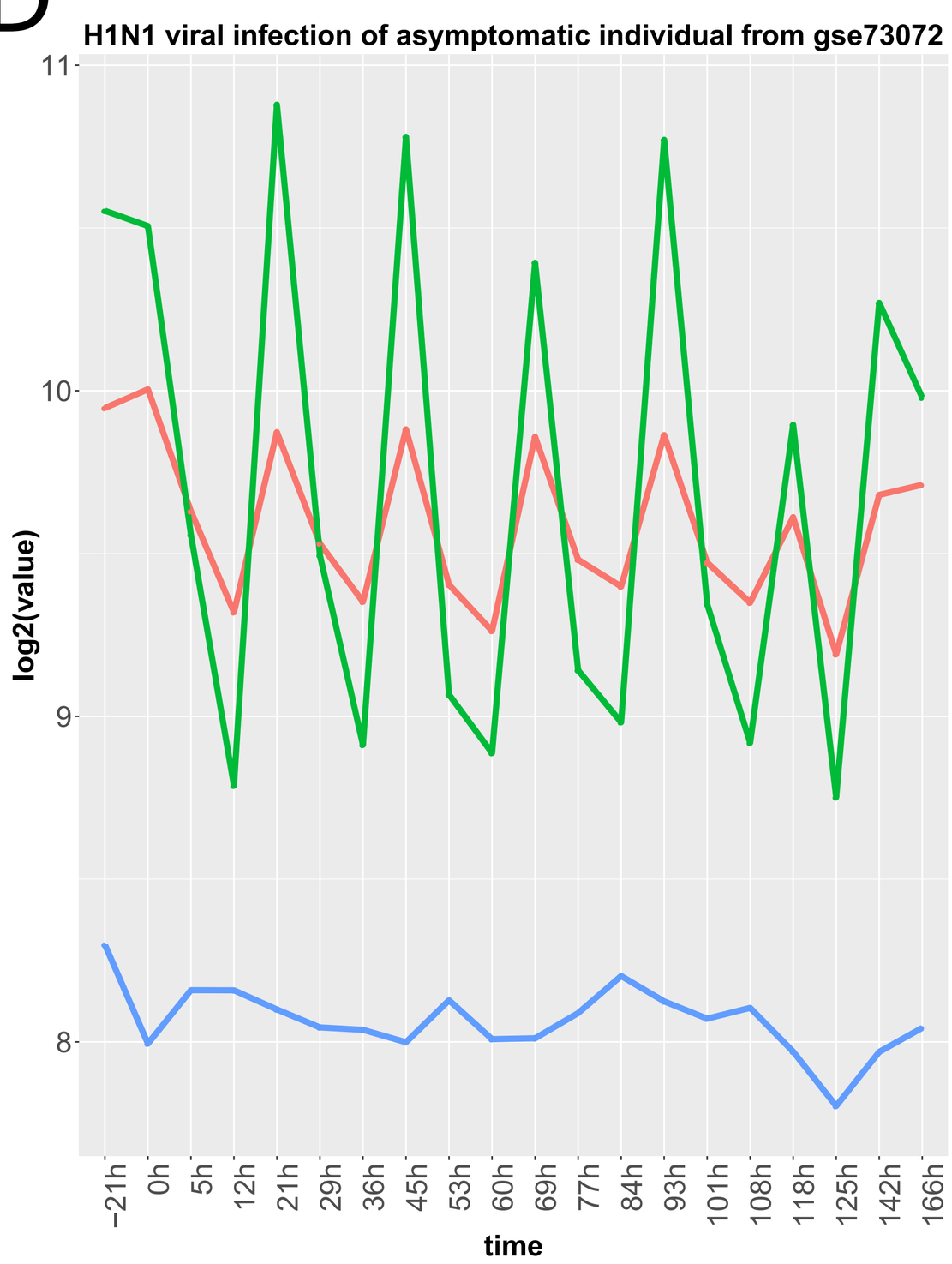
H1N1 viral infection of asymptomatic individual from gse73072
log2(value)
time

E

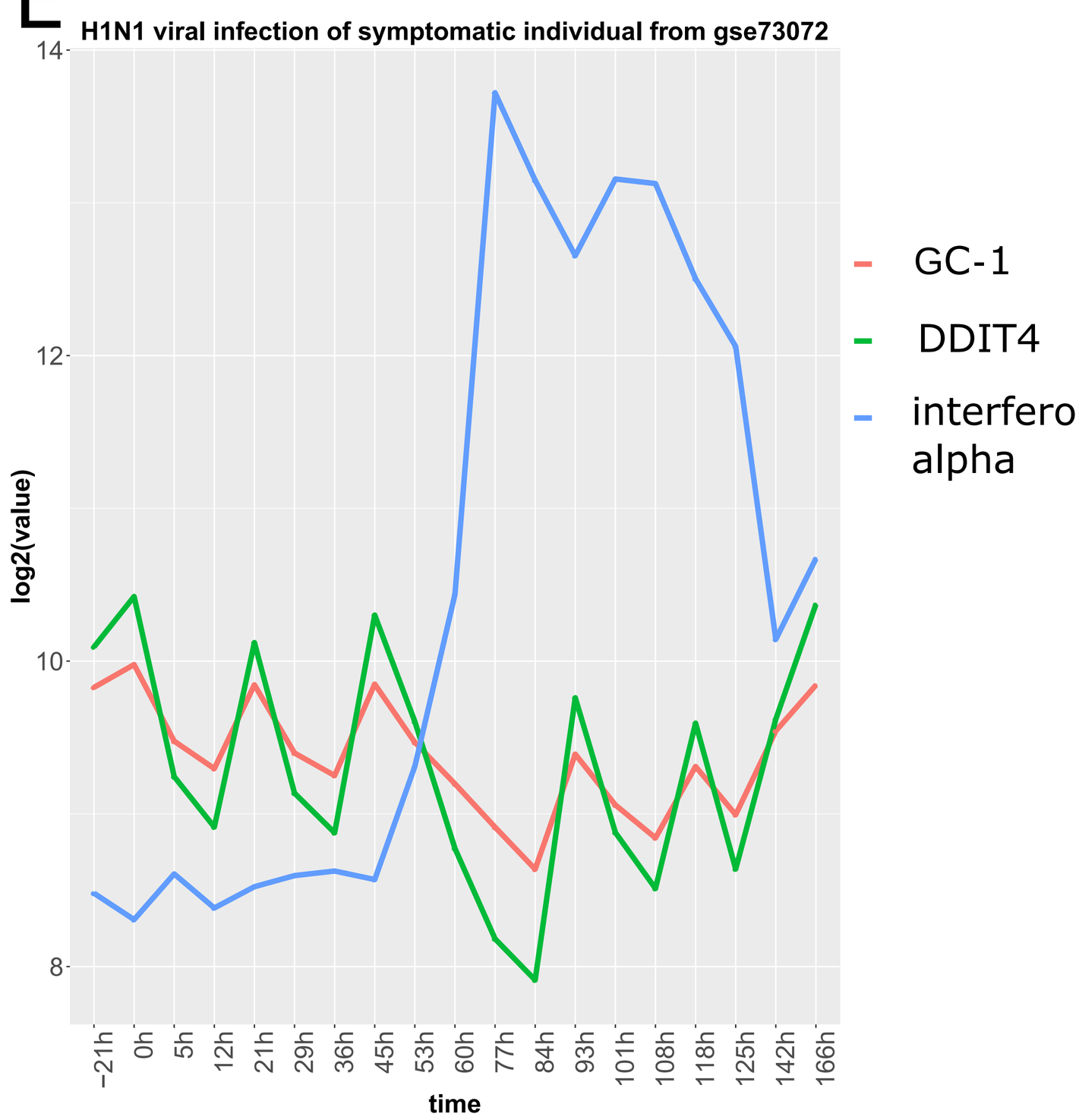
H1N1 viral infection of symptomatic individual from gse73072
log2(value)
time
GC-1
DDIT4
interferon alpha

A

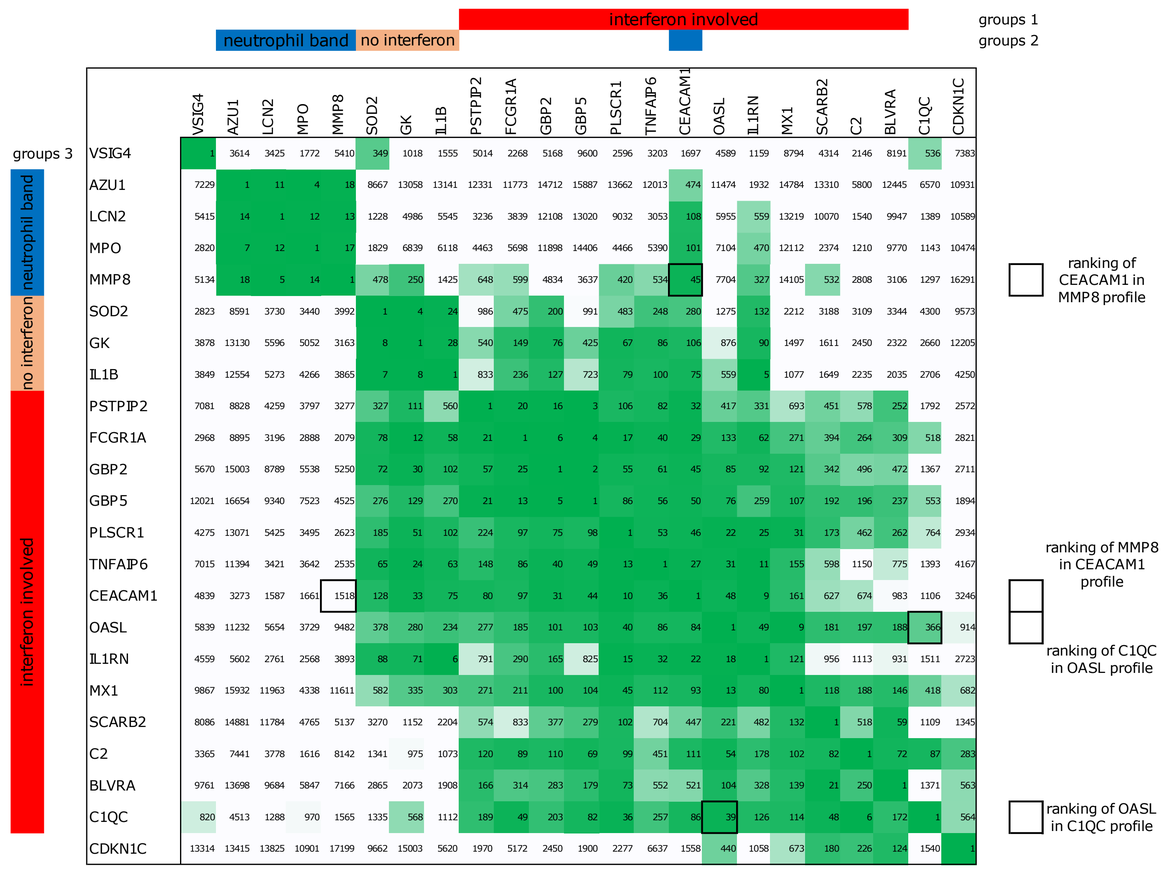
groups 1
groups 2
groups 3
neutrophil band
no interferon
interferon involved
ranking of CEACAM1 in MMP8 profile
ranking of MMP8 in CEACAM1 profile
ranking of C1QC in OASL profile
ranking of OASL in C1QC profile

B

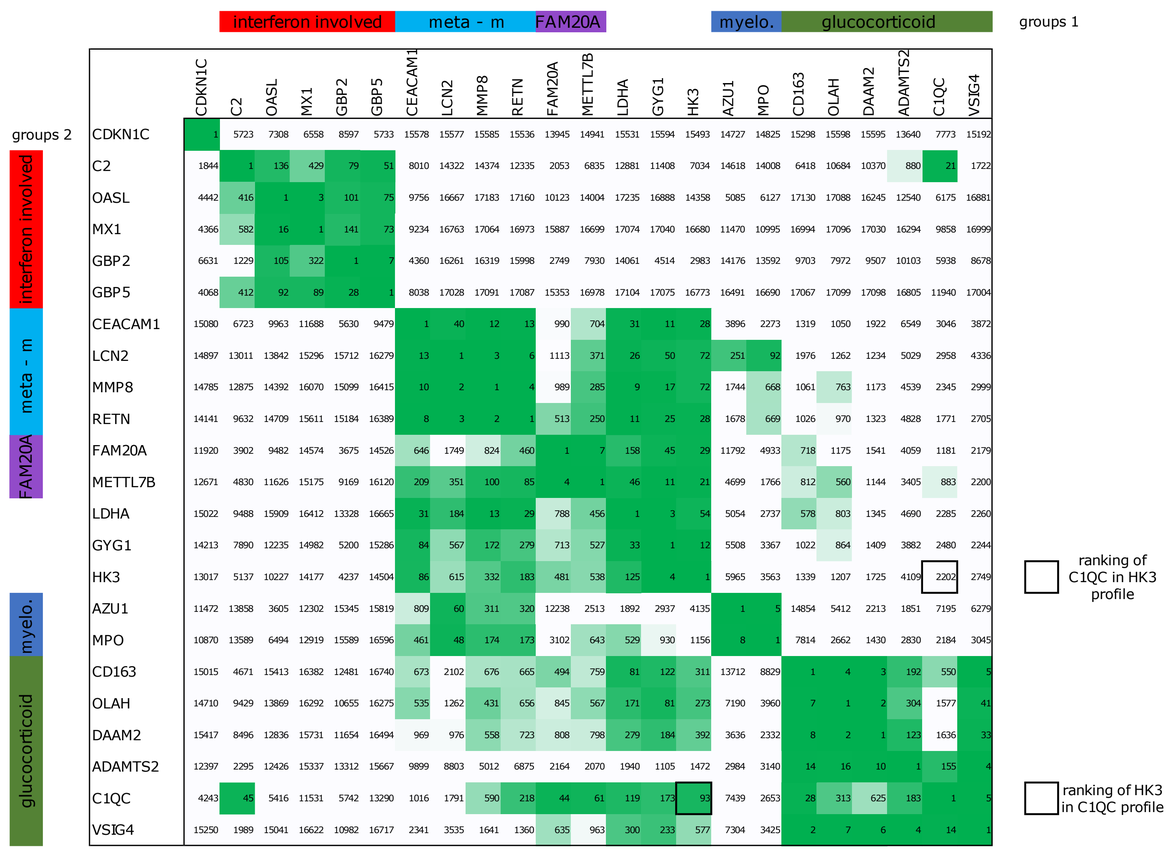
groups 1
groups 2
interferon involved
meta - m
FAM20A
myelo.
glucocorticoid
ranking of C1QC in HK3 profile
ranking of HK3 in C1QC profile

C

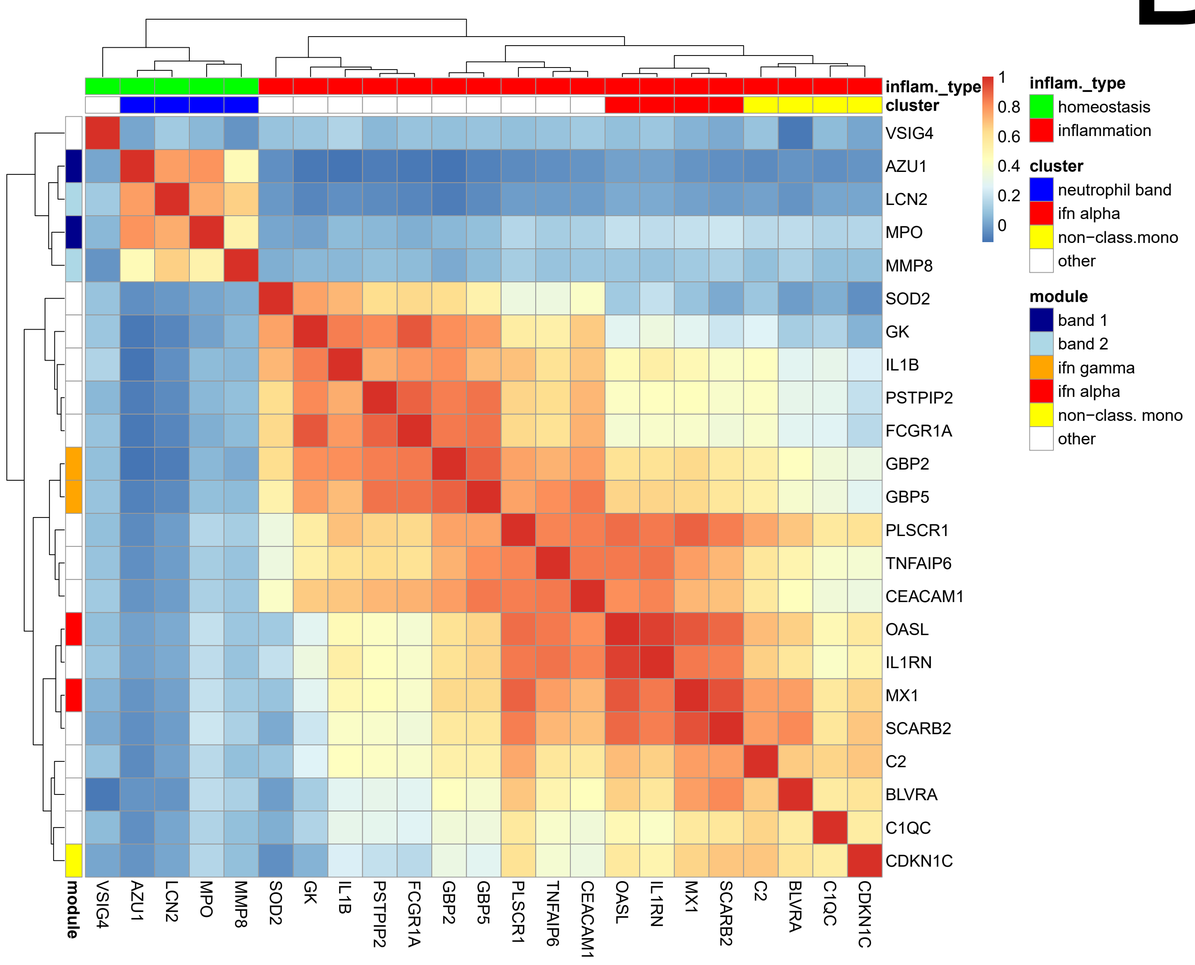
inflam._type
cluster
module
homeostasis
inflammation
neutrophil band
ifn alpha
non−class.mono
other
band 1
band 2
ifn gamma
non-class. mono

D

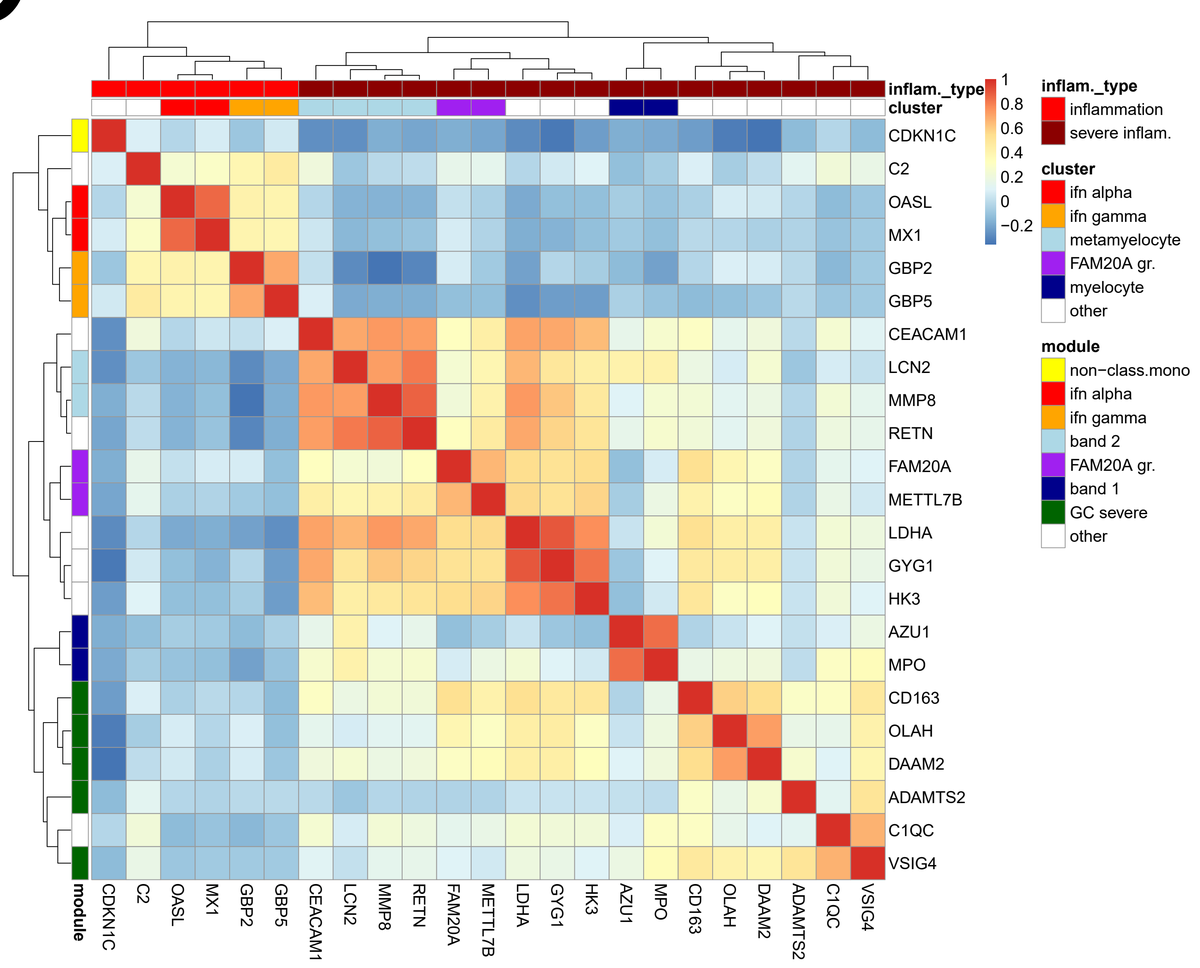
inflam._type
cluster
module
inflammation
severe inflam.
ifn alpha
ifn gamma
metamyelocyte
FAM20A gr.
myelocyte
other
non−class.mono
band 2
band 1
GC severe

E

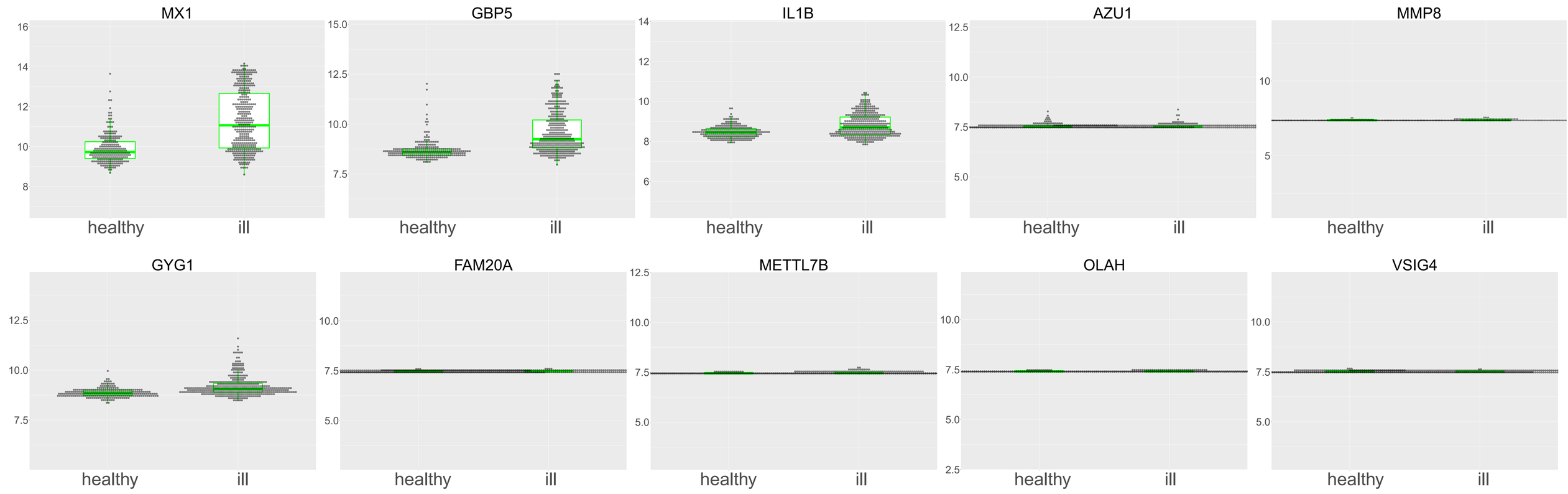
MX1
GBP5
IL1B
AZU1
MMP8
GYG1
FAM20A
METTL7B
OLAH
VSIG4
healthy
ill

F

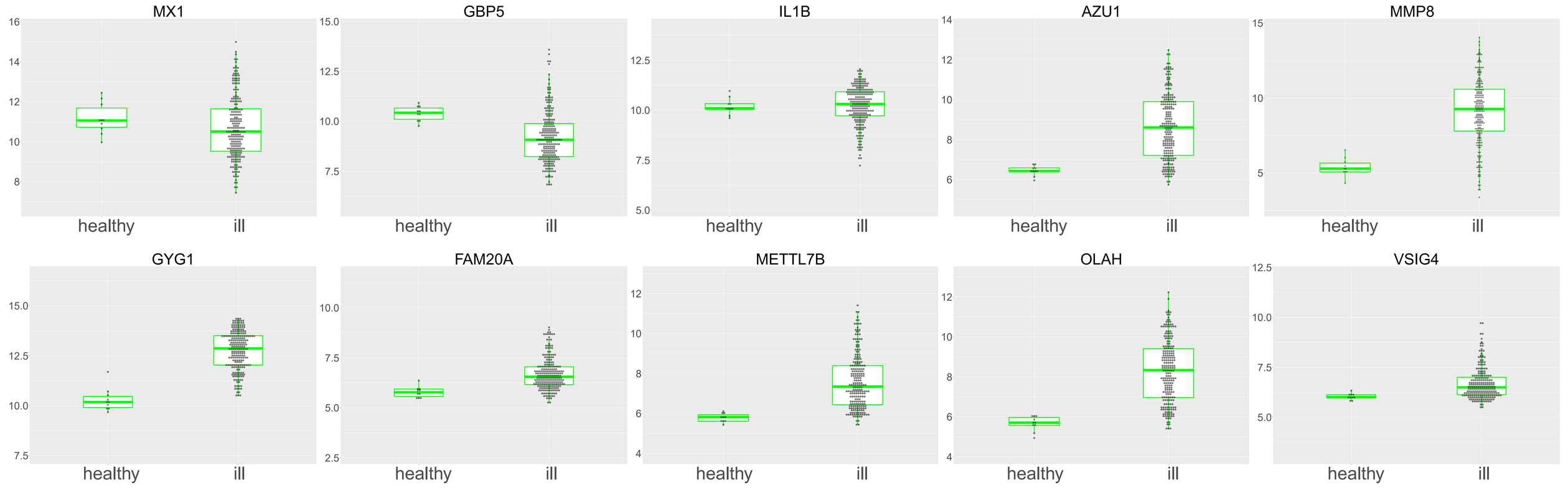
MX1
GBP5
IL1B
AZU1
MMP8
GYG1
FAM20A
METTL7B
OLAH
VSIG4
healthy
ill

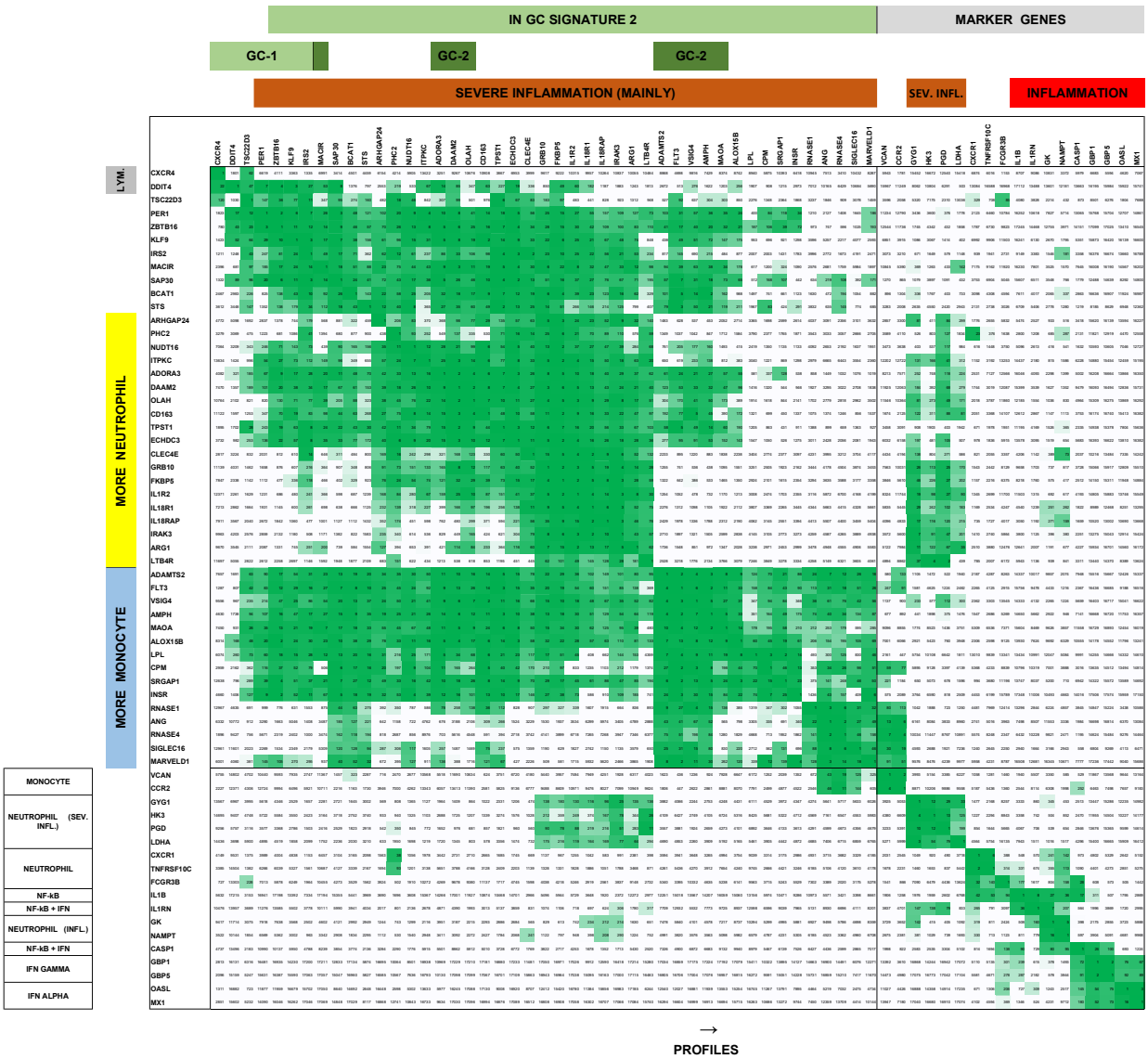

MODULE / SET GC-2 : MACIR, ADORA3, DAAM2, OLAH, ADAMTS2, FLT3, VSIG4, AMPH, MAOA

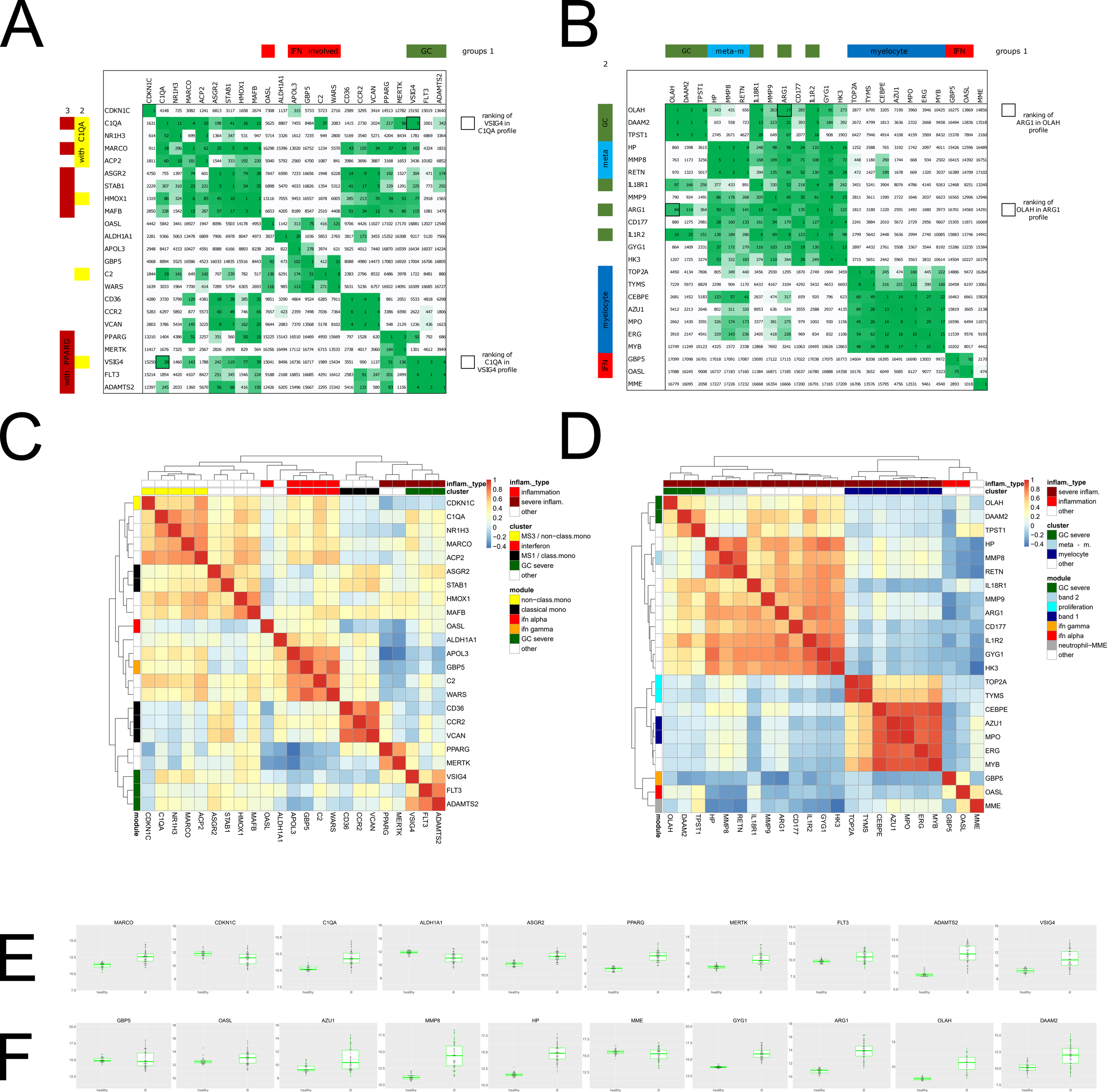
A
IFN involved
GC
groups 1
3
2
with C1QA
with PPARG
ranking of VSIG4 in C1QA profile
ranking of C1QA in VSIG4 profile
B
GC
meta-m
myelocyte
IFN
groups 1
2
GC
meta
myelocyte
IFN
ranking of ARG1 in OLAH profile
ranking of OLAH in ARG1 profile
C
inflam._type
cluster
inflammation
severe inflam.
other
cluster
MS3 / non−class.mono
interferon
MS1 / class.mono
GC severe
other
module
non−class.mono
classical mono
ifn alpha
ifn gamma
GC severe
other
D
inflam._type
cluster
severe inflam.
inflammation
other
cluster
GC severe
meta - m.
myelocyte
other
module
GC severe
band 2
proliferation
band 1
ifn gamma
ifn alpha
neutrophil−MME
other
E
MARCO
CDKN1C
C1QA
ALDH1A1
ASGR2
PPARG
MERTK
FLT3
ADAMTS2
VSIG4
F
GBP5
OASL
AZU1
MMP8
HP
MME
GYG1
ARG1
OLAH
DAAM2

A

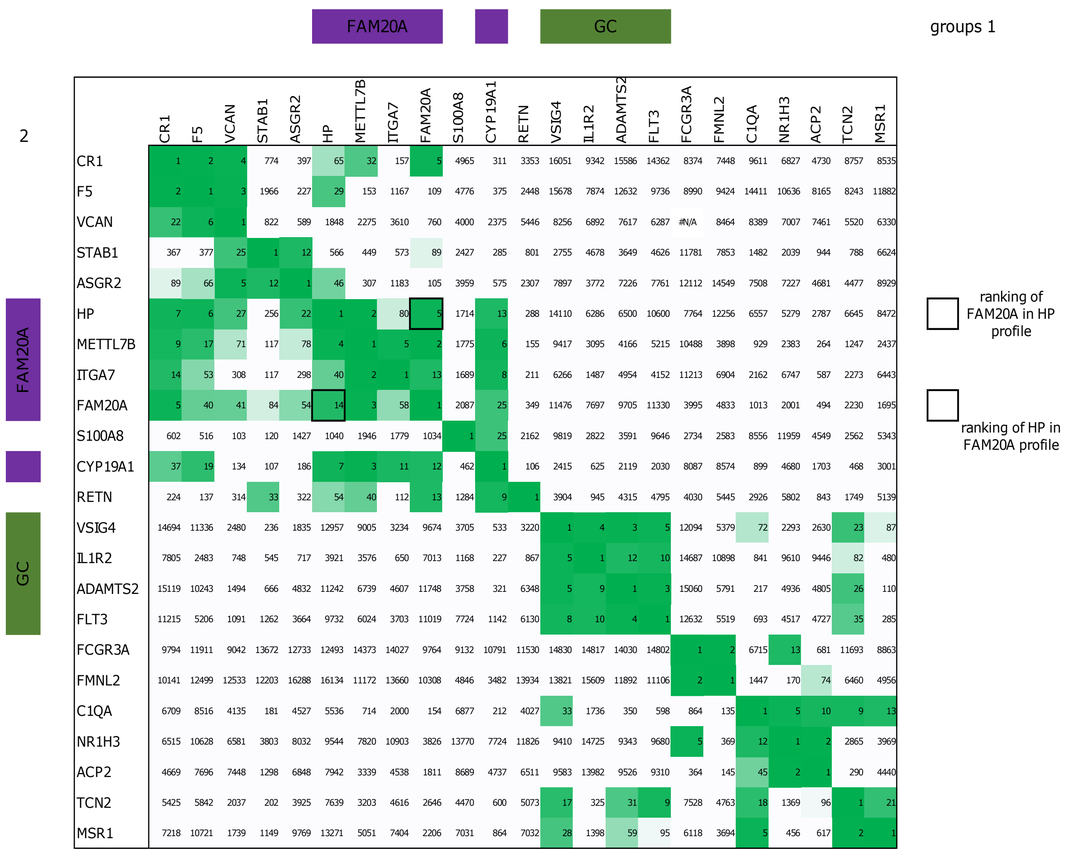
FAM20A
GC
groups 1
2
FAM20A
GC
ranking of FAM20A in HP profile
ranking of HP in FAM20A profile

B

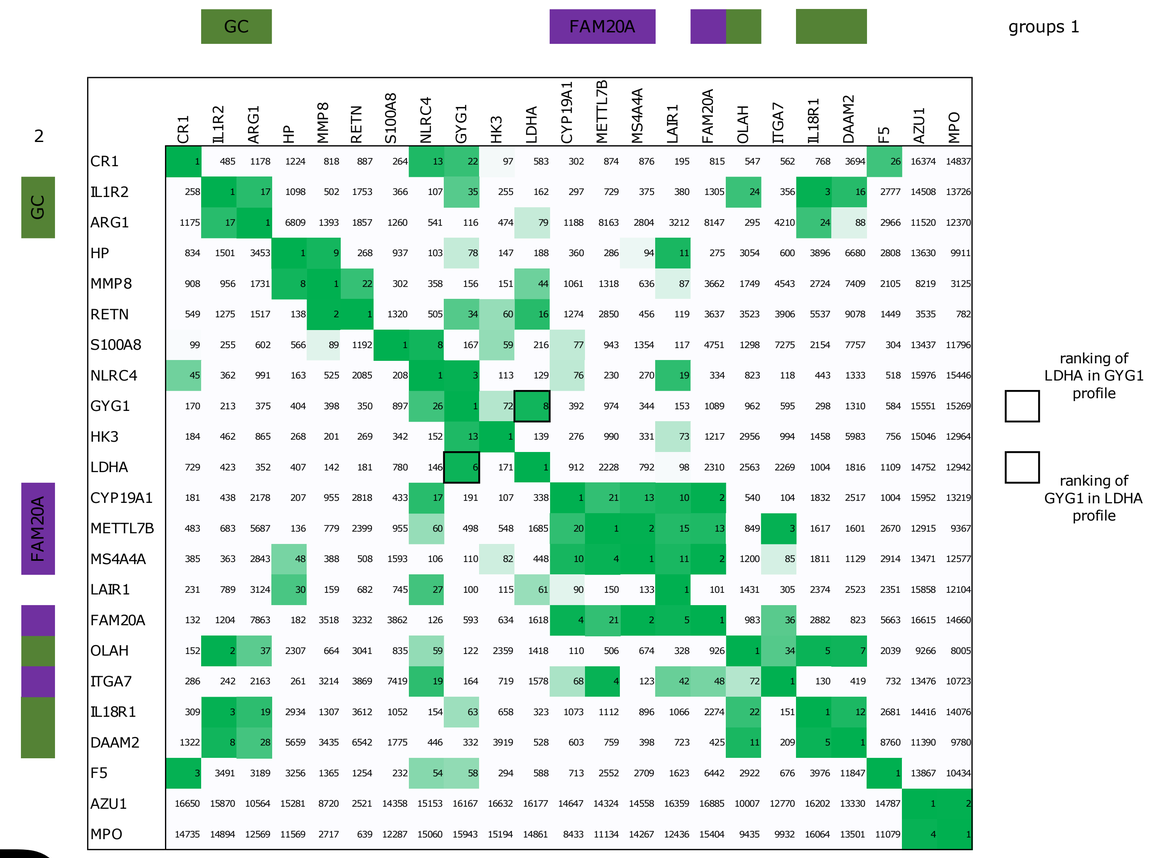
GC
FAM20A
groups 1
2
GC
FAM20A
ranking of LDHA in GYG1 profile
ranking of GYG1 in LDHA profile

C

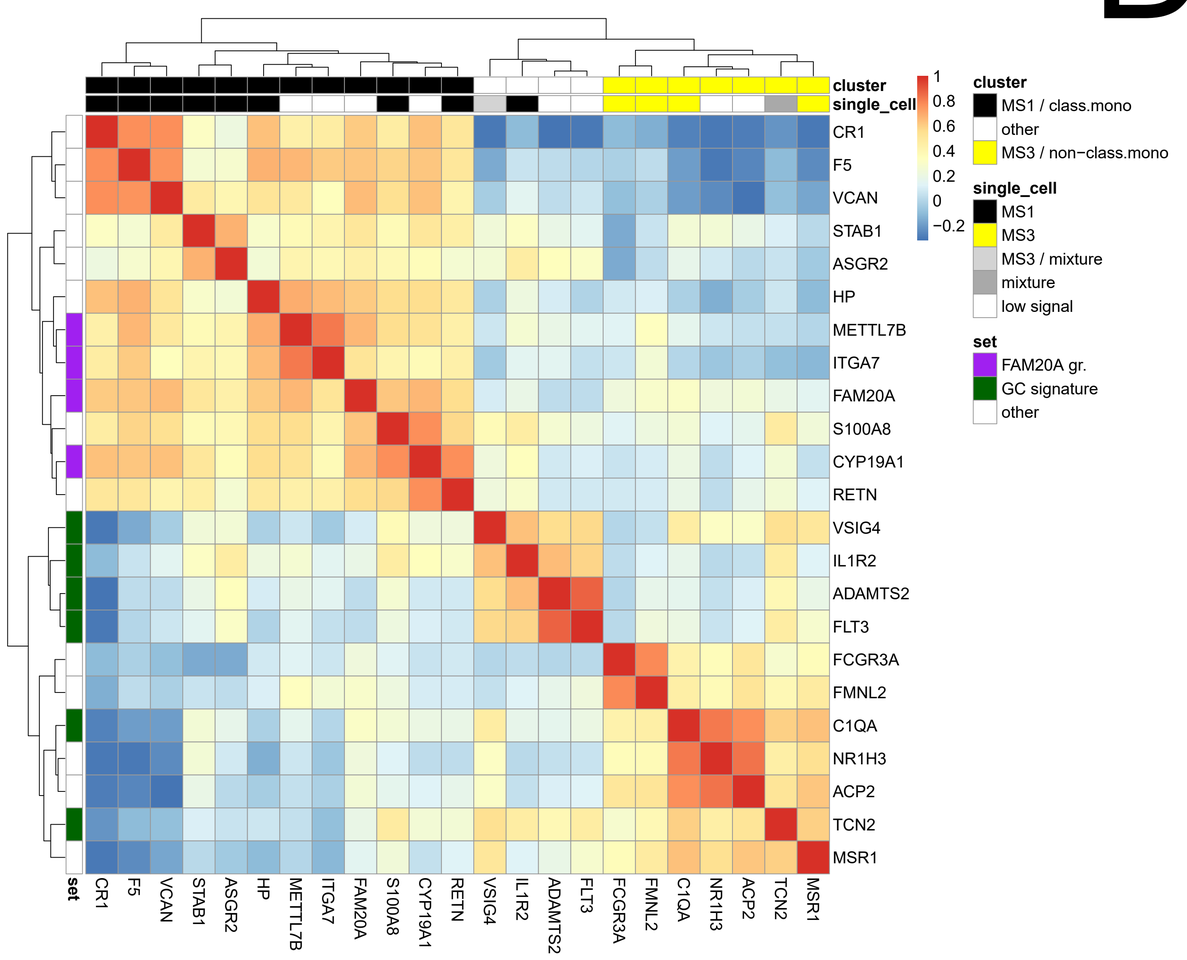
cluster
single_cell
set
cluster
MS1 / class.mono
other
MS3 / non−class.mono
single_cell
MS1
MS3
MS3 / mixture
mixture
low signal
set
FAM20A gr.
GC signature
other

D

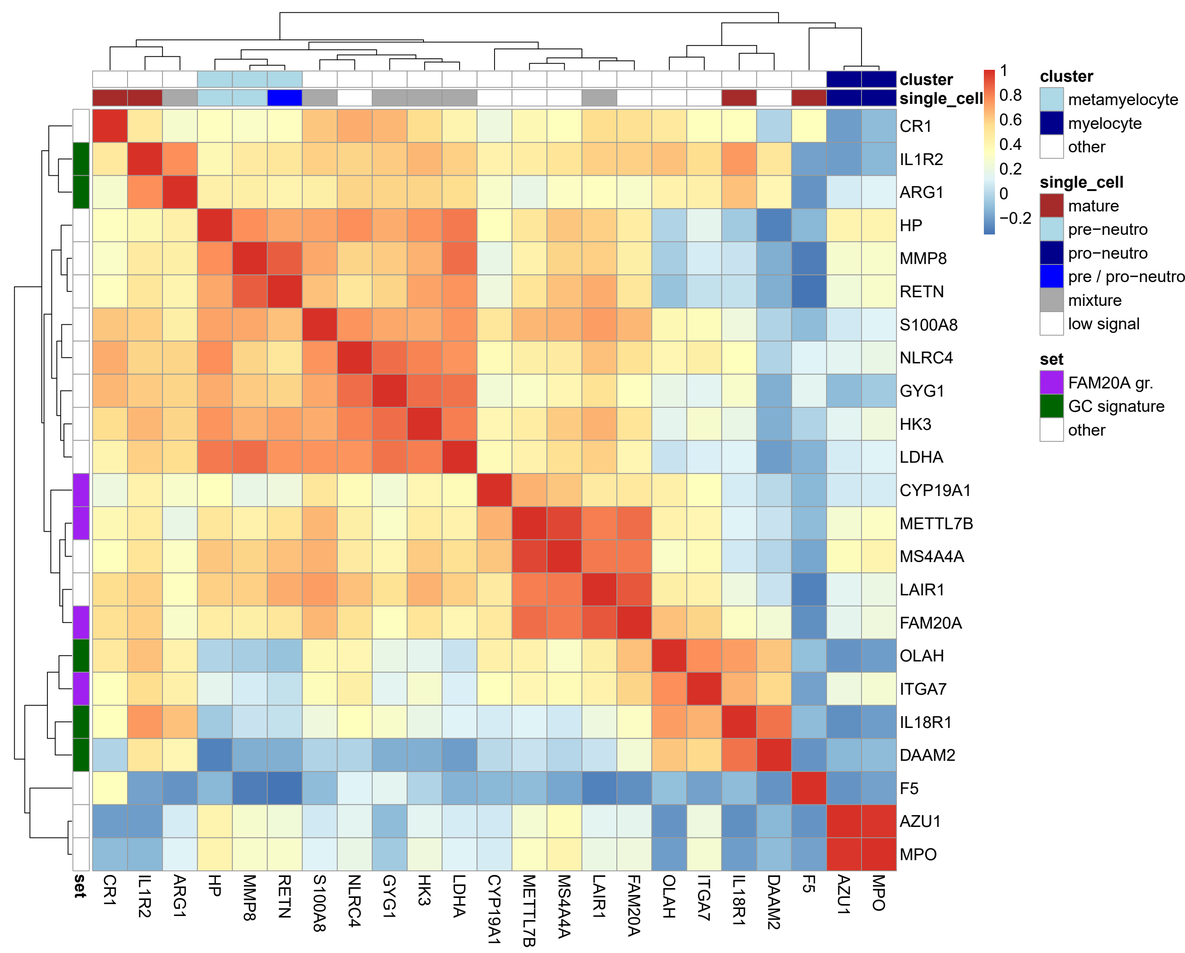
cluster
single_cell
set
cluster
metamyelocyte
myelocyte
other
single_cell
mature
pre−neutro
pro−neutro
pre / pro−neutro
mixture
low signal
set
FAM20A gr.
GC signature
other

E

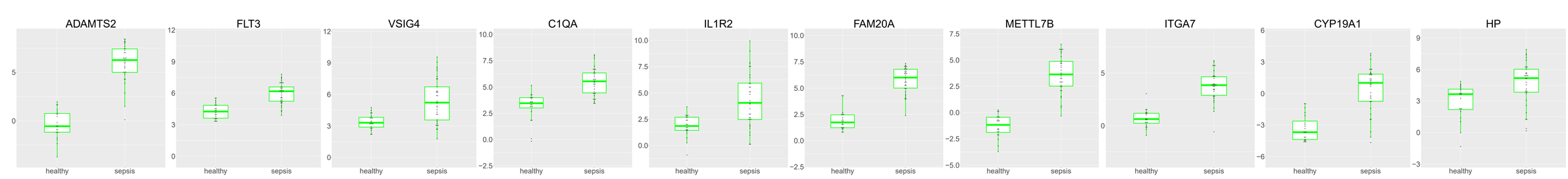
ADAMTS2
FLT3
VSIG4
C1QA
IL1R2
FAM20A
METTL7B
ITGA7
CYP19A1
HP
healthy
sepsis

F

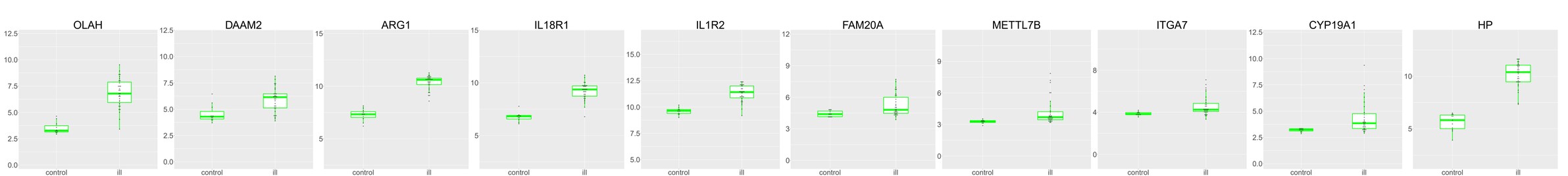
OLAH
DAAM2
ARG1
IL18R1
IL1R2
FAM20A
METTL7B
ITGA7
CYP19A1
HP
control
ill

	homeostasis	sev. inflam.
regulation of gene expression		
KLF9	M	M, N
ZBTB16	M	M, N
SAP30	M	M, N
PHC2	M, N	M, N
PER1	M, N	M, N
FKBP5	M, N	M, N
TSC22D3	M, N	M
energy metabolism		
BCAT1	no	M, N
PFKFB2	no	N
SIRT5	no	N
secretory pathway, ER		
ERN1	N	N
ERLIN1	M, N	M, N
TEX2	M	M, N
ERGIC1	no ?	M, N
secretory pathway, Golgi		
MAN2A2	M, N	M, N
CSGALNACT2	M ?	M, N
ST6GALNAC3	no	M, N
PXYLP1	no ?	N
B4GALT4	no ?	N
TPST1	M, N	M, N
sphingolipid synthesis		
SPTLC2	no ?	M, N
SGMS2	M	M, N
extracellular matrix		
ADAMTS2	no	M
THBS1	M	M
TIMP4	no	M
GPCR		
GPER1	M	M
ADORA3	M, N	M, N
GPCR (chemotaxis)		
CXCR4	M, N ?	no ?
LTB4R	no ?	M, N
phagocytosis and cell motility		
AMPH	M ?	M, N ?
SRGAP1	M ?	M
ARHGAP24	M ?	M, N
RALGAPA2	N	M, N
SIPA1L2	N	M, N
DAAM2	N	M, N
FMN1	no ?	M

	homeostasis	sev. inflam.
phagocytosis of apoptotic cells		
MFGE8	no	M
VSIG4	no	M
C1QA/B/C	no	M
PRR / phagocytosis receptors		
CLEC4E	M, N	M, N
CEACAM4	no	M, N
endocytosis receptor		
CD163	M ?	M, N
IL1 family receptors, etc		
IL1R1	no	N
IL1R2	M, N	M, N
IL18R1	N ?	N
IL18RAP	N ?	N
IRAK3	M, N	M, N
receptors, JAK/STAT		
IFNGR1	M	M, N
IL13RA1	M, N	M
receptor kinases		
FLT3	M	M
INSR	no	M
ACVR1B	M	M
intracellular signaling, misc.		
IRS2	M, N	M, N
GRB10	no	M, N
ITPKC	M	M, N
DDIT4	M, N	M
SESN1	no	M
PICK1	M	M
VSIR	N	N
prostaglandin and leukotriene		
ALOX15B	M	M
HPGD	M ?	M, N
ALOX5AP	no ?	M, N
angiogenesis and more		
RNASE1, ANG / RNASE4	no	M
miscellaneous		
ECHDC3	M ?, N	M, N
MACIR	N	N
OLAH	no	N
STS	N	N
ARG1	no	N
MAOA	no	M, N
PRL	no	M
APH1B	no	N

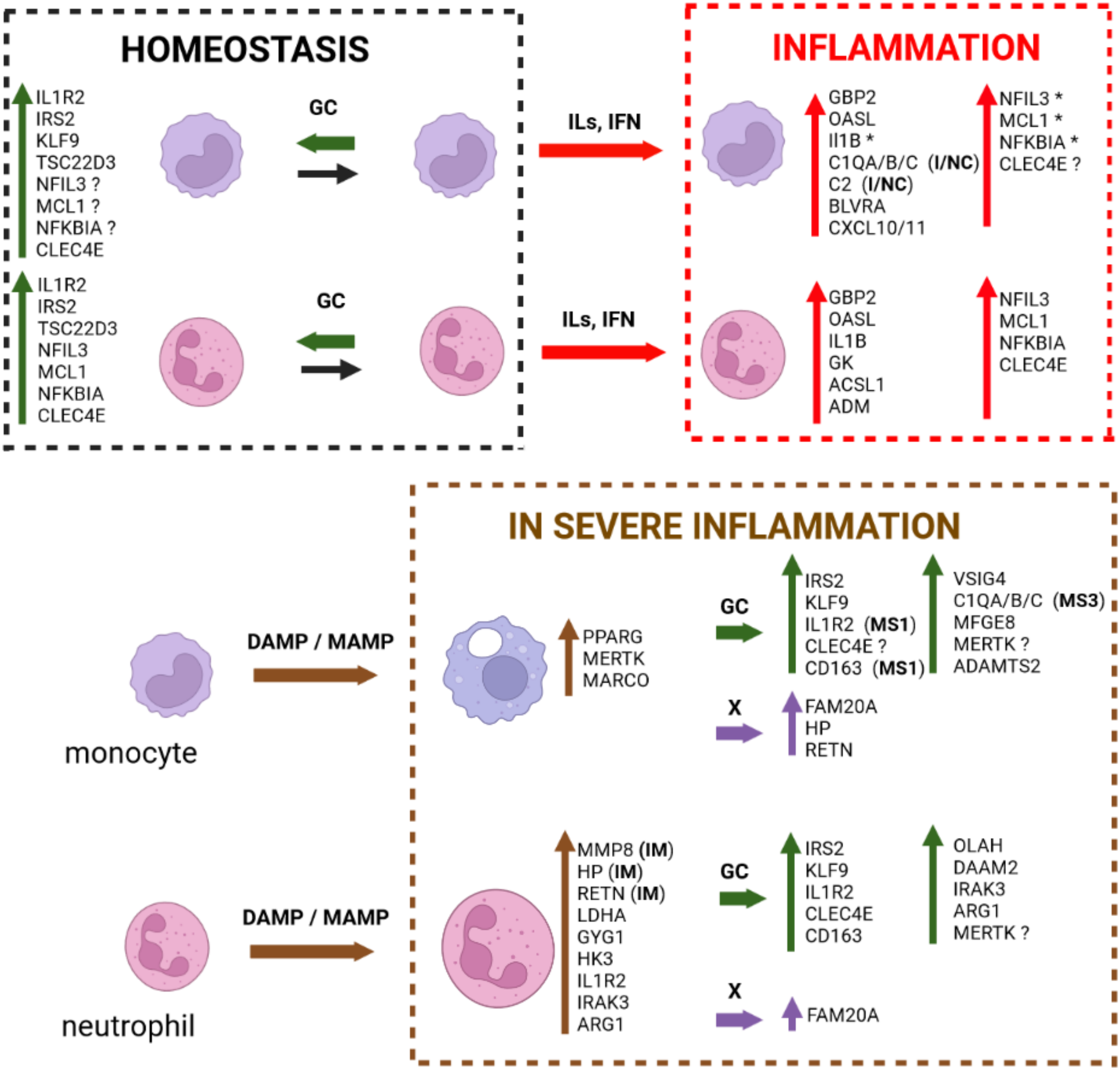

Created in BioRender.com bio

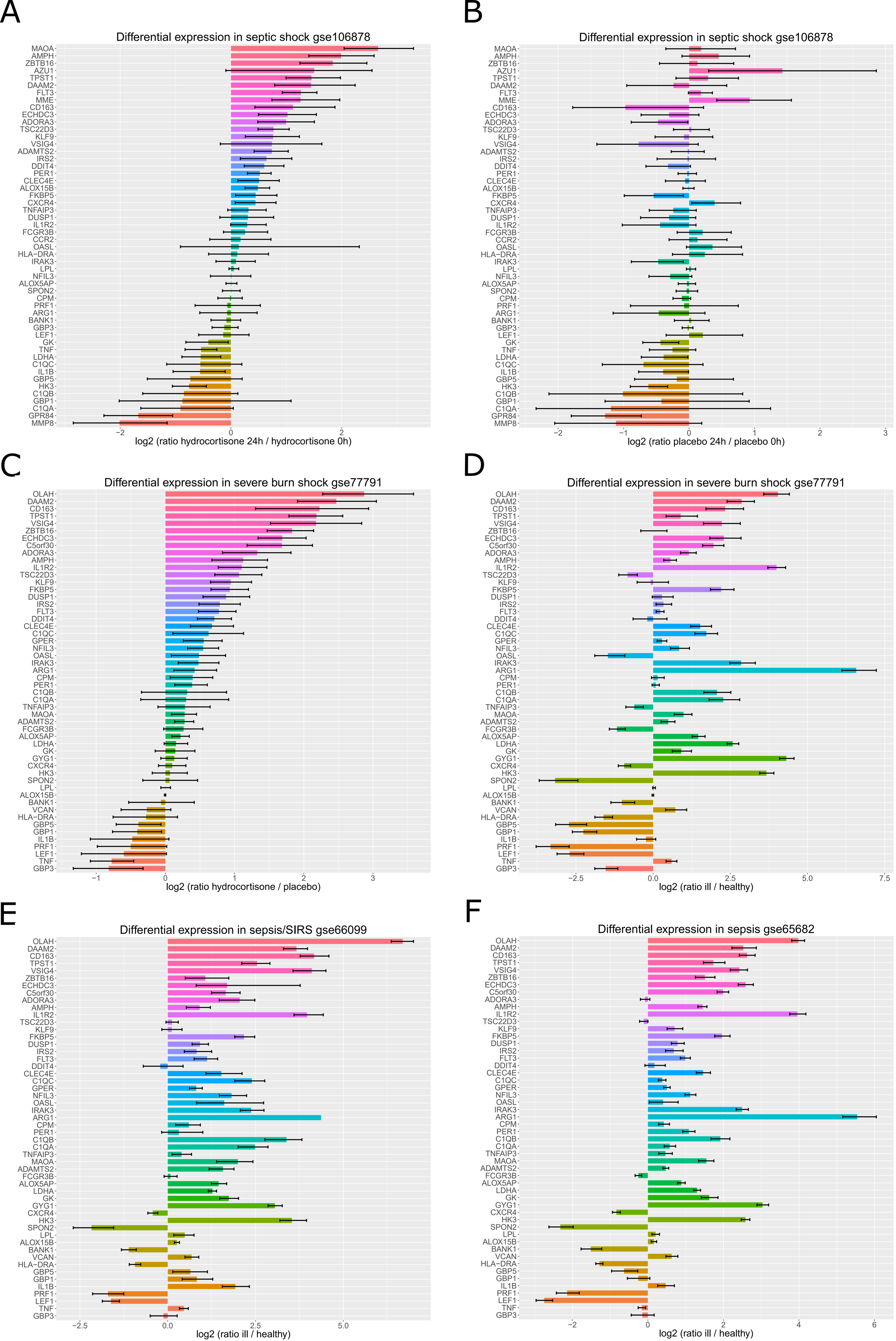
A
Differential expression in septic shock gse106878
log2 (ratio hydrocortisone 24h / hydrocortisone 0h)
B
Differential expression in septic shock gse106878
log2 (ratio placebo 24h / placebo 0h)
C
Differential expression in severe burn shock gse77791
log2 (ratio hydrocortisone / placebo)
D
Differential expression in severe burn shock gse77791
log2 (ratio ill / healthy)
E
Differential expression in sepsis/SIRS gse66099
log2 (ratio ill / healthy)
F
Differential expression in sepsis gse65682
log2 (ratio ill / healthy)

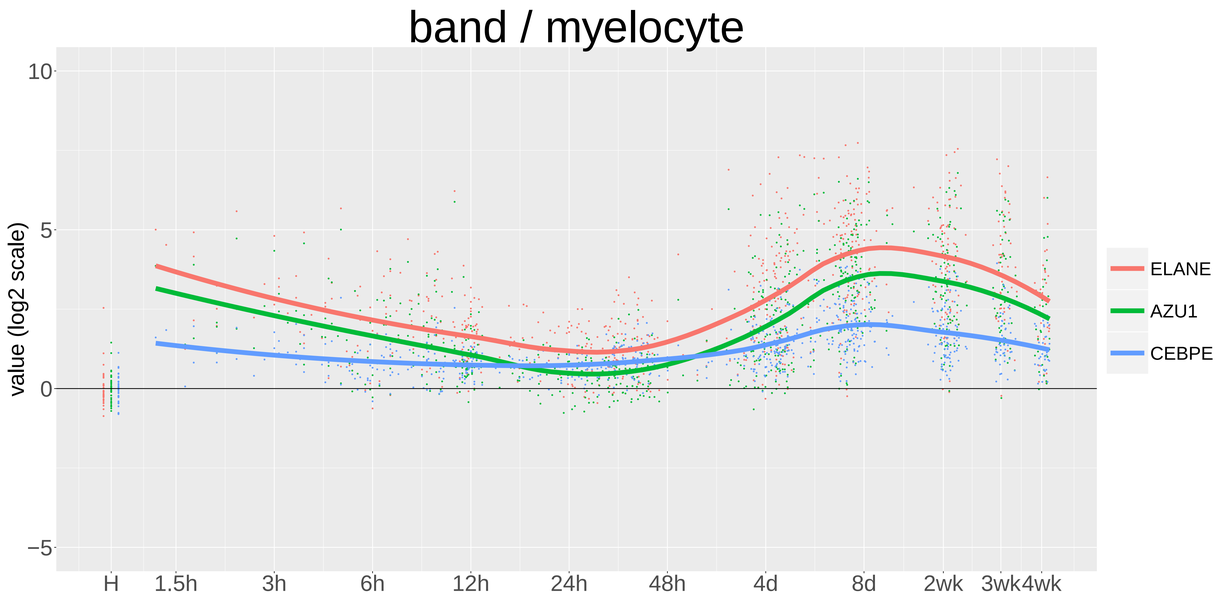
band / myelocyte
value (log2 scale)
10
5
0
−5
H
1.5h
3h
6h
12h
24h
48h
4d
8d
2wk
3wk
4wk
ELANE
AZU1
CEBPE

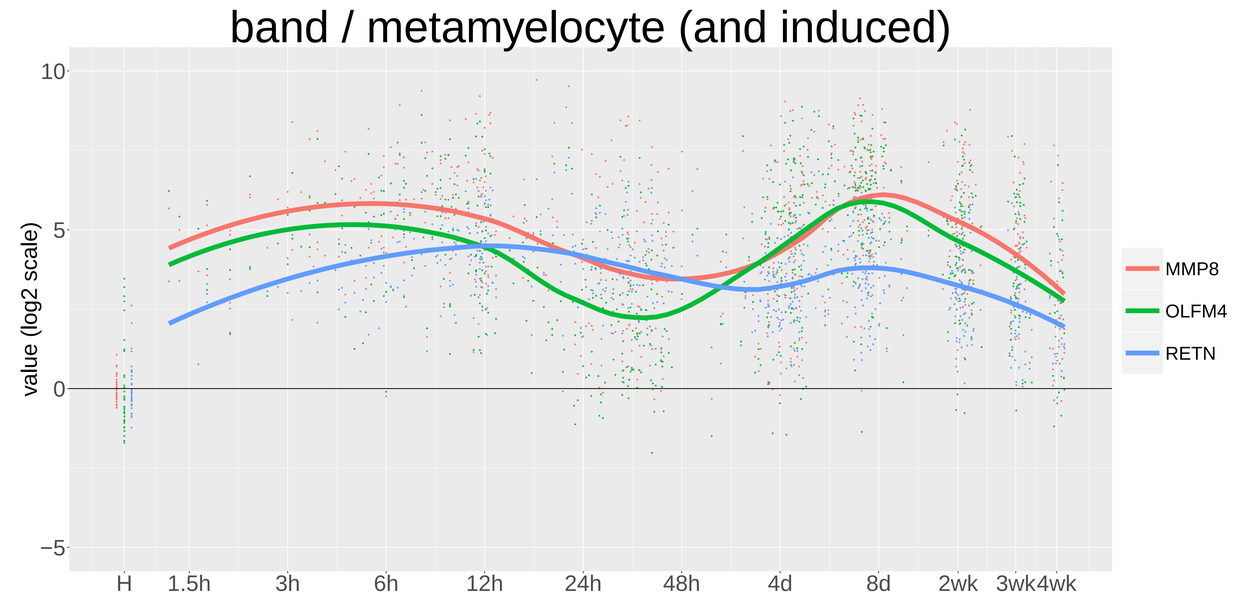
band / metamyelocyte (and induced)
value (log2 scale)
10
5
0
−5
H
1.5h
3h
6h
12h
24h
48h
4d
8d
2wk
3wk
4wk
MMP8
OLFM4
RETN

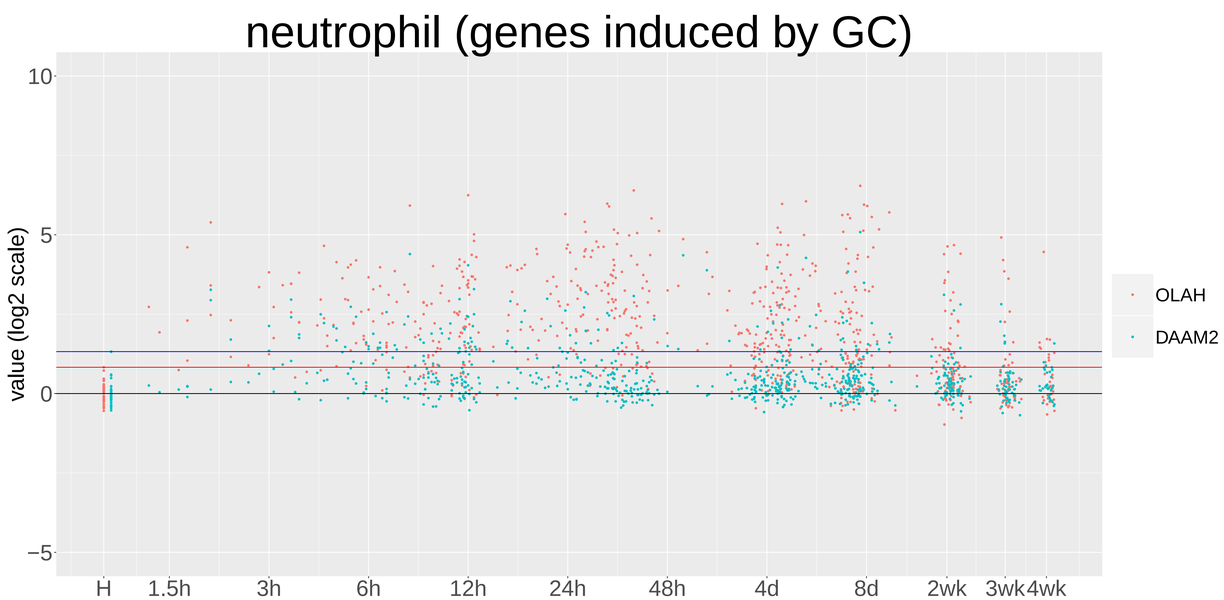
neutrophil (genes induced by GC)
value (log2 scale)
10
5
0
−5
H
1.5h
3h
6h
12h
24h
48h
4d
8d
2wk
3wk
4wk
OLAH
DAAM2

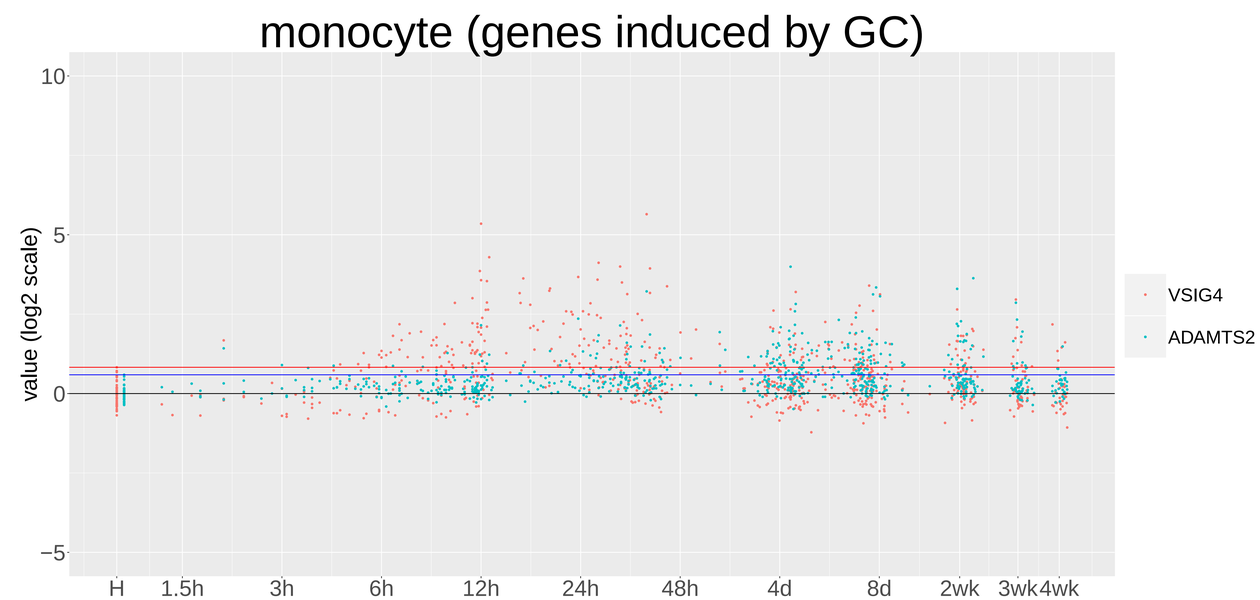
monocyte (genes induced by GC)
value (log2 scale)
10
5
0
−5
H
1.5h
3h
6h
12h
24h
48h
4d
8d
2wk
3wk
4wk
VSIG4
ADAMTS2

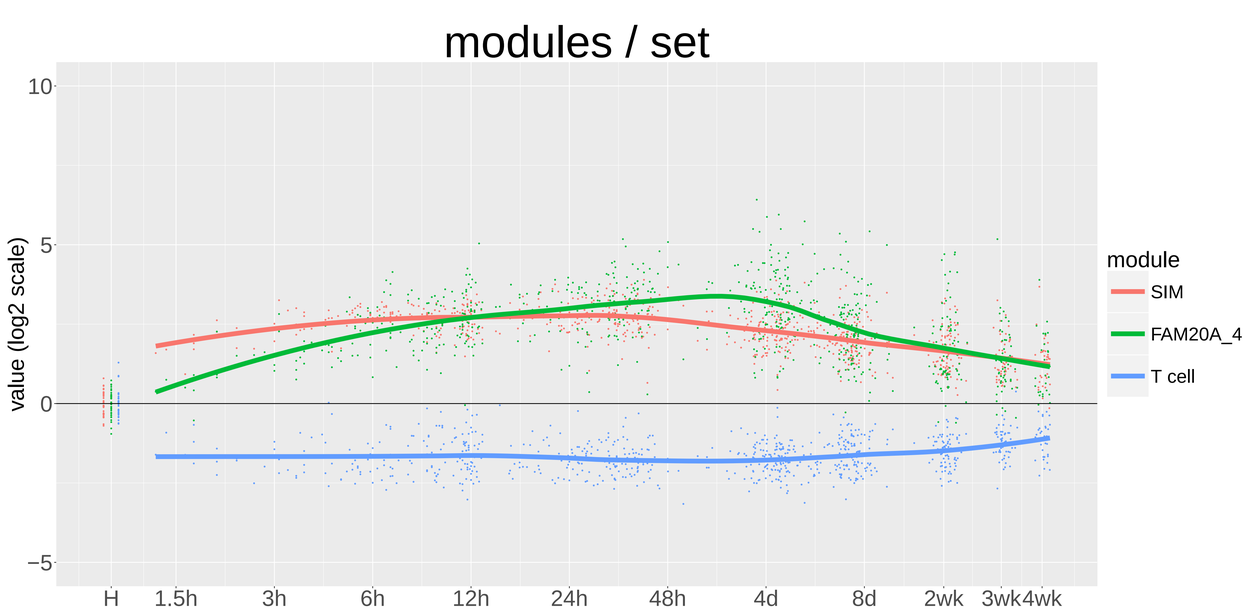
modules / set
value (log2 scale)
10
5
0
−5
H
1.5h
3h
6h
12h
24h
48h
4d
8d
2wk
3wk
4wk
module
SIM
FAM20A_4
T cell

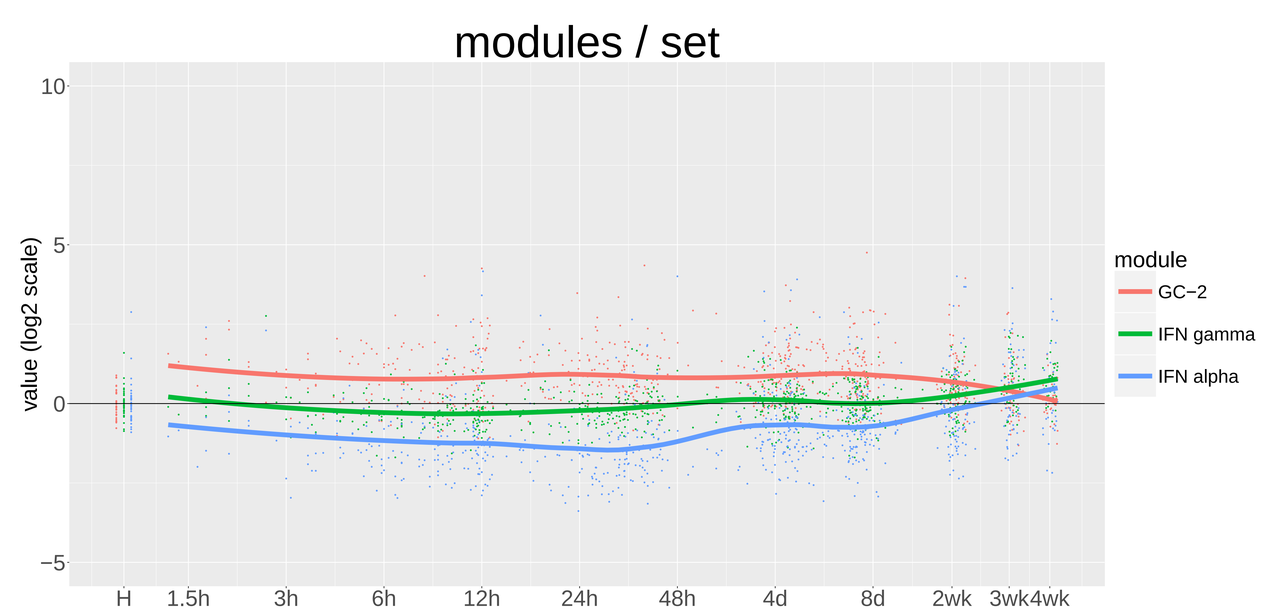
modules / set
value (log2 scale)
10
5
0
−5
H
1.5h
3h
6h
12h
24h
48h
4d
8d
2wk
3wk
4wk
module
GC−2
IFN gamma
IFN alpha

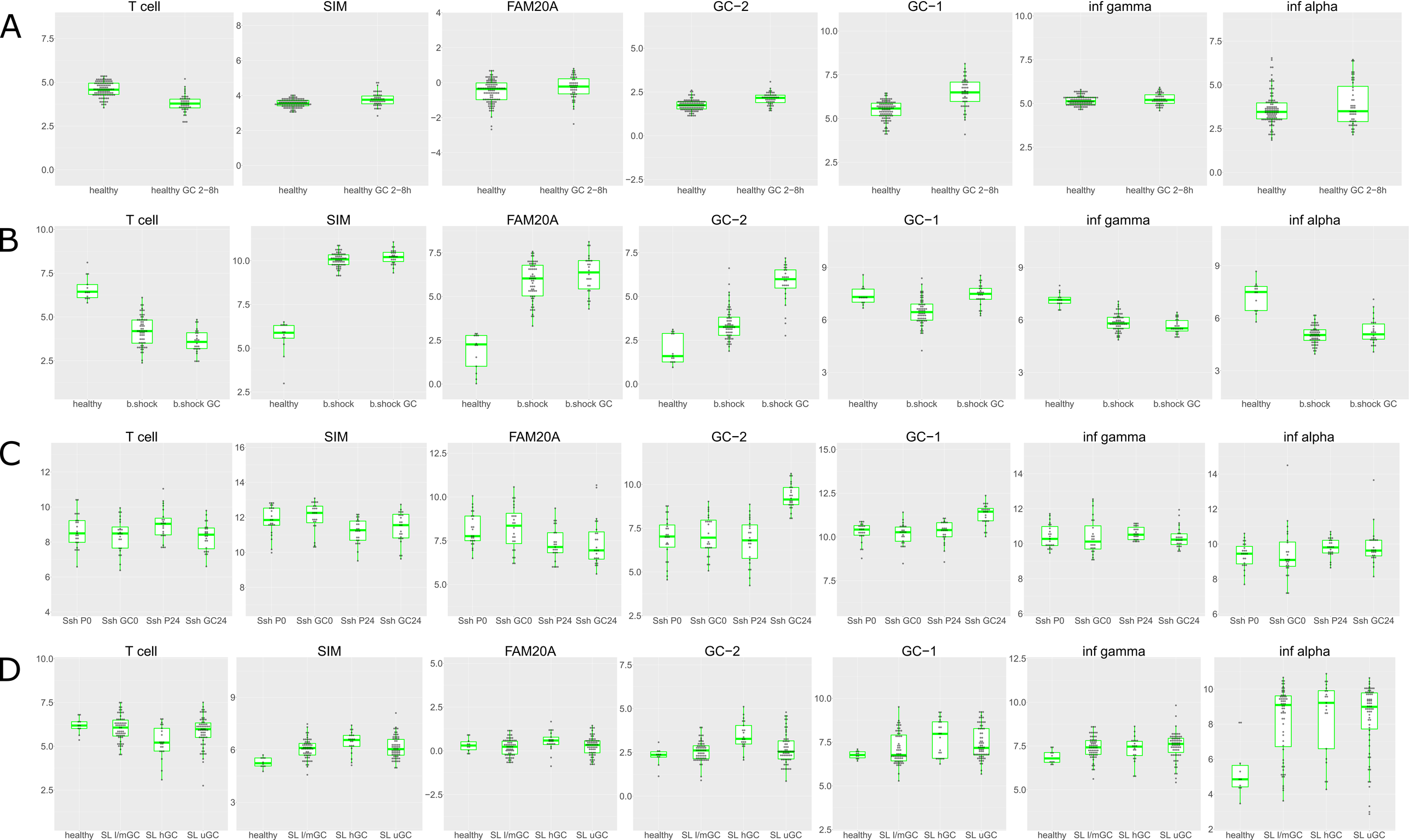
A
T cell
SIM
FAM20A
GC−2
GC−1
inf gamma
inf alpha
healthy
healthy GC 2−8h
B
healthy
b.shock
b.shock GC
C
Ssh P0
Ssh GC0
Ssh P24
Ssh GC24
D
healthy
SL l/mGC
SL hGC
SL uGC

disease	SIM	FAM (4)	GC-2	IFN-G	IFN-A	dataset	platform	supporting
PTSD	•	•	•	•	•	GSE97356	RNA-seq	Fig S6K
healthy + 7 days GC	↑	•	↑	•	•	GSE110160	GPL3921	Fig 15A
SLE	↑	↑	⬆	⬆	🔴⬆	GSE72509	RNA-seq	Fig S6H
SLE low SLEDAI	•	•	↑	⬆	🔴⬆	GSE138458	GPL10558	Fig S5H
SLE high SLEDAI	•	•	↑	⬆	🔴⬆	GSE138458	GPL10558	Fig S5H
SLE + low/medium GC	↑	•	•	⬆	🔴⬆	GSE110174	GPL13158	Fig 15D
SLE + high GC	⬆	•	⬆	⬆	🔴⬆	GSE110174	GPL13158	Fig 15D
SLE no GC	•	•	•	⬆	🔴⬆	GSE110169	GPL13667	Fig S7G/H
SLE + GC	↑	•	⬆	⬆	🔴⬆	GSE110169	GPL13667	Fig S7G/H
RA no GC	•	•	•	•	•	GSE110169	GPL13667	Fig S7G/H
RA + GC	↑	•	⬆	•	•	GSE110169	GPL13667	Fig S7G/H
RA	↑	•	↑	↑	↑	GSE93272	GPL570	Fig S4G
RA no GC	•	•	•	•	↑	GSE117769	RNA-seq	Fig S7D
RA + GC	↑	↑	⬆	•	?	GSE117769	RNA-seq	Fig S7D
JIA	•	↑	↑	?	↑	GSE112057	RNA-seq	Fig S6G
SJIA	↑	↑	⬆	?	↑	GSE112057	RNA-seq	Fig S6G
SJIA plus canakinumab	↑	⬆	↑	↑	↑	GSE80060	GPL570	Fig S4D
SJIA no canakinumab	⬆	⬆	↑	↑	↑	GSE80060	GPL570	Fig S4D
sarcoidosis	↑	•	•	⬆	⬆	GSE83456	GPL10558	Fig S5I
sarcoidosis	↑	↑	↑	⬆	↑	GSE19314	GPL570	Fig S4E
sarcoidosis (non active)	•	•	•	⬆	↑	GSE42834	GPL10558	Fig S5J
sarcoidosis (active)	↑	↑	?	⬆	⬆	GSE42834	GPL10558	Fig S5J
tuberculosis (active)	⬆	↑	↑	🔴⬆	⬆	GSE83456	GPL10558	Fig S5I
tuberculosis (latent)	•	•	•	•	•	GSE107793	RNA-seq	Fig S6J
tuberculosis (latent)	•	•	•	•	•	GSE107794	RNA-seq	Fig S6I
tuberculosis (active)	↑	⬆	↑	🔴⬆	↑	GSE107794	RNA-seq	Fig S6I
tuberculosis (active)	⬆	↑	?	🔴⬆	⬆	GSE42834	GPL10558	Fig S5J
lung cancer	⬆	↑	⬆	?	?	GSE42834	GPL10558	Fig S5J
IBD no GC	⬆	•	•	?	?	GSE126124	GPL6244	Fig S7I
IBD-Crohn	↑	↑	⬆	⬆	?	GSE112057	RNA-seq	Fig S6G
IBD-UC	⬆	↑	⬆	?	?	GSE112057	RNA-seq	Fig S6G
malaria (adults)	↑	↑	•	⬆	?	GSE52166	RNA-seq	Fig S6F
malaria (children)	⬆	⬆	⬆	⬆	↓↑	GSE34404	GPL10558	Fig S5F
malaria (cerebral)	⬆	⬆	⬆	?	↓↑	GSE117613	GPL10558	Fig S5G
malaria (anemia)	⬆	⬆	⬆	?	↓	GSE117613	GPL10558	Fig S5G
leishmaniasis	↑	⬆	?	⬆	⬆	GSE69597	RNA-seq	Fig S6E
brucellosis	•	↑	•	⬆	↑	GSE69597	RNA-seq	Fig S6E
diarrhea rota viral	↑	⬆	⬆	⬆	⬆	GSE69529	RNA-seq	Fig S6D
diarrhea bacterial	⬆	⬆	⬆	↑	⬆	GSE69529	RNA-seq	Fig S6D
bacterial (pneumonia/bacteremia)	⬆	⬆	⬆	↓⬆	↓↑	GSE176260	RNA-seq	Fig S7A
candidemia	⬆	⬆	⬆	⬆	↓↑	GSE176260	RNA-seq	Fig S7A
viral infection (acute)	⬆	⬆	?	🔴⬆	🔴⬆	GSE176260	RNA-seq	Fig S7A
mild resp. vir. influenza	↑	•	•	⬆	🔴⬆	GSE68310	GPL10558	Fig S5L
mild resp. vir. not influenza	↑	•	•	⬆	⬆	GSE68310	GPL10558	Fig S5M
COVID-19 not ICU *	⬆	⬆	⬆	⬆	⬆	GSE157103	RNA-seq	Fig S6B
COVID-19 ICU *	⬆	⬆	⬆	↑	⬆	GSE157103	RNA-seq	Fig S6B
COVID 19 (severe), **PBMC**	•	⬆	⬆	↑	⬆	GSE161918	RNA-seq	Fig S7F
COVID-19 (severe)	⬆	⬆	⬆	↑	⬆	GSE171110	RNA-seq	Fig S7C
COVID-19 (severe)	⬆	⬆	⬆	⬆	⬆	GSE152641	RNA-seq	Fig S6C
kawasaki acute no GC	⬆	⬆	⬆	↑	↓↑	GSE73463	GPL10558	Fig S5E
trauma < 99h	⬆	⬆	⬆	↓	↓↑	GSE36809	GPL570	Fig S4B
trauma > 99h	⬆	⬆	⬆	•	↓↑	GSE36809	GPL570	Fig S4B
burn shock	🔴⬆	🔴⬆	⬆	🔴⬇	🔴⬇	GSE77791	GPL570	Fig S4C/Fig 15B
burn shock + GC	🔴⬆	🔴⬆	🔴⬆	🔴⬇	🔴⬇	GSE77791	GPL570	Fig S4C/Fig 15B
SIRS	⬆	⬆	⬆	↓↑	⬇↑	GSE66099	GPL570	Fig S4A
sepsis	⬆	⬆	⬆	↓↑	⬇↑	GSE66099	GPL570	Fig S4A
septic shock	🔴⬆	🔴⬆	⬆	↓↑	⬇↑	GSE66099	GPL570	Fig S4A
sepsis SRS1	⬆	⬆	⬆	⬇↑	⬇↑	E-MTAB-5273	GPL10558	Fig S5B
sepsis SRS2	⬆	⬆	⬆	↓↑	↓↑	E-MTAB-5273	GPL10558	Fig S5B
sepsis pneumonitis	⬆	⬆	⬆	↓↑	↓↑	E-MTAB-5273	GPL10558	Fig S5A
sepsis peritonitis	⬆	⬆	⬆	⬇↑	⬇↑	E-MTAB-5273	GPL10558	Fig S5A
septic shock *	🔴⬆	🔴⬆	⬆	↓↑	⬇↑	GSE106878	GPL10295	Fig 15C
septic shock + GC *	🔴⬆	🔴⬆	🔴⬆	↓↑	⬇↑	GSE106878	GPL10295	Fig 15C